TRPML1: Role In Autophagy And Potential Target To Treat Lysosomal Storage Disorders

Thesis

The Open University
Degree of Doctor of Philosophy

PhD Thesis in
School of Life, Health and Chemical Sciences

TRPML1: role in autophagy and potential target to treat lysosomal storage disorders

Director of Studies:
Dr. Diego L. Medina

Candidate:
Anna Scotto Rosato

Supervisors:
Dr. Frances Platt; Dr. Antonella De Matteis

ARC:
Telethon Institute of Genetics and Medicine

Years 2017/2018

Abstract

The view of the lysosome as the terminal end of cellular catabolic pathways has been challenged by recent studies showing a central role of this organelle in the control of cell function. Here we show that a lysosomal Ca^{2+} signaling mechanism controls the activities of the phosphatase calcineurin and of its substrate TFEB, a master transcriptional regulator of lysosomal biogenesis and autophagy. Lysosomal Ca^{2+} release via mucolipin 1 (TRPML1) activates calcineurin, which binds and de-phosphorylates TFEB, thus promoting its nuclear translocation. Induction of autophagy and lysosomal biogenesis via TFEB required TRPML1-mediated calcineurin activation, linking lysosomal calcium signaling to both calcineurin regulation and autophagy induction. In addition to the role of TRPML1 on sustaining transcriptional autophagy program, through the activation of TFEB, we also found that TRPML1-activation induces the recruitment of PtdIns(3)P-binding proteins to the nascent autophagosome, whereas genetic or pharmacological inhibition of TRPML1 channel inhibits autophagy initiation. Importantly, alteration of this function has pathological consequences, and thus we found that autophagosome formation is impaired in human fibroblasts from patients affected of mucolipidosis IV (MLIV; a severe lysosomal storage disorder caused by mutations in TRPML1). By using specific compound inhibitors during starvation, we found that TRPML1-mediated induction of autophagosome biogenesis requires calmodulin, CaMKKβ, and the PtdIns(3)-generating enzyme VPS34. Therefore, we hypothezise that during starvation, TRPML1 activation releases lysosomal calcium that activates a calcium-depedent pathway involving CaMKKβ and the induction of two essential protein complexes involved in autophagy initiation such as ULK1 and PIK3C3 complexes.

In parallel studies, we used high content (HC) screening approaches to identify small molecules able to ameliorate the MLIV phenotype. In one of them, we tested whether previously identified drugs (150 FDA compounds) inducing TFEB translocation and cellular clearance might be active in MLIV patient cells. This screening resulted in the identification of 3 drugs able to induce TFEB nuclear translocation confirming the importance of the TRPML1-mediated signalling to promote TFEB activity. In addition, only one of these hits were able to reduce the pathological accumulation of autophagic substrates such as p62 and NBR1 in MLIV human fibroblasts. In a second independent HC-screening, we developed a cell-based assay to identify FDA-drugs able to reduce cholesterol accumulation in MLIV cells. We identify 8 small molecules able to reduce cholesterol accumulation in MLIV human fibroblasts that will need further characterization to define their ability to ameliorate the phenotype of this devastating disease. In summary, we found two novel signaling pathways triggered by TRPML1-dependent lysosomal calcium release that regulate cellular homeostasis by both promoting autophagy initiation and sustaining transcriptional programs inducing autophagic and lysosomal genes during starvation. Finally, we use part of this knowledge to develop cell-based high content screening assays that identified 9 FDA-approved compounds able to ameliorate the autophagic impairment and reduce lipid storage in MLIV disease cells.

Index

Introduction

TRP channels

The family of transient receptor potential (TRP) channels is formed by seven subfamilies: TRPC (canonical), TRPV (vanilloid), TRPM (melastatin), TRPP (polycystin), TRPML (mucolipin), TRPA (ankyrin) and TRPN (NOMPC-like), with the last one only found in invertebrates and fish. These channels are ubiquitously expressed and could be classified as non – selective cation channels with only few of them classified as highly selective for calcium ions. The *Trp* gene was firstly identified in *Drosophila melanogaster* by Montell and Rubin in 1989 (Montell and Rubin, 1989). Going through the sequence, TRP family members share 35 % of homology except for the ones which come from duplication, like TRPC6 and TRPC7, TRPM4 and TRPM5, and TRPV5 and TRPV6, where the homology goes from 50 to 80% (Nilius and Owsianik, 2011).

All TRP proteins have the same structure, they are composed by six transmembrane domains with the pore region located within the 5^{th} and 6^{th} transmembrane segments. In addition, they present an amino and a carboxyl tail that could vary among channel members. For instance, it has been reported that the carboxyl terminal could contain an entire catalytic site, like the Nudix hydrolase domain in TRPM2 (Perraud et al., 2001). On the other hand, the amino terminal is enriched of ankyrin repeats, the number of repeats varies among different TRP members, and the function seems to be connected with tetramerization of the channel and interactions with ligands and protein partners (Gaudet, 2008). Other additional domains and motifs could be part of the channel structure and are strictly connected with the channel function. Generally, these domains are coiled coils, calmodulin-binding sites, lipid-interaction domains, EF hands or

phosphorylation sites, and are firmly preserved within the same TRP subfamily (Owsianik et al., 2006).

TRPs are principally located on cellular membranes with the only exception for the nuclear envelope and the mitochondrial membrane (Nilius and Owsianik, 2011). The majority of TRP channels is located on plasma membrane (PM) and is involved in cation transport (Ca^{2+}, Mg^{2+}, trace of metal ions) thus, many of them are involved in different biological processes such as homeostatic functions, muscle contraction and vasomotor control. Generally, for the correct execution of their function TRP channels are associated with accessory proteins, for instance TRPV4 interacts with PACSIN3, a protein kinase C and casein kinase II substrate, which modulates synaptic vesicular membrane traffic and dynamin-mediated endocytic processes in neurons (D'Hoedt et al., 2008, Cuajungco et al., 2006).

In the last decade, several mechanisms have been described for TRP channels activity. They could be activated by different stimuli such as membrane voltage, membrane phospholipids, phosphorylation and interaction with ligand. Membrane voltage activation is generally used by TRP channels involved in sensorial perception (Nilius et al., 2005, Nilius et al., 2003). This activation takes place thanks to positively charged amino acid (aa), like lysine and arginine in the 4^{th} and 5^{th} transmembrane domain (Voets et al., 2007). Due to their principal location on plasma membranes, it is not a surprise that TRP channels are particularly sensitive to membrane phospholipids, as in the case of TRPA1 and TRPV1 (Kim et al., 2008, Karashima et al., 2008). The phosphatidylinositol 4,5-bisphosphate (PI(4,5)P2) is one of the principal phospholipids on plasma membrane and with the help of phospholipase C (PLC) and phosphatidylinositol kinases/phosphatases could rapidly modify its concentration modulating TRP channels activity (Rohacs and Nilius, 2007, Voets and Nilius, 2007, Liu and Qin, 2005). This is true for the cold- and

menthol-sensitive TRPM8 and the Ca^{2+}-activated taste-transducing TRPM5 channels. It has been shown that the activation of PLC mediated by calcium rapidly reduces the PI(4,5)P2 levels leading to a decrease in the affinity of the channel for its ligands (menthol for TRPM8 and calcium for TRPM4) (Liu and Qin, 2005, Nilius et al., 2006). In addition, also TRPML1, an endo-lysosomal TRP channel is modulated by phospholipids. TRPML1 could directly interact with PI(3,5)P2 leading to an highly specific channel activation (Dong et al., 2010). Two major kinases have been identified as TRP channels modulator by direct phosphorylation, and those are protein kinase C (PKC) and protein kinase A (PKA). PKC seems to sensitize TRPV1 to its ligand (heat or capsaicin) (Premkumar and Ahern, 2000, Bhave et al., 2003) and through phosphorylation of TRPM8 leads to channel inactivation (Premkumar et al., 2005). PKA, on the other hand, directly phosphorylates TRPML1 inducing a reduction in channel activity (Vergarajauregui et al., 2008b). In fact, two serine belonging to the PKA consensus motif were found in the C-terminus of TRPML1 (Vergarajauregui et al., 2008b). Also TRPV1 could be phosphorylated by PKA and this phosphorylation potentiates its activity (Bhave et al., 2003). More recently, Brenman and colleagues have shown that also the target of rapamycin (TOR), a nutrient sensitive kinase that is involved in negative regulation of the autophagic flux, directly phosphorylates the *Drosophila* trpml and inactivates it (Onyenwoke et al., 2015). Finally, the best stimulus which activates TRP channels is mediated by the interaction with a large number of exogenous and endogenous ligands. For instance, temperature sensitive TRP channels prefer plants derived compounds, indeed, TRPV1 is activated by capsaicin (Caterina et al., 1997), resiniferatoxin (Szallasi et al., 1999), piperine (McNamara et al., 2005) and camphor (Xu et al., 2005). Not only plants derived compounds could interact with TRP channels, but also a wide range of synthetic ligands are available and the majority of them represents useful pharmacological tools to modulate channel activity (Nilius and

Owsianik, 2011). Some of these compounds bind to more than one TRP channel, like 2-aminoethyl diphenylborinate which activates TRPV1, TRPV2 and TRPV3 (Chung et al., 2004, Hu et al., 2004) and icilin which activates TRPM8 and TRPA1 (McKemy et al., 2002, Story et al., 2003). Other compounds exist which are more specific and very selective for one TRP channel such as olvanil for TRPV1 (Iida et al., 2003) and 4α-phorbol-12,13-didecanoate (4α-PDD), lumiphorbols, phorbol-hexonates and GSK 1016790A for TRPV4 (Watanabe et al., 2002, Klausen et al., 2009, Thorneloe et al., 2008).

TRPMLs

The transient receptor potential mucolipin (TRPML) channel group is one of the TRPs subfamilies and is formed by three members, TRPML1, TRPML2 and TRPML3 which share about 75% of similarity in the amino acid sequence (Di Paola et al., 2017). Being a sub-group of the TRP channel family these channels share specific structural features like the pore-forming re-entrant loop between the 5th and the 6th trans-membrane segment and two cytoplasmic amino- and carboxyl- termini (Li et al., 2011), but characteristic features of TRPMLs are the large extracellular-intraluminal loop between the 1st and the 2nd transmembrane segment and the short cytosolic tails, which range from 61 to 72 aa in length. The presence of negatively charged glutamate and aspartate residues within the pore region defines TRPMLs selectivity to cations. Since high similarity in the pore sequence of TRPMLs exists, it is likely that differences in their regulation and conductance are defined by structural determinants located outside the pore (Di Paola et al., 2017).

TRPML1 channel structure and function

MCOLN1 gene and the associated disease mucolipidosis type IV (MLIV)

Human TRPML1 is encoded by the MCOLN1 gene which is located on chromosome 19 and, unlike the murine homolog, does not have splicing variants (Falardeau et al., 2002). Genetic mutations leading to inactivation of TRPML1 cause a rare genetic disorder called

Mucolipidosis Type IV (MLIV). In 2000, three research groups independently identified MCOLN1 as the mutated gene causing MLIV (OMIM 252650), an autosomal recessive lysosomal storage disease (LSD) characterized by mental retardation, corneal opacities, elevated blood gastrin levels, achlorhydria and delayed motor milestones (Bargal et al., 2000, Berman et al., 1974, Bassi et al., 2000, Sun et al., 2000, Frei et al., 1998, Amir et al., 1987, Altarescu et al., 2002, Lubensky et al., 1999). Distribution of the disease is relatively rare in the whole population with a prevalence of 1 in 40,000 individuals (Altarescu et al., 2002, Bach, 2001, Kogot-Levin et al., 2009, Bargal et al., 2002). Of note, 70-80% of affected individuals were identified as Ashkenazi Jewish (AJ) descent, with carrier frequency in AJ population estimated to be 1:100 (Bargal et al., 2000). In individuals affected by MLIV, two main mutations, originated from AJ, were isolated. The major AJ mutation, present on 72% of the AJ MLIV alleles, is an A>G transition at the 3′ spliceosome acceptor site for intron 3 that causes the deletion of exon 4 (Bargal et al., 2000, Bassi et al., 2000, Sun et al., 2000, Altarescu et al., 2002), the minor AJ mutation, found on 23% of the AJ MLIV alleles, is a 6434 bp genomic deletion that spans exons 1–6 and the first 12 bp of exon 7 (Altarescu et al., 2002). Other mutations in the MCOLN1 gene account for the remaining 5% of affected individuals. These novel mutations have been documented as nonsense, missense and one in-frame deletion which generally cause milder phenotypes (Sun et al., 2000, Altarescu et al., 2002, Bach, 2001). MCOLN1 is ubiquitously transcribed in all tissues, with brain, spleen, liver and heart expressing the highest levels of the transcript (Samie et al., 2009). To dissect the role of TRPML1 in cellular physiology, many cell-based studies have been performed on MLIV-derived fibroblasts or through TRPML1 acute silencing in heterologous cells (Di Paola et al., 2017). Early studies on MLIV patient fibroblasts have shown lysosomal accumulation of heterogeneous macromolecules, like gangliosides, phospholipids and

mucopolysaccharides, which are not due to defects in enzymatic degradation (Bargal and Bach, 1988, Bargal and Bach, 1989, Zeigler et al., 1992). Indeed, MLIV fibroblasts as well as cells depleted of TRPML1 show defective transport of lipids from acidic organelles to the Golgi apparatus or the plasma membrane and a delayed lipid metabolism, which causes lysosomal accumulation of substrates and indirectly interferes with other transport pathways (Chen et al., 1998, Bargal and Bach, 1997, Pryor et al., 2006, Jansen et al., 2001, Thompson et al., 2007, Miedel et al., 2008). Animal models for MLIV disease have been generated in mice, *C. elegans*, and *Drosophila* showing similar substrate accumulation and endo-lysosomal trafficking alterations (Fares and Greenwald, 2001, Venkatachalam et al., 2008, Micsenyi et al., 2009).

Channel structure and regulation

The late endo-lysosome (LEL) compartment is the primary site of TRPML1 localisation in mammalian cells (Pryor et al., 2006, Manzoni et al., 2004). Similar localisation has been reported for TRPML1 orthologs in other animal models, such as *Drosophila*, *C. elegans* and *Xenopus* (Fares and Greenwald, 2001, Venkatachalam et al., 2008, LaPlante et al., 2002). TRPML1 can also reach the plasma membrane, through the biosynthetic pathway from the Golgi apparatus or by lysosomal exocytosis, a process responsible for the repair/reseal of plasma membrane injuries, secretion of lysosomal enzymes or clearance of lysosomal content (Pryor et al., 2006, Rodriguez et al., 1997, Medina et al., 2011, Clark and Griffiths, 2003, Vergarajauregui and Puertollano, 2006). Lack or dysfunction of TRPML1 causes impairment in lysosomal functions, with an abnormal accumulation of heterogeneous material in the lysosomes. The discovery of TRPML1 as an endo-lysosomal Ca^{2+}-permeable channel has been very relevant for the study of lysosomal biology as Ca^{2+} is an universal second messenger required for many intracellular processes such as membrane trafficking, phagocytosis, exocytosis and vesicular fusion (Medina et al., 2011,

Sudhof and Rothman, 2009, Li et al., 2013, Cooper and McNeil, 2015). Early studies on TRPML1 channel activity relied on the measurement of whole-cell and single channel currents using standard voltage-clamp techniques. These measurements showed that TRPML1 acts as a non-selective channel permeable to various cations such as Ca^{2+}, Na^{+} and K^{+} (LaPlante et al., 2002, LaPlante et al., 2004). Although most of these studies were performed *in vitro* and using plasma membrane-mislocalised mutant versions of TRPML1, recent work using patch-clamp on isolated lysosomes confirmed that TRPML1 is an inwardly rectifying current channel, able to transport cations from the lumen of the lysosome, or from the extracellular space, to the cytosol (Xu et al., 2007). Mutagenesis studies on the linker between the 4^{th} and 5^{th} transmembrane tracts and the last part of the 5^{th} transmembrane tract, led to the identification of the amino acidic residues that are critical to modulate channel permeability (Dong et al., 2009).

In addition to Ca^{2+}, TRPML1 is able to mobilize heavy metals such as Fe^{2+} and Zn^{2+} from the lumen of the lysosome (Eichelsdoerfer et al., 2010, Dong et al., 2008). Various studies reported the existence of a zinc regulatory circuit in which the lysosomal Zn^{2+}-importer ZnT4, the Zn^{2+}-responsive transcription factor MTF-1 and TRPML1, which interacts with the putative lysosomal Zn^{2+} extruder TMEM163, contribute to cellular balance of chetable Zn^{2+} in the cell (Kukic et al., 2013, Kukic et al., 2014, Cuajungco et al., 2014). These data suggest that accumulation of Fe^{2+} and Zn^{2+} might be the deleterious process promoting cell death and neurodegeneration in MLIV disease.

As for many other proteins localised in specific cellular compartments, the correct targeting of TRPML1 to the lysosome is probably one of the first mechanisms of regulation and quality control. TRPML1 is a 580aa long six-pass transmembrane channel with both the N-, and C-termini exposed to the cytoplasm (Fig. 1). The two cytosolic tails contain one di-leucine motif each, which dictate targeting of the protein to the LEL

compartment. The N-terminal di-leucine motif (L15L) promotes TRPML1 transport from the trans-Golgi network (TGN) to early endosomes and then to lysosomes, through a mechanism that requires the adaptor protein (AP)-1. The C-terminal di-leucine motif (L577L) instead, signals through AP-2 for the recycling of plasma membrane TRPML1 to the LEL compartment (Vergarajauregui and Puertollano, 2006, Miedel et al., 2006). In addition, the C565CC palmitoylation motif is involved in TRPML1 recycling by facilitating the interaction of the C-terminal endocytic motif with AP-2 (Vergarajauregui and Puertollano, 2006). Differently, the R200P201 site in the intraluminal loop is sensitive to the enzymatic cut mediated by cathepsin B (CTSB) which inactivates the channel generating different forms of the protein (Kiselyov et al., 2005). Likely, inactivation of TRPML1 by cleavage is a regulatory mechanism to limit the duration of the channel activity. The cytosolic portions of TRPML1 are also the most affected by post-translational modifications or binding to regulatory molecules. Protein kinase A (PKA) phosphorylates TRPML1 on S557 and S559 in the C-terminal cytosolic domain, inducing a decrease in the channel conductance. Because of large distance between the target serines and the pore region, it is conceivable that phosphorylation affects the channel activity impairing its multimerization (e.g. with other TRPMLs) or interaction with other proteins (Vergarajauregui et al., 2008b, Venkatachalam et al., 2006, Curcio-Morelli et al., 2010b). Protein kinase D (PKD) is also involved in the phosphorylation of TRPML1 at its C-terminal region. This modification seems to be critical for the trafficking of TRPML1 from the Golgi apparatus to the lysosome, although the target residues have not yet been identified (Marks et al., 2012). In *Drosophila*, TRPML1 is a target of the lysosome associated TORC1 kinase, a master regulator of cell growth and metabolism. TORC1 phosphorylates TRPML1 on two serines, S572 and S576 (Onyenwoke et al., 2015).

Once in the lysosome, the highly acidic environment has been proposed to modulate the activity of TRPML1. Conflicting reports have shown both activating and inhibitory effect of pH on the channel conductance or even postulated a role for TRPML1 in the mobilisation of protons out of the lysosome (Xu et al., 2007, Dong et al., 2009, Raychowdhury et al., 2004, Soyombo et al., 2006, Cantiello et al., 2005, Goldin et al., 2008). A very recent study shed new light on the role played by pH in the regulation of TRPML1 channel (Li et al., 2017). Li and colleagues resolved the crystal structure of the intraluminal loop between the first and the second transmembrane domains of TRPML1. This loop is able to form a tetramer, which acts as an intraluminal pore that participates in ion transport across the membrane. Interestingly, specific aspartate residues in each loop are critical for the channel conductance. Thus, at pH 7.4, the negative charge of these aspartate residues inhibits Ca^{2+} conductance whereas at pH 4.6 the aspartates are protonated, promoting conductance. These evidences, collectively suggest that pH differently regulates the TRPML1 function depending on the cellular compartment. In the lysosomes, the acidic pH favours the release of Ca^{2+} from the lumen through TRPML1 activation, whereas on the plasma membrane, the high pH of the extracellular milieu inhibits Ca^{2+} influx (Li et al., 2017).

Phosphoinositides (PIPs) are important regulators of TRPML1 in membranes. In eukaryotes, PIPs metabolism covers a key role in the maintenance of organelle identity, intracellular trafficking and other aspects of cell physiology. Different PIPs localise in different membrane compartments and this diversification dictates the identity of each organelle (Schink et al., 2016). The importance of PIP metabolism in human disease is supported by the existence of various disorders caused by mutations in different PI-metabolising enzymes. Signalling mediated by PIPs is exerted through well-known protein domains (PH, PX, FYVE, FERM, etc.) or basic amino acid stretches contained in PIPs-

recognizing proteins. Membrane PIPs as well as Ca^{2+} release are both necessary for fusion-fission events in intracellular trafficking. As described above, different members of TRPC, TRPM and TRPV channel families are regulated by PIPs and TRPMLs undergo the same regulation (Rohacs, 2014). The first evidence of such regulation of TRPML1 was provided by the activatory role of PI(3,5)P2, a low abundant endo-lysosomal specific PIP (Dong et al., 2010). In animal cells, PI(3,5)P2 is generated by the phosphorylation of PI3P by the PIKfyve kinase, whereas Sac3/FIG4 and MTMR lipid phosphatases de-phosphorylate PI(3,5)P2 to PI3P and PI5P, respectively (Tronchere et al., 2004, Gary et al., 2002). As expected, conversion of PI(3,5)P2 to PI5P, by over-expressing the PI3-phosphatase MTM1, decreases TRPML1 channel activity (Dong et al., 2010). As already mentioned, TRPML1 can also localise to the plasma membrane in which PI(4,5)P2, is abundant. Analysis performed on TRPML1 exposed to PI(4,5)P2 showed an inhibitory effect on channel gating (Zhang et al., 2012). PI(3,4)P2 and PI(3,4,5)P3 also inhibit TRPML1 gating, although with lower efficacy. Both PI(3,5)P2 and PI(4,5)P2 bind to a very well conserved aa stretch in the N-terminal region of TRPML1, with R61 and K62 selectively required for PI(3,5)P2 activation and R41/R42/R43 specifically required for PI(4,5)P2 inhibition (Zhang et al., 2012). The importance of PIPs modulation for TRPML1 activation has been confirmed in a recent work describing the role of the PI(4,5)P2 phosphatase OCRL on lysosomal function. Upon nutrient starvation, the fusion of autophagosomes with lysosomes stimulates the translocation of OCRL from the endosomal compartment to the lysosomes, where it interacts with TRPML1. On the lysosome, OCRL de-phosphorylates PI(4,5)P2 to PI4P thus sustaining the activation of TRPML1 and the progression of the autophagic flux. Interestingly, in Lowe syndrome cells, in which OCRL is mutated, TRPML1 activation is delayed, and an accumulation of autophagosomal structures is observed. Stimulation by specific activators (Table 1) or

over-expression of TRPML1 in these cells can ameliorate the lysosomal phenotype, confirming that OCRL is important for TRPML1 channel activity (De Leo et al., 2016).

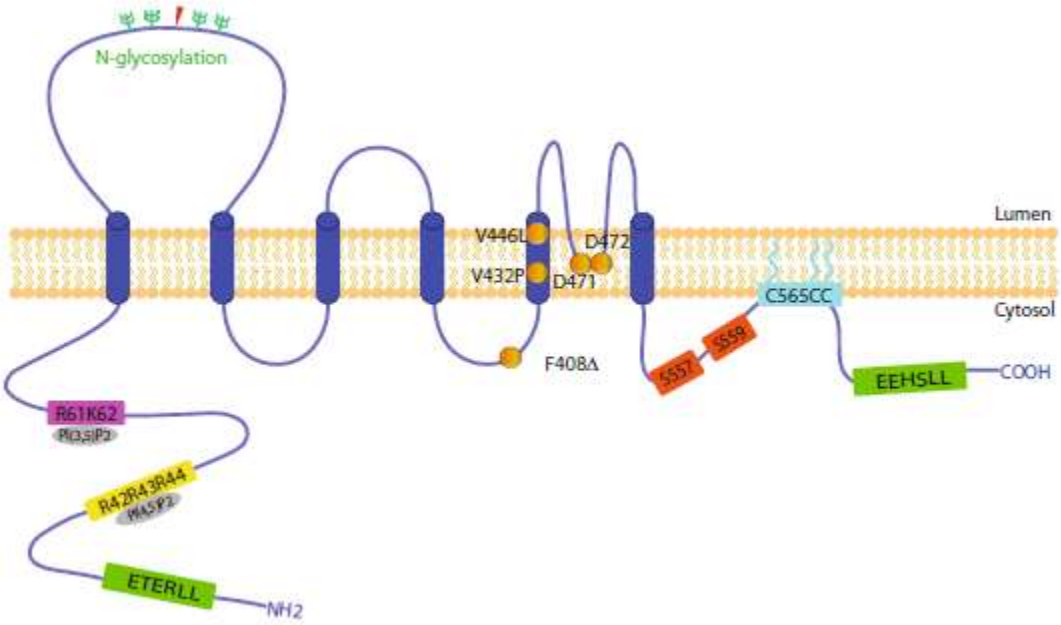

Figure 1: TRPML1 channel structure consists of six transmembrane (6TM) domains with the amino-terminal (NH2) and carboxyl-terminal (COOH) tails facing the cytosol. In this cartoon the major channel characteristics are highlighted: the large loop between the 1st and 2nd TM domains, the two di-leucine motifs necessaries for channel localisation (in green), the phosphoinositide binding sites (in purple and yellow), the two serines phosphorylated by PKA at the C-terminus (in red) the key aa residues in the pore region (orange dots), whose mutation leads to gain or loss of function mutant. Reproduced with permission from: Wuyang Wang et al. (Wang et al., 2014)

TRPML1 biological function

Lysosomal biogenesis, exocytosis and positioning

The studies performed on cells and animal models lacking TRPML1 underlined gross defects in the LEL compartment. Null mutations in cup-5, the ortholog of MCOLN1 in *C. elegans*, cause impairment in the maturation of lysosomes from late endosomes (Fares and Greenwald, 2001, Treusch et al., 2004, Campbell and Fares, 2010). Similar accumulation of immature LEL has also been observed in the *Drosophila* trpml null-model (trpml1) and in neuronal cells isolated from TRPML1 KO mice (Venkatachalam et al., 2008, Micsenyi et al., 2009). The possible explanation for these alterations could lie into vesicular fusion/fission impairment due to abolished TRPML1 channel activity and reduced lysosomal Ca^{2+} release (LaPlante et al., 2002, LaPlante et al., 2004, Pryor et al., 2000, Miller et al., 2015). The absence of TRPML1 has been correlated to multiple trafficking defects such as in the retrograde transport of lactosyl-ceramide to the Golgi compartment, in the transport and degradation of different substrates into the lysosomes, and in the delivery of lysosomes to the plasma membrane via exocytosis (Chen et al., 1998, Pryor et al., 2006, Thompson et al., 2007, Miedel et al., 2008). The latter is still a very intriguing cellular process, as the protein components and the regulatory mechanisms modulating it still need to be fully characterised, in particular in cells not derived from the hematopoietic lineage. Lysosomal exocytosis is a two-step process that initially requires the docking of lysosomes to the close proximity of the PM and then the elevation of intracellular Ca^{2+} levels to favour membrane fusion. The lysosomal membrane protein synaptotagmin VII (SytVII) plays a crucial role in the binding of Ca^{2+} and subsequent tethering of lysosomal and plasma membrane SNAREs preceding membrane fusion (Martinez et al., 2000, Reddy et al., 2001). Upon release of lysosomal content, lipids and lysosomal membrane proteins, including LAMP1 and TRPML1, fuse to the plasma membrane and are recycled-back through endocytosis (LaPlante et al., 2002).

The first evidence suggesting a role for TRPML1 in lysosomal exocytosis came from studies in human MLIV fibroblasts (LaPlante et al., 2006). In this regard and unexpectedly, the discovery of the transcription factor EB (TFEB), a master gene for lysosomal biogenesis and autophagy, has contributed to confirm the positive role of TRPML1 channel in lysosomal exocytosis. Indeed, TFEB over-expression is able to induce cellular clearance of lysosomal storage in various *in vitro* and *in vivo* models of LSDs (Medina et al., 2011). The silencing of TRPML1, a direct transcriptional target of TFEB, inhibits lysosomal exocytosis while the over-expression of TFEB in MLIV fibroblasts is not able to induce lysosomal exocytosis (Medina et al., 2011, Palmieri et al., 2011). Most importantly, this discovery raised a novel and promising therapeutic approach to treat LSDs by activating lysosomal exocytosis to clear pathological storage (Medina et al., 2011, LaPlante et al., 2006). Subsequently, many other research groups have obtained similar results and also extended this approach for the clearance of toxic cargoes in more common neurodegenerative disorders such as Alzheimer, Parkinson, and Huntington disease (Napolitano and Ballabio, 2016, Settembre et al., 2013).

TRPML1 has also been involved in phagocytosis and clearance of exogenous particles in macrophage cells (Dayam et al., 2015, Samie et al., 2013). Upon exposure of cell to external particles, TRPML1 is stimulated by endogenous PI(3,5)P2, leading to exocytosis of lysosomes near the site of phagocytosis (Samie et al., 2013). Once the particles are internalized, TRPML1 activity may promote the fusion of the phagosome with the lysosome to stimulate particle degradation (Dayam et al., 2015).

More recently, TRPML1 has been implicated in the centripetal movement of lysosomes upon nutrient starvation (Li et al., 2016). During autophagy (see next paragraph), the lysosomes are recruited to the perinuclear area where they become proximal to autophagosomes to which they fuse into autolysosomes (Korolchuk et al., 2011). In basal

endocytic conditions, trafficking of lysosomes towards the centre of the cell is mediated by a Rab7/RILP/dynein mechanism. Conversely, upon starvation, a PI(3,5)P2/TRPML1-mediated Ca^{2+} release activates the Ca^{2+}-binding protein ALG-2, which binds to TRPML1 and in turn recruits the dynein-dynactin complex for retrograde transport of lysosomes (Li et al., 2016, Vergarajauregui et al., 2009). Thus, TRPML1 may control different lysosomal functions depending on the position of the lysosome and the specific interaction with partner proteins localised in different regions of the cell. For instance, TRPML1 activation in a lysosomal pool close to the PM might promote lysosomal exocytosis, whereas perinuclear TRPML1-lysosomes might trigger autophagosome-lysosome fusion.

Autophagy

Macroautophagy, hereafter referred to as autophagy, is a multi-step intracellular catabolic process which mediates the sequestration of damaged organelles and macromolecules into specialised vesicles, named autophagosomes. Mature autophagosomes are finally delivered to lysosomes for fusion and degradation of their content (Yorimitsu and Klionsky, 2005). Autophagy exists in basal conditions and is further activated by cellular stress conditions, such as nutrient deprivation. The main purpose of this process is to clear the cells from toxic material and produce nutrients from digested macromolecules. In both human fibroblasts derived from MLIV patients and heterologous cells depleted of TRPML1, alterations in the autophagic pathway with the elevation of lipidated LC3 protein and accumulation of the autophagic substrate SQSTM1/P62 have been found (Vergarajauregui et al., 2008a, Jennings et al., 2006). Immunofluorescence analysis has shown marked increase in the co-localisation of LC3-puncta with SQSTM1/P62 and delayed fusion of autophagosomes with LEL during nutrient deprivation (Vergarajauregui et al., 2008a). Similar findings were also described in neuronal cells

derived from a MLIV mouse model (Micsenyi et al., 2009, Venugopal et al., 2007, Curcio-Morelli et al., 2010a).

Studies performed on *Drosophila* trpml1 mutants described similar autophagy defects, with increased number of autophagosome structures and reduced degradation of cargo in autolysosomes (Venkatachalam et al., 2008). In addition, the defect in TRPML1-mediated Ca^{2+} release from late endosomes also impairs the fusion of amphisomes (single membrane structures derived from the fusion of autophagosomes and late endosomes) with lysosomes (Wong et al., 2012).

Different signalling pathways regulate the execution of the autophagic process, and among them, the mTORC1-regulated pathway is probably the most important. mTORC1 senses amino acid content on the lysosomal surface. In normal nutrient rich conditions mTORC1 is active and inhibits autophagy. In *Drosophila* trpml1 mutants, defective vesicular fusion results in lower catabolic activity and reduced amino acid levels. Such condition leads to an inhibition of TORC1 mimicking starvation and causing aberrant accumulation of autophagic substrates and cell death (Wong et al., 2012).

A role of TRPML1 in autophagy has also been reported in cup-5 null mutant in *C. elegans*. In addition to the defects in sorting of material from endosomes to lysosomes with its aberrant accumulation in large vacuoles, loss-of-function cup-5 mutants results in impairment of degradation of autophagy substrates (Fares and Greenwald, 2001, Treusch et al., 2004, Sun et al., 2011). Accumulation of T12G3.1 and LGG-1 (SQSTM1/P62 and LC3 homologues) in enlarged LEL structures indicates that mutations in cup-5 do not affect fusion between lysosomes and autophagosomes but interferes with degradation in autolysosomes. It has been previously shown that cup-5 null mutation is responsible for maternal-lethal effect (Hersh et al., 2002). In such embryos, the increase in autophagy is

likely due to the onset of a starvation phenotype caused by a decrease in nutrient and biosynthetic compound availability (Schaheen et al., 2006). Suppression of the autophagic pathway partially relieves death in such mutant, suggesting that impaired lysosomal function strongly contributes to lethality (Sun et al., 2011, Schaheen et al., 2006).

More recently, studies performed in mammals have given important hints to the dissection of the molecular mechanisms behind the regulation of autophagy by TRPML1. Indeed, TRPML1 is a crucial factor in the activation of TFEB (Settembre et al., 2011, Sardiello et al., 2009). In nutrient rich condition TFEB is inactivated by mTORC1 mediated phosphorylation on two key serine residues (S142 and S211) and localises in the cytoplasm. Conversely, in conditions of nutrient starvation, mTORC1 is inhibited and TFEB is de-phosphorylated shuttling into the nucleus to activate the transcription of lysosomal and autophagy genes (Settembre et al., 2012). Starvation triggers the release of lysosomal Ca^{2+} through the activation of TRPML1 (Medina et al., 2015, Wang et al., 2015), Ca^{2+} activates the Ca^{2+}-CaM-dependent Calcineurin (CaN) phosphatase, which in turn binds and de-phosphorylates S142 and S211 on TFEB (Medina et al., 2015). De-phosphorylated TFEB enters into the nucleus to drive a transcriptional program to activate and sustain autophagy. Interestingly, TRPML1 is a transcriptional target of TFEB, therefore establishing a positive feedback loop which boosts TRPML1-TFEB response (Settembre et al., 2011, Medina et al., 2015, Wang et al., 2015). Depletion of TRPML1 or CaN impairs TFEB activation, demonstrating that the three proteins cooperate in a lysosome-to-nucleus signalling pathway to coordinate starvation-mediated autophagy (Medina et al., 2015).

Of note, the over-expression of TRPML1 results in a significant increase of the autophagic flux, whereas its silencing reduces PI3P-positive vesicles and WIPI2 positive spots upon

starvation, raising the possibility that TRPML1 might also have some role in the early steps of autophagy (Medina et al., 2015). Intriguingly, nutrient starvation causes a decrease in levels of PI(3,5)P2, the only known endogenous agonist of the TRPML1 channel, raising the unresolved question of how nutrient deprivation controls TRPML1 channel activity (Zhang et al., 2012, Medina et al., 2015, Spooner et al., 2013, Zolov et al., 2012). Since TRPML1 channel activity is sensitive to pH, a potential explanation may be related to changes in the cytosolic pH during starvation (Li et al., 2016).

Recently, a similar TRPML1/TFEB pathway has been described upon reactive oxygen species (ROS) production. In this case, TRPML1 acts as a sensor for ROS levels in the cell and becomes activated or sensitised upon high ROS condition, such as mitochondrial damage. TRPML1-mediated Ca^{2+} release from the lysosome stimulates CaN and activates TFEB transcription to promote autophagy and lysosomal biogenesis (Zhang et al., 2016). In a context in which TRPML1 function is abolished, such as MLIV, lysosomal Fe^{2+} accumulation could contribute to ROS production, which in turn provokes impairment of mitochondrial membrane potential and accumulation of damaged mitochondria which cannot be recycled because of the block of autophagy (Zhang et al., 2016, Coblentz et al., 2014).

Despite the emerging interest in the role of TRPML1 on autophagy, there are still many open questions about the precise role of this channel and of lysosomal calcium in this important catabolic process. Indeed, most of the studies in mammalian cells are limited to human fibroblasts or heterologous cell lines that have been depleted of TRPML1 by transient siRNA-silencing. Another important aspect that has not been addressed yet is whether the mTOR pathway alteration observed on invertebrate models such as *C. elegans* or *Drosophila* can be observed in mammalian cells. The use of new approaches such as CRISPR/Cas9 technology and human fibroblast reprogramming (such as induced

pluripotent stem cell, iPSCs) might contribute to the generation of better models to study TRPML1 function in specific cell types that are relevant in MLIV disease. Finally, a few lysosomal Ca^{2+} effectors involved in specific TRPML1 functions have been identified. Some examples are SytVII, CaN, and ALG-2 therefore it is likely that other TRPML1 effectors and interactors, signalling cascades and molecular events modulating TRPML1 will be identified in the next future.

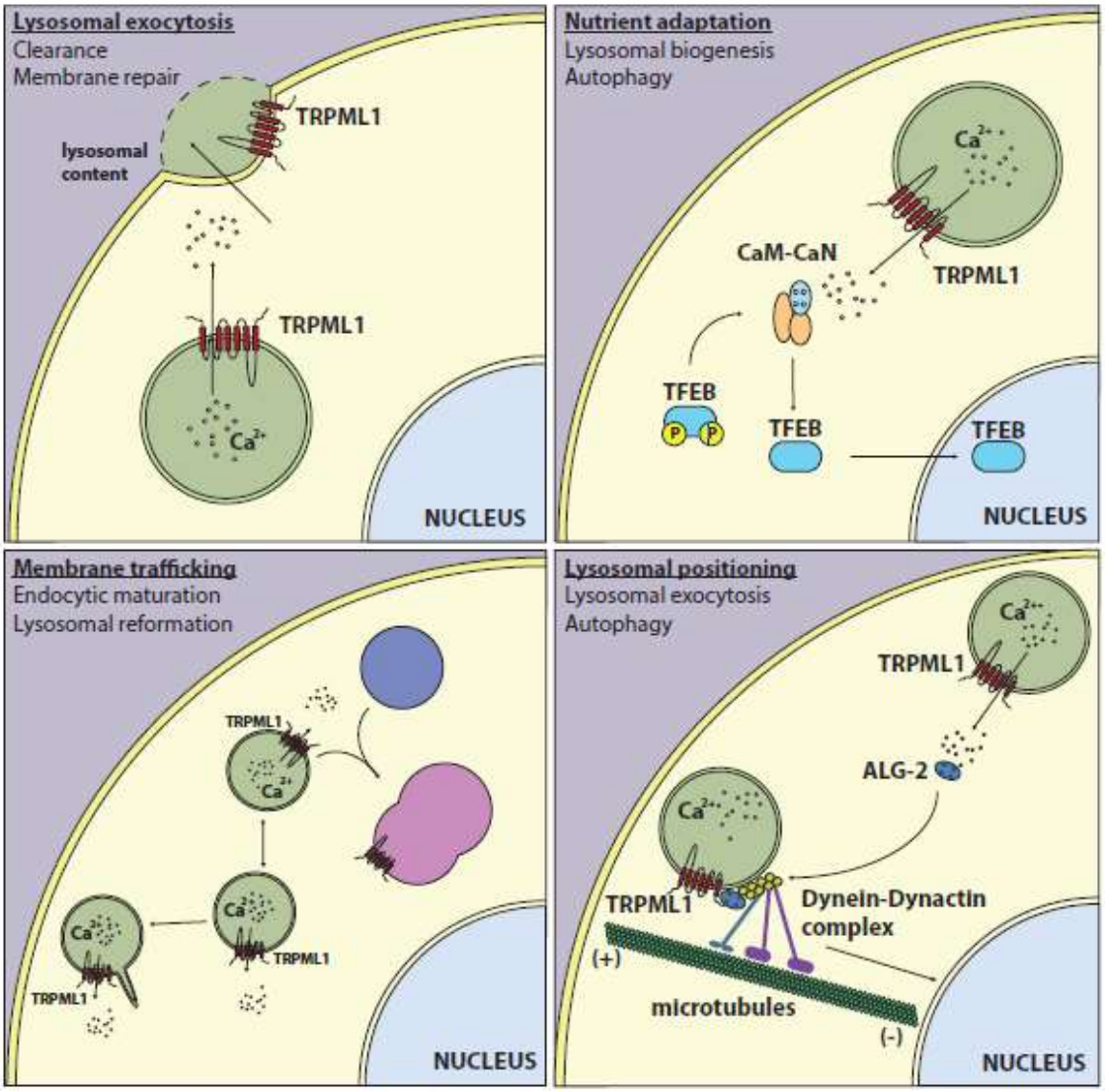

Figure 2: Scheme of the major TRPML1 functions. Lysosomal Ca2+ release by TRPML1 is important for the execution of different intracellular pathways. TRPML1 has been involved in the regulation of Ca2+-dependent lysosomal exocytosis (top left). TRPML1 activity has been involved in vesicular fusion events and lysosomal re-formation (bottom left). Upon different environmental cues, such as nutrient deprivation, TRPML1 activation induces TFEB-mediated transcriptional program (top right). TRPML1 triggers in-ward lysosomal movement by a mechanism that requires ALG-2 and the Dynein-Dynactin complex (bottom right). Reproduced with permission from: Di Paola et al. (Di Paola et al., 2017)

Lysosomal calcium release trough TRPML1 regulates autophagy through calcineurin and TFEB

Lysosomes are membrane-bound organelles present in all cell types. Their role in degradation and recycling processes has been extensively characterized (Luzio et al., 2007, Saftig and Klumperman, 2009, de Duve, 2005). The acidic pH of the lysosomal lumen with the presence of a broad variety of hydrolases able to degrade an ample spectrum of substrates, makes these organelles extraordinary machineries for the recycling of cellular waste. Extracellular substrates reach the lysosome mainly via the endocytic and phagocytic pathways, while intracellular substrates are the delivered to the lysosome by the autophagic pathway via the fusion of autophagosomes with lysosomes (Luzio et al., 2007, Saftig and Klumperman, 2009). Thus, lysosomes are the "terminal end" of most cellular catabolic pathways. The role of the lysosomes in degradation and recycling processes has always been considered as a cellular "housekeeping" function and little attention has been paid to the regulation of these processes and to the influence of environmental cues, such as starvation and physical exercise.

The discovery that the Transcription Factor EB (TFEB) is a master regulator of lysosomal and autophagic function and of energy metabolism (de Duve, 2005, Saftig and Klumperman, 2009, Luzio et al., 2007) suggested that environmental cues may control lysosomal function via the induction of a broad transcriptional program. TFEB activity is regulated by phosphorylation (He and Klionsky, 2009, Luzio et al., 2009, de Duve, 2005, Saftig and Klumperman, 2009, Luzio et al., 2007), which keeps TFEB inactive in the cytoplasm, while de-phosphorylated TFEB travels to the nucleus to activate transcriptional target genes. TFEB phosphorylation is mediated by mTORC1, a major kinase complex that positively regulates cell growth and negatively regulates autophagy.

Interestingly, it is known mTORC1 exerts its activity on the lysosomal surface and is positively regulated by lysosomal nutrients (Sardiello et al., 2009, Settembre et al., 2011). The regulation of TFEB by lysosomal mTORC1 and the shuttling of TFEB to the nucleus revealed a lysosome-to-nucleus signalling mechanism (de Duve, 2005). Thus, these studies identify the lysosome as a signalling hub controlling cellular homeostasis via both post-translational and transcriptional mechanisms (He and Klionsky, 2009, de Duve, 2005, Saftig and Klumperman, 2009, Luzio et al., 2007).

An important aspect emphasised in this chapter is the classification of the lysosome, not only as the terminal end of all the material that needs to be degraded, but as calcium storage organelle that actively participate to calcium signalling processes. Calcium ions are important second messengers that are involved in several biological processes. Rapid and highly localised Ca^{2+} spikes regulate membrane fusion (Berridge et al., 2003), cellular motility and could regulate enzyme activity, permeability of ion channels (Ali et al., 2016), activity of ion pumps, and components of the cytoskeleton. To execute their function Ca^{2+} ions should diffuse through the cytoplasm and since this diffusion is not energetically favoured in a cytoplasm crowded of organelles there are many calcium binding proteins that amplify the calcium wave signal (Clapham, 2007). Furthermore, endoplasmic reticulum and mitochondria, which represent the major calcium storage in the cytoplasm, are widely spread in the cytoplasm providing a calcium source in the whole cell. This underlies how calcium signalling requires proximity and rapidity, a valid example is given by the sarcoplasmic reticulum in the skeletal muscles providing Ca^{2+} to the adjacent muscle proteins in an efficient and rapid manner (Clapham, 2007). Equally, lysosome could store Ca^{2+} and participate to calcium signalling processes. Several calcium channels reside on the lysosomal membrane. Recent studies have investigated the role of these lysosomal calcium channels in fundamental cellular processes and their involvement in

disease mechanisms (Morgan et al., 2011). One of the major channels on the lysosome is represented by MCOLN1, a non-selective cation channel which releases Ca^{2+} from the lysosomal lumen into the cytoplasm. In this chapter the mechanism by which the release of calcium via MCOLN1, leads to calcium increase in the proximity of the lysosomes triggering autophagy via calcineurin-mediated induction of TFEB will be discussed.

Starvation induces lysosomal Ca^{2+}via TRPML1

Since starvation-induced TFEB nuclear translocation requires the activity of calcineurin and the subcellular localisation of TFEB is calcium mediated, the effect of starvation on cytosolic $Ca^{2+}$was evaluated in collaboration with Dr. De Stefani and Dr. Rizzuto (affiliation). The overall levels of cytosolic Ca^{2+}were measured by an aquaporin-based probe localising in the bulk cytoplasm which remained unaltered during starvation (Fig. 3 a). Moreover, while a fast calcium chelator, like BAPTA-AM, was able to reduce starvation-mediated TFEB nuclear translocation, a slower calcium chelator, like EGTA-AM (Morgan et al., 2013), did not (Fig. 3 b). To address this point the release of calcium from the endoplasmic reticulum (ER) was quantified by measuring cytosolic calcium transiently evoked by the IP3-mobilising hormone histamine in fed and starved cells (Fig. 3 a,c). To specifically measure the lysosomal calcium release a plasmid developed in Dr. Xu's laboratory was used (Samie et al., 2013). This plasmid called ML1-GCaMP3 allows the expression of the calcium channel TRPML1 fused with GFP protein, which thanks to a calmodulin binding domain, is sensitive to calcium ions (Samie et al., 2013). The GFP fluorescence is quenched in basal condition but once Ca^{2+} is released by TRPML1 the calmodulin domain allows structural changes in the GFP which becomes able to emit green fluorescence. HeLa cells transiently transfected with this construct clearly showed that starvation is able to release calcium from TRPML1 (Fig. 3 d). The same was observed in HEK293 cells stably overexpressing ML1-GCaMP3 (Fig. 3 e). The increase in Ca^{2+} levels

induced by starvation detected by ML1-GCaMP3 were not affected by the removal of extracellular Ca^{2+} (ruling out the contribution of plasma membrane calcium channels), but was blunted by treatment with the lysosomotropic agent GPN (Fig. 3 f).

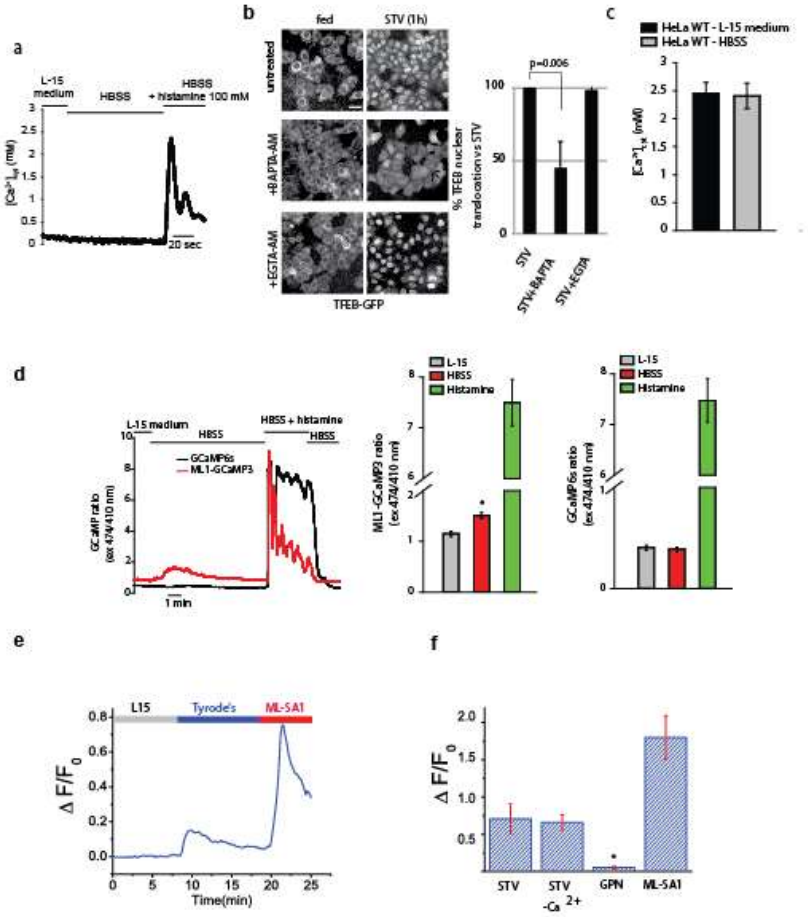

Figure 3: Starvation induces lysosomal Ca^{2+} release through MCOLN1. (a) Starvation does not induce bulk cytosolic Ca^{2+} elevation in HeLa cells transfected with the Ca^{2+}-sensitive probe aequorin. Bulk cytosolic [Ca^{2+}] was monitored during perfusion with complete L-15 medium, HBSS and HBSS supplemented with 100µM histamine as indicated. (b) Stable HeLa TFEB–GFP cells were left untreated or pre-treated for 30min with the Ca^{2+} chelators BAPTA-AM or EGTA-AM (5µM each). After washing, cells were left untreated or starved for 1h. After treatment, cells were fixed and a high-content imaging analysis was performed. The plot shows the percentage of TFEB nuclear translocation in BAPTA-treated cells compared with untreated and EGTA treated. (c) Average and s.d. of cytoplasmic [Ca^{2+}] evoked by maximal histamine stimulation in wild-type HeLa cells. Agonist stimulation was carried out in complete L15 medium or after a three-minute starvation with HBSS. (d) Representative traces of the cytosolic GCaMP6s and the perilysosomal ML1-GCaMP3 calcium probes. HeLa cells were transfected with the indicated probe and ratiometric imaging (474 and 410nm excitation) was performed. Cells were continuously perfused with the indicated solutions. The bottom left plot represents the average perilysosomal calcium peak values induced by perfusion of the indicated buffer, as recorded by the GCaMP3–ML1 probe. The bottom right plot represents the average cytosolic calcium peak values induced by perfusion of the indicated buffer, as recorded by the GCaMP6s probe. (e) Ca^{2+} release (measured with 1F/F0 fluorescence intensity) was detected right after the L-15 medium (containing 2mM [Ca^{2+}], amino acids and 10% FBS) was switched to Tyrode's solution (2mM [Ca^{2+}]) in HEK293 cells stably expressing GCaMP3–ML1. The agonist of MCOLN1 ML-SA1 (10µM) was applied to induce MCOLN1-mediated Ca^{2+} release. (f) Similarly, the lysosomotropic drug GPN blunted starvation-mediated calcium release detected by GCaMP3– ML1.

Moreover, neither the silencing of the lysosomal two-pore channel TPCN2 nor the overexpression of a critical regulator of mitochondrial Ca2+ uptake, MICU1 altered TFEB subcellular localisation (Fig. 4 a, b). These data clearly demonstrate that during starvation the lysosomes, via TRPML1, release calcium generating a local calcium spike responsible of PPP3CB activation. Successively, the involvement of TRPML1 in the modulation of TFEB nuclear translocation was assessed (Dong et al., 2010, Shen et al., 2012, Samie et al., 2013, Medina et al., 2011).

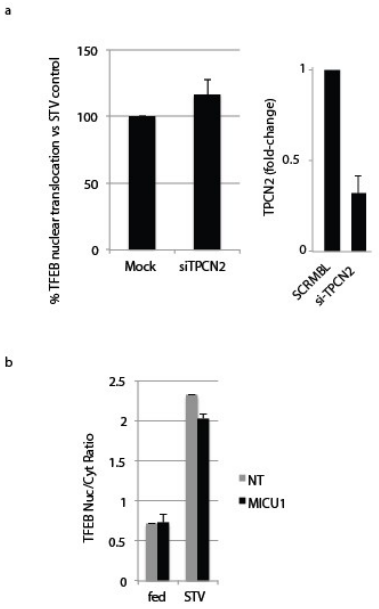

Figure 4: TPCN2 and MICU1 calcium channels do not regulate TFEB localisation. (a) Depletion of the lysosomal two-pore channel TPCN2 does not affect TFEB nuclear translocation during starvation (1 hour) (left graph). Quantification of the efficiency of TPCN2 gene silencing by qPCR analysis (right graph). (b) Overexpression of the essential mitochondrial Ca^{2+} regulator MICU1 does not impact on the subcellular localisation of TFEB in fed and starvation conditions (1hr), as compared to untransfected cells. High content imaging analysis was used to quantify TFEB localisation using HeLa-TFEB-GFP cells.

A significant reduction in nuclear localisation during starvation of TFEB both overexpressed and endogenous was observed by using a cell line stably transfected with a short hairpin RNA (shRNA) targeting TRPML1. (Fig. 5 a). This endorsed consistently that this process requires lysosomal calcium release. Similar results were obtained by nucleus/cytoplasm fractionation

(Fig. 5 b). Consistently, depletion of TRPML1 reduced the downshift of endogenous TFEB molecular weight during starvation, suggesting a defective de-phosphorylation (Fig. 5 d). Mutations in the TRPML1 gene cause Mucolipidosis type 4 (MLIV), a lysosomal storage disease (Bassi et al., 2000, Bargal et al., 2000). Starvation-induced nuclear translocation of TFEB is inhibited in fibroblasts from MLIV patients (Fig. 5 c).

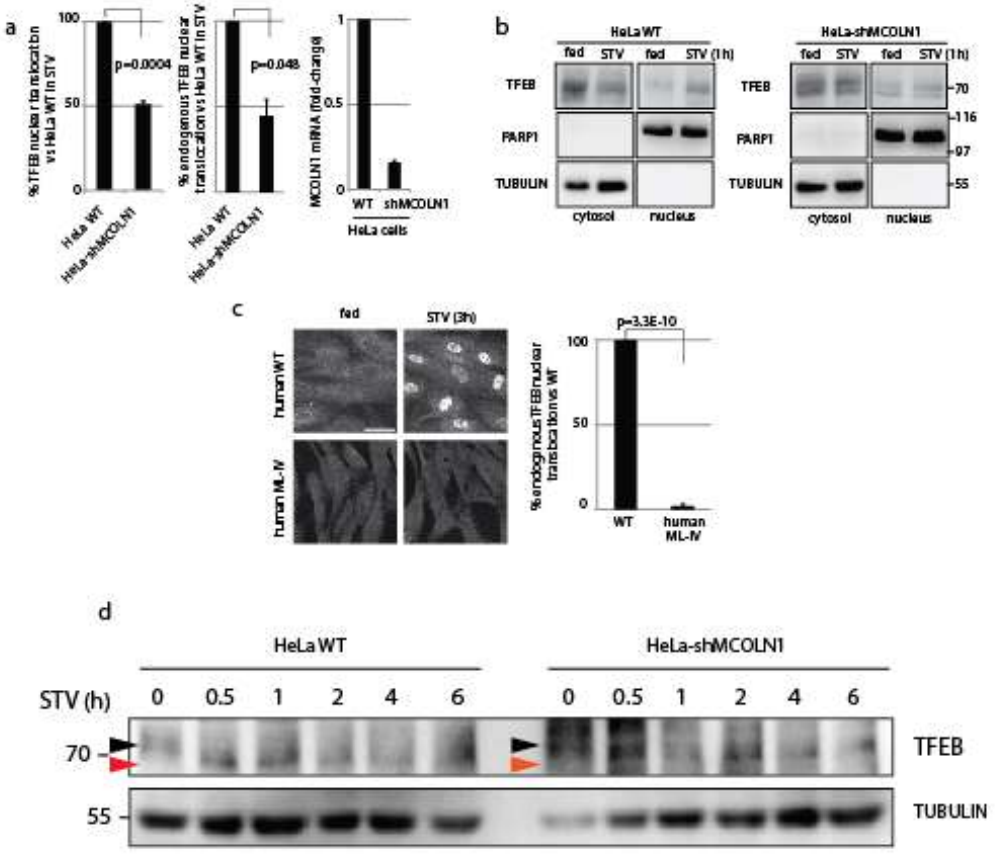

Figure 5: MCOLN1-mediated calcium release induces TFEB nuclear translocation. (a, b) Silencing of MCOLN1 reduces starvation-mediated TFEB nuclear translocation. (a) HeLa cells or a HeLa cell line stably-transfected with a MCOLN1 shRNA was left untreated or transiently transfected with a TFEB–GFP plasmid. The left plot shows the percentage of TFEB–GFP nuclear translocation in starved (3h) HeLa-MCOLN1 shRNA cells compared with starved HeLa cells. Similarly, the middle plot shows the results on endogenous TFEB nuclear translocation. The right plot shows the efficiency of MCOLN1 silencing. (b) Silencing of MCOLN1 reduces starvation-mediated TFEB nuclear translocation. HeLa and HeLa-MCOLN1 shRNA cells were transfected with a TFEB–3×FLAG construct. Following starvation, of 100µg nuclear and 50µg of cytosolic extracts were prepared and probed using anti-Flag antibody. (c) Endogenous TFEB nuclear translocation analysis of human wild-type and mucolipidosis IV fibroblasts in fed conditions and after a 3h starvation of serum and amino acids. The graph shows the percentage of TFEB nuclear translocation in human MLIV cells when compared with WT cells in starvation conditions. (d) Depletion of the lysosomal calcium channel MCOLN1 reduces starvation mediated TFEB nuclear translocation. WT HeLa and HeLa-shMCOLN1 cells were starved at different time-points. Following starvation, 50µg of protein extracts were prepared and probed for endogenous TFEB using anti-TFEB antibodies. TFEB mobility downshift after starvation is reduced in MCOLN1 depleted cells during starvation (black arrows point-out the phosphorylated forms, while red arrows show the downshift corresponding to de-phosphorylated TFEB forms).

On the other hand, overexpression of TRPML1 and of gain of function mutants (GOFs) in HeLa TFEB-GFP promotes TFEB nuclear translocation (Fig. 6 a) in a calcineurin dependent fashion (Fig. 6 b). Furthermore, similar results were obtained using a TRPML1 specific agonist, SF-51 (Shen et al., 2012) (Fig. 6 c, d).

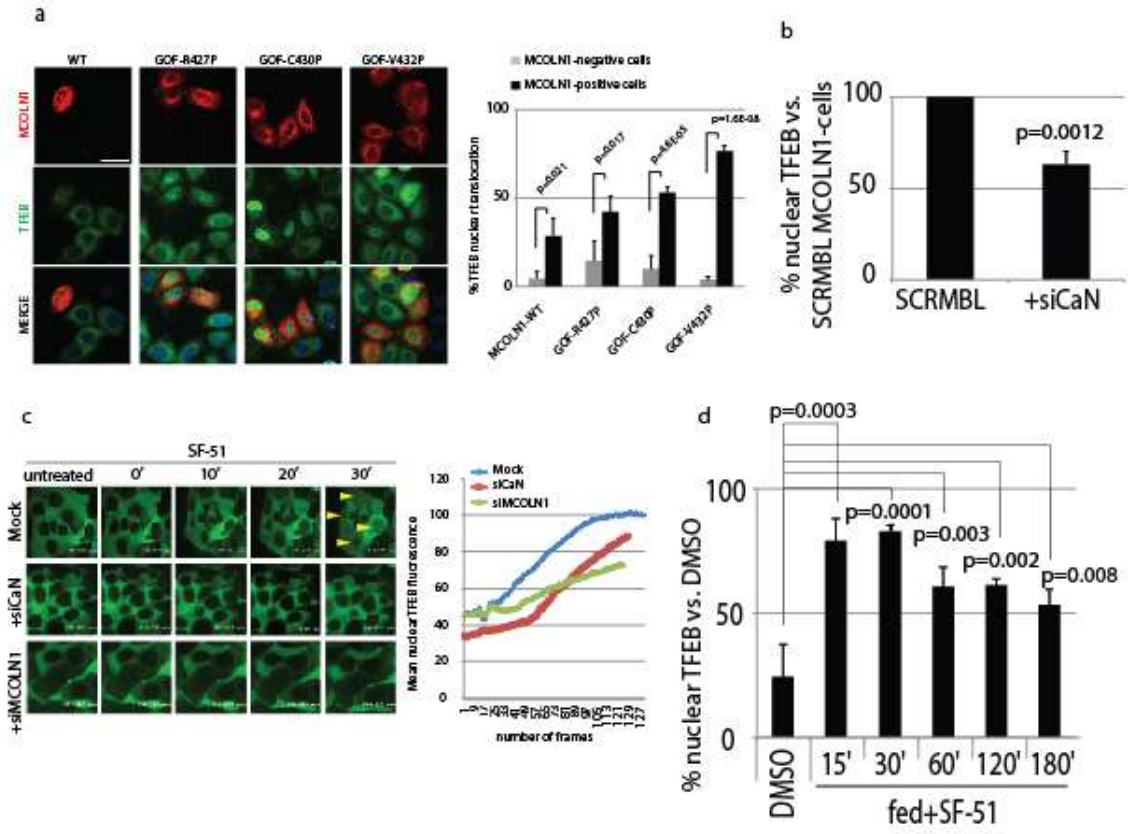

Figure 6: MCOLN1-mediated calcium release induces TFEB nuclear translocation. (a) Overexpression of MCOLN1 induces TFEB nuclear translocation. HeLa cells stably expressing TFEB–GFP were transfected with plasmids carrying wild-type or constitutively active mutant forms of FLAG-tagged MCOLN1. TFEB subcellular localisation was assessed in FLAG-positive (red-stained cells) and negative cell populations. The graph shows the percentage of TFEB nuclear translocation in the different GOF mutation carrying cells, compared with non-transfected cells. (b) MCOLN1-mediated induction of TFEB nuclear localisation is calcineurin-dependent. HeLa TFEB-GFP cells were transfected with FLAG-tagged MCOLN1 gene in combination with siRNAs against PPP3CB and PPP3R1 (siCaN) or scramble siRNA oligonucleotides (SCRMBL). TFEB subcellular localisation was assessed in FLAG-positive population using HC imaging. The graph shows the percentage of nuclear TFEB in siCaN knock-down cells compared with control SCRMBL-transfected cells. (c) Frames of time-lapse experiments in HeLa TFEB–GFP cells treated with the MCOLN1 agonist SF-51 (200µM) after the transfection of PPP3CB+PPP3R1 (CaN) siRNA, MCOLN1 or scramble siRNAs. Yellow arrowheads indicate TFEB nuclear localization. The plot shows the kinetics of TFEB nuclear localisation during the time of recording. (d) The MCOLN1 agonist SF-51 induces TFEB nuclear translocation. The effect of SF-51 treatment on HeLa TFEB-GFP cells at the time points indicated in the plot

was quantified using an HC assay. The graph shows the percentage of treated cells with nuclear TFEB compared to DMSO control cells.

Since TRPML1 and the release of lysosomal calcium are required for calcineurin activation, whether also the silencing of TRPML1 generate the same autophagy impairment was investigated. Consistently with previous data, the silencing of TRPML1 significantly reduced the number of PI(3)P-positive vesicles as measured by the GFP–2×FYVE reporter (Fig. 7 a). Conversely, overexpression of TRPML1 significantly increased the level of the autophagosome marker LC3, and co-treatment with bafilomycin A1 led to a further increase, indicating an induction of autophagy, rather than an impairment of autophagosome degradation (Fig. 7 b, c). Thus, lysosomal calcium signalling via MCOLN1 controls autophagy through calcineurin-mediated activation of TFEB. Intriguingly, TRPML1 is a direct transcription target of TFEB (Medina et al., 2011, Palmieri et al., 2011). This suggests the existence of a positive feedback loop by which TFEB regulates the expression of TRPML1, which in turn promotes TFEB activity via Ca^{2+}-mediated activation of calcineurin.

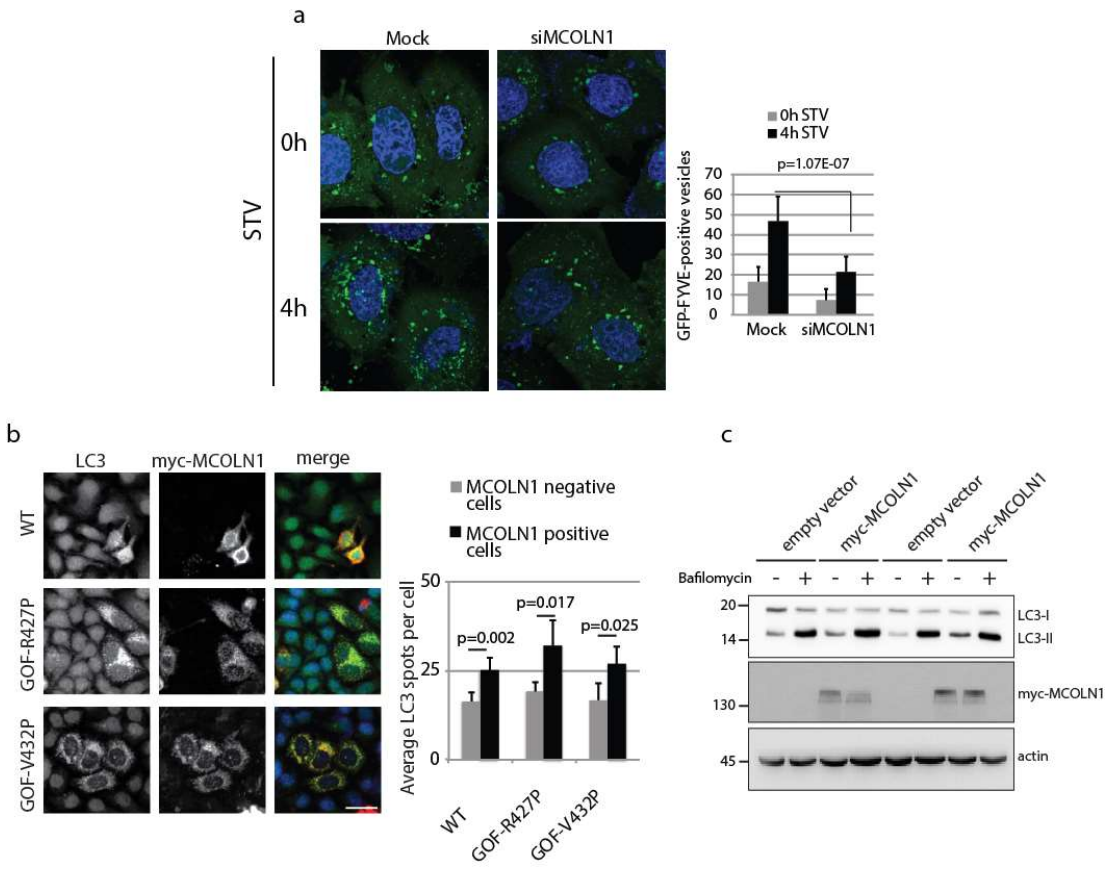

Figure 7: MCOLN1 regulates the lysosomal/autophagic pathway. (a) Representative images and analysis of the overexpression of the autophagy related PI(3)P reporter GFP–2×FYVE during starvation in wildtype (Mock) HeLa cells, and in cells silenced for MCOLN1. GFP–2×FYVEpositive vesicles (in green) were counted using ImageJ software. (b) MCOLN1 overexpression leads to a significant increase in LC3 levels. HeLa cells were transfected with Myc-tagged MCOLN1 or gain-of-function mutants R427P and V432P respectively. Immunofluorescence was performed using antiLC3 antibodies. The number of LC3 spots per cell was quantified using high-content imaging analysis. (c) Fifty micrograms of protein extracts from HeLa cells treated with bafilomycin (BAFA) and overexpressing an empty vector of a Myc–MCOLN1 plasmid for 24h was immunoblotted against LC3.

Autophagy is an evolutionary conserved mechanism by which cells degrade and recycle self-components in order to maintain cellular homeostasis (Mizushima et al., 2008). This degradative lysosomal pathway is tightly regulated and the nutritional stress is considered the major stimulus triggering it (Lum et al., 2005, Onodera and Ohsumi, 2005). Due to its relevance, regulation of autophagy is thought to be a biphasic process, with a fast induction which relies on post-translational and protein-protein interaction events, and a sustained response which is mediated by transcriptional mechanisms (Fullgrabe et al., 2014). In this chapter, the mechanism by which a calcium release via TRPML1 from

lysosome could regulate autophagy by activating a TFEB-mediated transcriptional program has been described. Although it has been well-established that autophagy is negatively regulated by the mTOR kinase (Yang and Klionsky, 2010) the pathway identified in the present study is mediated by the Ca^{2+}-dependent phosphatase calcineurin and seems to operate independently from mTOR. The results discussed in this chapter allow to delineate a working model of how starvation and exercise regulate TFEB via both the mTOR and calcineurin pathways (Fig. 8). In basal feeding/sedentary conditions mTORC1 phosphorylates TFEB allowing its interaction with 14-3-3 proteins, thus preventing its nuclear translocation. Conversely, during starvation and physical exercise mTORC1 activity is inhibited and, at the same time, calcineurin activity is locally induced by lysosomal calcium release via MCOLN1. This leads to both a decreased rate of TFEB phosphorylation, via mTORC1 inhibition, and an induction of TFEB de-phosphorylation, via calcineurin induction. De-phosphorylated TFEB is free to travel to the nucleus and to induce the expression of lysosomal and autophagic genes (Fig. 8).

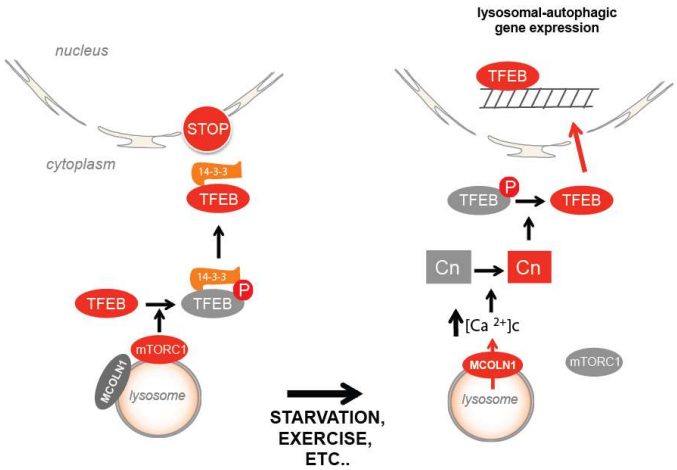

Figure 8: Model of Ca^{2+} mediated regulation of TFEB. Under feeding conditions TFEB is phosphorylated on the lysosomal surface and is sequestered in the cytoplasm by the 14-3-3 proteins. During starvation and physical exercise Ca^{2+} is released from the lysosome via MCOLN1, thus establishing a Ca^{2+} microdomain. This leads to calcineurin activation and TFEB de-phosphorylation. De-phosphorylated TFEB is no longer able to bind 14-3-3 proteins and can freely translocate to the nucleus where it transcriptionally activates the lysosomal/autophagic pathway.

Previous studies reported that exercise induces autophagy in muscle (He et al., 2012, Grumati et al., 2011, Jamart et al., 2013). The results described in this chapter provide a mechanistic link between calcineurin activation and autophagy induction during exercise. To date, the transcription factors of the NFAT family, master regulators of T cell activation (Macian, 2005), have been considered the main transcriptional mediators of calcineurin function. The discovery that TFEB, a master controller of autophagy, is a calcineurin substrate expands the current view on the mechanism of action of calcineurin. Interestingly, starvation induces calcineurin-mediated de-phosphorylation and nuclear translocation of both TFEB and NFAT, suggesting a coordinated regulation of the two different transcriptional networks. Previous studies implicated calcineurin in a variety of both physiological and pathological processes, such as neuronal synaptic transmission, adaptive immune response and muscle remodelling after physical exercise (Rusnak and Mertz, 2000, Kasahara et al., 2013). The data reported here suggest that some of these processes may be linked to the lysosomal/autophagic pathway via TFEB. In addition, other calcineurin substrates may also play a role in autophagy.

Calcium is considered a key regulator of the autophagy pathway, its availability and distribution inside storage compartment and cytoplasm is critical for autophagy regulation. A key role is fulfilled by calcium storage organelles, endoplasmic reticulum (with a Ca^{2+} concentration of about 0.4 – 0.8mM), mitochondria (with a Ca^{2+} concentration of about 200nM) and lysosome (with a Ca^{2+} concentration of about 0.4 – 0.6mM) (Christensen et al., 2002, Shigetomi et al., 2016), even if, more than the storage organelles per se, there are fundamental players located in those compartment that dynamically control the release of calcium to the cytosol and vice versa (Filippi-Chiela et al., 2016). Indeed, the inositol 1,4,5 – triphosphate receptor (IP3-R) is located on the endoplasmic reticulum (Berridge, 2009), the voltage dependent anion channel (VDAC1)

and the mitochondria calcium uniporter regulator 1 (MCUR1) are found on the mitochondrial outer and on inner membrane respectively (Williams et al., 2013), while on the lysosome there are TRPML1 and 3 (Christensen et al., 2002). IP3-R is the main Ca^{2+} effector, it links environmental signals to autophagy since its ligand IP3 increases in response to ATP, hypoxia, hormones, growth factors and neurotransmitters (Berridge, 2009). On the other hand, VDAC1, is involved together with IP3-R, in calcium transfer from endoplasmic reticulum to mitochondria. Calcium storage inside mitochondrial lumen is fundamental for Krebs cycle and ATP production, thus impairment in this calcium transfer leads to mitochondrial malfunction and autophagy (Mallilankaraman et al., 2012, Williams et al., 2013). In addition, regarding lysosome in this chapter we have dissected a Ca^{2+}-dependent pathway that thanks to calcium release, via MCOLN1, regulates autophagy at the transcriptional level. Our study demonstrates that local calcineurin activation near the lysosome occur due to the calcium microdomain generated by the calcium release of MCOLN1. In addition, our data also revealed a positive feedback loop by which the TFEB is activated by the calcium channel MCOLN1, which is known to be a TFEB transcriptional target (Palmieri et al., 2011).

In conclusion, the identification of a mechanism by which lysosomal Ca^{2+} regulates autophagy via MCOLN1 and the activation of the transcription factor TFEB by calcineurin further support the role for the lysosome as a signalling hub. It is likely that future studies will lead to the identification of other signalling pathways originating from the lysosomal surface.

TRPML2 and TRPML3

Other than TRPML1, the TRPMLs subfamily is made of other 2 members, TRPML2 and TRPML3. TRPML2 mRNA is expressed in high levels in thymus, spleen, lymphatic nodes and kidney (Samie et al., 2009, Grimm et al., 2010, Sun et al., 2015). Interestingly,

transcript levels of TRPML2 co-vary with those of TRPML1. Indeed, in lymphoid tissues and primary cells from mouse or human cell models, TRPML2 transcript levels is significantly reduced in the absence of TRPML1 and increased upon TRPML1 over-expression or stimulation by specific activators or nicotinic acid adenine dinucleotide phosphate (NAADP). This suggests a regulatory role for TRPML1 in the expression and function of TRPML2 in these specialised tissues (Samie et al., 2009). Different studies using over-expressed TRPML2 reported the localisation of the protein to the lysosomes and partially to the plasma membrane (demonstrated by whole cell current recording) (Venkatachalam et al., 2006, Zeevi et al., 2009, Song et al., 2006). Moreover, TRPML2 has been also found to localise onto tubular recycling endosomes, where it is associated with the ARF6-dependent pathway (Karacsonyi et al., 2007). In activated macrophages and microglia, intracellular distribution of the endogenous TRPML2 protein is almost exclusively present in recycling endosomes (Sun et al., 2015). By using a GOF mutant (TRPML2Va; A369P), which carries the same constitutively active Varitint-Waddler mutation described for TRPML3 (see below), it has been demonstrated that TRPML2 is a non-selective Ca^{2+}-, Na^{2+}- and Fe^{2+}-permeable channel. Like other mucolipin family members, TRPML2 can generate inwardly rectifying current, thus transporting cations from the lumen of endosomes, lysosomes or extracellular space to the cytosol (Dong et al., 2008, Grimm et al., 2012, Grimm et al., 2007). Wild-type TRPML2 single channel current has been only measured in synthetic membrane bilayers containing translated TRPML2 produced *in vitro* or in mammalian cells. TRPML2 shows limited single channel conductance, although the *in vitro* approach used to perform the measurements may underestimate the effective conductance of the channel (Curcio-Morelli et al., 2010b). TRPML2 can interact with the other two members of the family to form dimers, although these interactions are present to a very limited extent (Venkatachalam et al., 2006, Zeevi

et al., 2009). Hetero-dimerization of over-expressed wild type or dominant negative TRPML2 with TRPML1 and TRPML3 gives rise to channel complexes with altered conductance, suggesting that these interactions may be physiologically relevant for the regulation of TRPMLs channel activity upon specific conditions (Curcio-Morelli et al., 2010b, Zeevi et al., 2010). As described for TRPML1, activity of TRPML2 channel can be physiologically stimulated by both protons and PI(3,5)P2 (Dong et al., 2008, Dong et al., 2010, Lev et al., 2010). In addition to endogenous stimuli, three synthetic compounds, named SF-21, SF-41 and SF-81 (Table 1), have been characterized as activators of both wild type TRPML2 and TRPML3 (Grimm et al., 2010, Grimm et al., 2012). These molecules may be of particular interest in the development of therapeutic strategies to treat MLIV, caused by loss-of-function mutation in the TRPML1 gene. Thus, the activation of potential and functional redundant TRPMLs may mitigate the symptoms of MLIV disease. Unlike TRPML1, no monogenic diseases correlated with TRPML2 loss-of-function have been identified so far. Interestingly, the enrichment of TRPML2 transcript in lymphoid tissues, like spleen and thymus, and immune cells, such as B-cell lines and primary B-lymphocytes, raised the hypothesis of a regulatory role of TRPML2 in the immune system (Samie et al., 2009, Grimm et al., 2010, Sun et al., 2015, Lindvall et al., 2004). TRPML2 has been found significantly down-regulated in B-cells lacking the Bruton Tyrosine Kinase (BTK), a kinase involved in B-lymphocyte development, thus suggesting a role of BTK signalling cascade in the regulation of TRPML2 expression (Lindvall et al., 2004, Lindvall et al., 2005). Furthermore, it has been shown that the transcription factor PAX5, also known as B-cell specific activator protein (BSAP), controls the expression of TRPML2 gene (Valadez and Cuajungco, 2015). Finally, TRPML2 is a molecular partner of the plasma membrane protein TMEM176A, which negatively regulates the maturation and activation of dendritic cells (Chen et al., 2014). Interestingly, a role for TRPML2 on innate immune

response has also been recently described. Indeed, TRPML2 is present at very low levels in resting macrophages, but its expression dramatically increases in response to TLRs activation, whereas the mRNA levels of TRPML1 and TRPML3 do not change during similar stimuli (Sun et al., 2015). Furthermore, by generating a knockout mouse model, it has been assessed that the absence of TRPML2 reduces chemokine release from bone marrow-derived macrophages (BMDMs) and, subsequently, their ability to migrate. Altogether these evidences strongly suggest a specific role for TRPML2 in immune response, although further investigations are needed to clarify the mechanism of TRPML2 activation, such as the identification of the physiological events activating TRPML2 expression and function, likely via BTK and PAX5, and its possible role in the internalisation and recycling of plasma membrane proteins acting as immune receptors.

Similarly to TRPML1 and TRPML2, TRPML3 is an inwardly rectifying non-selective cation channel. TRPML3 was primarily identified as the gene carrying the causative mutation of the Varitint-Waddler (Va) phenotype in mice. The typical Va mutation affects hair cells of the cochlea causing severe stereocilia disorganisation in both the inner and outer hair cells (Di Palma et al., 2002). Va mutant mice suffer early-onset hearing loss, vestibular defects, pigmentation abnormalities and perinatal lethality. The mutated TRPML3 gene can produce two semi-dominant alleles: Va and VaJ. The Va allele is responsible for the most severe phenotype and is the result of the Ala to Pro substitution that occurs at the position 419 (A419P) located on the fifth transmembrane domain of TRPML3. In the VaJ mutant a second sequence alteration (I362T) occurring in *cis* partially rescues the Va allele. Va/Va mice are severely affected and exhibit multiple symptoms and reduced viability. +/VaJ mice show the mildest phenotype, are viable, display only limited variegation and coat colour dilution and have some residual hearing. VaJ/VaJ and +/Va mice show intermediate and similar phenotypes (Di Palma et al., 2002).

Studies performed on the TRPML3 channel properties have shown that the mutation occurring in the Va mutant mice (A419P) results in the constitutive activation of the channel (Xu et al., 2007, Grimm et al., 2007, Nagata et al., 2008, Kim et al., 2007),more precisely, introduction of a proline substitution in positions 413 to 419 of the fifth transmembrane domain causes helix-breaking which leads to channel activation. The generation of a TRPML3 GOF on the plasma membrane leads to massive Ca^{2+} overload, membrane depolarisation and subsequent cell death by apoptosis (Xu et al., 2007, Grimm et al., 2007, Nagata et al., 2008, Kim et al., 2007). The presence of a second mutation (I362T) in the VaJ allele attenuates current density and reduces protein localisation at the plasma membrane, resulting in a milder phenotype (Grimm et al., 2007, Kim et al., 2007). Endogenously expressed TRPML3 mRNA and protein have been found in the inner ear of wild type mice (Di Palma et al., 2002, Nagata et al., 2008). In HEK293 and CL4 cellular models, over-expressed TRPML3 localises on cytosolic vesicular structures and plasma membrane (Xu et al., 2007, Venkatachalam et al., 2006, Di Palma et al., 2002, Nagata et al., 2008). In ARPE19 cells, these structures were identified as early and late endosomes (Martina et al., 2009). The silencing of TRPML3 accelerates endocytosis of EGF and transferrin, whereas TRPML3 over-expression results in the opposite effect (Kim et al., 2009). TRPML3 has also been linked to the autophagy pathway (Kim et al., 2009). Indeed, upon starvation, the over-expression of the channel stimulates formation of autophagosomes, with a strong co-localisation of TRPML3 protein within these structures (Kim et al., 2009). Interestingly, TRPML3 specifically binds to GATE16, a mammalian ATG8 homolog important for autophagosome maturation (Choi and Kim, 2014). However, the link between TRPML3, GATE16 and autophagosome maturation, as well as the relevance of TRPML3 in autophagy has not yet been fully clarified. Finally, a novel function for TRPML3 in the neutralisation of bacterial infection has been recently described. In

particular, TRPML3 acts as a pH sensor during bacterial internalisation promoting lysosomal exocytosis to clear bacteria and therefore re-establishes proper lysosomal function (Miao et al., 2015).

Table 1 : List of endogenous and synthetic modulators of TRPML channels activity. Modified with permission from: *Di Paola et al. (Di Paola et al., 2017)*

Name	Target	Type	Reference
phosphatidylinositol (3,5) bisphosphate (PI(3,5)P2)	TRPML1, TRPML2, TRPML3	Activator	(Dong et al., 2010)
ML-SA1	TRPML1, TRPML2, TRPML3	Activator	(Grimm et al., 2010, Shen et al., 2012)
MK6-83	TRPML1, TRPML3	Activator	(Chen et al., 2014)
SF-22; SF-51	TRPML1, TRPML3	Activator	(Grimm et al., 2010, Shen et al., 2012)
SF-21; SF-41, SF-81	TRPML2, TRPML3	Activator	(Grimm et al., 2012)
Na^+	TRPML2	Activator	(Grimm et al., 2012)
SF-11; SN-1; SN-2	TRPML3	Activator	(Grimm et al., 2010)
SF-23; SF-24; SF-31; SF-32; SF-33; SF-61; SF-71	TRPML3	Activator	(Grimm et al., 2010)
ML268; ML269	TRPML3	Activator	(Saldanha et al., 2010)
Sphingomyelins	TRPML1	Inhibitor	(Shen et al., 2012)
phosphatidylinositol (4,5) bisphosphate (PI(4,5)P2)	TRPML1	Inhibitor	(Zhang et al., 2012)
Verapamil	TRPML1, TRPML3	Inhibitor	(Xu et al., 2007)
La^{3+}	TRPML1	Inhibitor	(Dong et al., 2010)
Na^+	TRPML3	Inhibitor	(Grimm et al., 2012, Kim et al., 2007)
Gd^{3+}	TRPML3	Inhibitor	(Nagata et al., 2008)

Chapter 1

TRPML1 links lysosomal calcium to autophagy initiation

Abstract

TRPML1 (or Mucolipin 1) is a cation-permeable channel localized on the membranes of late endosomes and lysosomes (LELs) of mammalian cells. TRPML1 has been involved in vesicular trafficking, vesicular fusion, phagocytosis of large particles, and lysosomal exocytosis (Medina et al., 2011, Samie et al., 2013, Manzoni et al., 2004, Di Paola et al., 2017). We have recently shown that lysosomal Ca^{2+} release, through TRPML1, plays a major role in lysosomal adaptation to starvation by inducing calcineurin that de-phosphorylates and activates TFEB, a master gene of lysosomal function (Medina et al., 2015). While studying the role of TRPML1 in autophagy, we also observed that the inhibition of TRPML1 significantly reduced the recruitment of the WD-repeat PtdIns(3)P effector protein WIPI2 to vesicles. Since WIPI2 is an essential effector at the nascent autophagosome (Mauthe et al., 2011), we reasoned that the activity of the lysosomal calcium channel TRPML1 may play a role in autophagosome biogenesis. Indeed, we found that TRPML1-activation induces the recruitment of PtdIns(3)P-binding proteins to the nascent autophagosome, whereas genetic or pharmacological inhibition of TRPML1 channel inhibits autophagy initiation. Importantly, alteration of this novel identified function may be involved in the pathology of LSDs since we found that autophagosome formation is impaired in human fibroblasts from patients affected of mucolipidosis IV (MLIV; a severe LSD caused by mutations in TRPML1). We also found that WIPI2 puncta formation was closely to lysosomes overexpressing TRPML1-GFP suggesting that PtdIns(3)P nucleation occurs in the vicinity of TRPML1 activation. By silencing VAPs

proteins, that have been involved in the formation of numerous different membrane contact sites, we consistently reduced TRPML1-mediated induction of WIPI2 puncta formation upon agonist treatment. In addition, by using specific compound inhibitors during starvation, we found that TRPML1-mediated induction of autophagosome biogenesis requires calmodulin, CaMKKβ, and the PtdIns(3)-generating enzyme PIK3C3 (also called VPS34). Therefore, we propose a new lysosomal calcium signalling that through the activation of TRPML1 induces autophagosome biogenesis via the CaMKKβ/AMPK pathway, and the induction of two essential protein complexes involved in autophagy initiation the ULK1 and PIK3C3 complexes.

Introduction

Ca^{2+} is an universal second messenger that plays a fundamental role in cellular physiology regulating processes such as gene transcription, cell proliferation, migration and death (Berridge et al., 2000). By definition Ca^{2+} levels are extremely low in resting cells to allow a rapid release upon specific stimulus. Thus, the variety of cellular processes modulated by changes in Ca^{2+} concentration requires an exquisitely control of its intracellular levels to create a wide range of spatial and temporal signals (Berridge et al., 2000). An important manner to regulate Ca^{2+} is through the generation of gradients by intracellular Ca^{2+} stores, of which the endoplasmic reticulum (ER) is the major Ca^{2+} store organelle in the cell. Such compartmentalization allows the rapid mobilization of Ca^{2+} by the regulation of the expression and activity of Ca^{2+} permeable channels and thereby the modulation of Ca^{2+}-dependent processes, such as cell proliferation, ER stress, and apoptosis (La Rovere et al., 2016). In addition, in the last years evidence is accumulating for a role of intracellular Ca^{2+} in autophagy (Decuypere et al., 2011b, Cardenas and Foskett, 2012, Yao and Klionsky, 2015, Medina et al., 2015, Medina et al., 2011). The role of Ca^{2+} in autophagy started to emerge in the early 90s, in which a first study

revealed that chelation of Ca^{2+} as well as the elevation of cytosolic Ca^{2+} suppressed autophagy (Gordon et al., 1993). This controversy has continued with the publication of many different studies supporting both positive and negative effects of Ca^{2+} on autophagy activation (Cardenas et al., 2010, East and Campanella, 2013, Decuypere et al., 2011a, Su et al., 2013, Gastaldello et al., 2010, Smaili et al., 2013). Thus, we are still far away to fully understand the precise mechanisms by which Ca^{2+} controls this important catabolic process, and how these mechanisms are integrated in well-known triggers/regulators of autophagy initiation such as nutrient deprivation, low cellular energy levels, ER stress, hypoxia and oxidative stress (Kroemer et al., 2010).

Recently, lysosomal organelles are emerging as intracellular Ca^{2+} stores that play major roles in vesicular trafficking and autophagy. Most importantly, impairment of lysosomal Ca^{2+} homeostasis has been implicated in many human diseases such as lysosomal storage diseases (Morgan et al., 2011, Shen et al., 2012, Lloyd-Evans et al., 2008), neurodegeneration (Funk and Kuret, 2012, Bae et al., 2014, Ezeani and Omabe, 2016), muscular dystrophy, and cancer (Cheng et al., 2014, Kondratskyi et al., 2013, Galluzzi et al., 2015). The non-selective cation channel TRPML1 is the major calcium-release channel on the lysosomal membrane. TRPML1 activity has been involved in a variety of membrane trafficking processes such as endocytosis, exocytosis, phagocytosis and autophagy (Xu and Ren, 2015). In addition, mutations in the TRPML1 gene cause mucolipidosis type IV (MLIV: OMIN 252650), an autosomal recessive lysosomal disease characterized by psychomotor alterations, corneal opacities, and achlorhydia (Frei et al., 1998, Bargal et al., 2000). At the cellular level, both human fibroblasts affected of MLIV and TRPML1-/- neurons from a MLIV mouse model present autophagy impairment characterized by the accumulation of autophagic markers such as LC3 and p62 (Vergarajauregui et al., 2008b, Curcio-Morelli et al., 2010a). This phenotype is not exclusive of MLIV, and many other

LSDs present defects in autophagy that have been mainly explained as a consequence of global lysosomal dysfunction and/or defects of autophagosome-lysosome fusion. However, recent evidences strongly suggest that TRPML1 activity plays a direct role in the activation of autophagy. Thus, we have shown that lysosomal Ca^{2+} signalling regulates autophagy through calcineurin and its substrate TFEB (Medina et al., 2015). Lysosomal Ca^{2+} release through TRPML1 stimulates the calcium-dependent phosphatase calcineurin which binds and dephosphorylates its substrate TFEB, and thereby promoting its nuclear translocation to initiate the transcription of lysosomal and autophagic genes (Medina et al., 2015). In addition, we also observed that acute TRPML1 depletion reduces the formation of autophagosomes by using the PtdIns(3)P-binding reporter GFP-2xFYVE (Medina et al., 2015), suggesting a potential role of TRPML1-mediated lysosomal calcium release on the early steps of phagophore formation and therefore on autophagy initiation.

The autophagy pathway starts with the formation of autophagosomes and could be divided in four steps: initiation, nucleation, elongation and finally closure of the double-membrane structure to form an autophagosome (Roberts and Ktistakis, 2013). The main kinase which regulate signals leading to autophagy initiation is mammalian target of rapamycin 1 (mTORC1) (Weidberg et al., 2011, Mizushima et al., 2011, Rubinsztein et al., 2012, Kuballa et al., 2012). In fully fed condition mTORC1 is active and suppress autophagy by phosphorylating ULK1 on serine 757 (Roberts and Ktistakis, 2013). When nutrients are removed mTORC1 is inactive and these leads to ULK1 de – phosphorylation and to autophagy initiation (Roberts and Ktistakis, 2013). Together with ATG13 and FIP200, ULK1 constitute the ULK1 complex. The formation of this complex is essential for autophagy initiation and in starvation is recruited on the site of autophagosome formation (Mizushima et al., 2011). More recently, it has been demonstrated that also

the AMP activated protein kinase (AMPK) can phosphorylate ULK1, this phenomenon is even emphasized in the presence of mTORC1 inhibitor like rapamycin, meaning that mTORC1 negatively regulate this phosphorylation (Kim et al., 2011, Egan et al., 2011b). Furthermore, not only nutrient deprivation but also, intracellular Ca^{2+} levels can trigger autophagy by a Calmodulin- Dependent Kinase Kinase β (CaMKKβ)-mediated activation of AMPK without requiring a change in AMP or ADP levels (Hawley et al., 2005, Woods et al., 2005). It has been observed that different Ca^{2+} mobilizing agents, such as vitamin D, induce autophagy by CaMKKβ and AMPK phosphorylation and activation. Conversely, both pharmacological inhibition and genetic depletion of CaMKKβ causes the inactivation of AMPK and an attenuation of autophagy (Hoyer-Hansen et al., 2007). Thus, autophagy initiation is a balance among mTORC1 and AMPK, the first one suppresses ULK1 activity in nutrient-rich condition, whereas the phosphorylation by the second one can activate it (Egan et al., 2011a). After the recruitment of the ULK1 complex, the next complex required for autophagosome formation is the VPS34 complex 1 that is composed by phosphoinositide 3-kinase C (hVPS34 or PIK3C3), ATG14L, Beclin1 and phosphoinositide-3-Kinase regulatory subunit 4 (hVPS15 or PIK3R4). PIK3C3 lipid kinase activity is crucial for phosphatidylinositol 3-phosphate (PtdIns(3)P) production (Mizushima and Komatsu, 2011, Weidberg et al., 2011, Kuballa et al., 2012) since membranes enriched with PtdIns(3)P are thought to be the site of phagophore nucleation (Axe et al., 2008). Generation of PtdIns(3)P is a crucial step since it is necessary for the recruitment of several accessory proteins: double FYVE domain-containing protein 1 (DFCP1) (Ridley et al., 2001) and the WD-repeat protein interacting with phosphoinositides (WIPI) family (Proikas-Cezanne et al., 2004, Polson et al., 2010, Proikas-Cezanne et al., 2007). DFCP1 possess an endoplasmic reticulum targeting domain and two FYVE domain required for PtdIns(3)P binding. When autophagy is induced DFCP1 translocates to the phagophore

nucleation site, and these structures partially colocalize with LC3 and ATG5 (Ridley et al., 2001). DFCP1 recruitment on autophagosome generation site is inhibited by PI3K inhibitors such as wortmannin or 3-methyladenine, or by using siRNA targeting PIK3C3 and Beclin1, indicating that both are required for PtdIns(3)P formation. On the other hand, the WIPI family members (WIPI1, WIPI2, WIPI3 and WIPI4) have been all implicated in autophagy (Proikas-Cezanne et al., 2004, Polson et al., 2010, Proikas-Cezanne et al., 2007) with WIPI2 and WIPI4 (Proikas-Cezanne et al., 2004) behaving similarly to DFCP1 (Roberts and Ktistakis, 2013). In addition, WIPI2 recruitment to the phagophore is necessary for the subsequent recruitment of lipidated LC3 during autophagosome maturation (Dooley et al., 2014). Here we investigated the role of TRPML1 activation in the modulation of autophagy initiation. We found that TRPML1-mediated lysosomal calcium release promotes the recruitment of PtdIns(3)P-binding proteins to the autophagosome nucleation site during autophagy initiation in a process that requires calmodulin, CaMKKβ, and the subsequent activation of the ULK1 complex and the the PtdIns(3)-generating enzyme PIK3C3. We also found that the recruitment of PtdIns(3)-binding proteins occurs in the close vicinity of TRPML1 activation in agreement the triggering of a local increase of lysosomal calcium in the phagophore nucleation site during autophagy initiation.

Results and discussion

TRPML1 regulates autophagosome biogenesis

We have recently discovered a new lysosomal signalling pathway modulating autophagy that involves the release of lysosomal calcium through the activation of TRPML1 (Medina et al., 2015), a mechanism that may be important to sustain autophagy during starvation (Medina et al., 2015). Interestingly, we also preliminary observed that the acute silencing of TRPML1 significantly reduced the recruitment of PtdIns(3)P-binding reporter GFP-

2xFYVE (Medina et al., 2015). PtdIns(3)P is a phosphoinositide detected at the surface of early endosomes, on intraluminal vesicles of multivesicular endosomes, and autophagosomes (Burman and Ktistakis, 2010, Di Paolo and De Camilli, 2006). Thus, during nutrient starvation the activation of the PIK3C3 complex, most likely in the ER increases the production and recruitment of PtdIns(3)P to the omegasome, the early precursor of autophagosomes (Knaevelsrud et al., 2013). Since PtdIns(3)P is an essential effector at the nascent autophagosome (Proikas-Cezanne et al., 2015), our observation may suggest that the activity of the lysosomal calcium channel TRPML1 plays a role in autophagosome biogenesis during autophagy initiation. First of all, we reproduced the data previously obtained by overexpressing the GFP-2xFYVE reporter (Medina et al., 2015), by detecting endogenous WIPI2, a marker of autophagosome formation which is able to bind PtdIns(3)P too. We found that the acute silencing of TRPML1 by siRNAs reduces endogenous WIPI2 puncta formation upon starvation with EBSS (fig. 9 a). Then, as TRPML1 mutations cause the human lysosomal storage disease mucolipidosis IV (Bargal et al., 2000, Bassi et al., 2000), we investigated whether the recruitment of endogenous WIPI2 during starvation was also impaired in human MLIV fibroblasts from different patients (GM02525, GM02526). Indeed, we found a significant reduction in the induction of WIPI2 puncta formation during starvation compared with the normal starvation response in human WT cells. Similar reduction in the induction of WIPI2 puncta were obtained in a human cellular model of TRPML1 depletion, generated by CRISPR/Cas9, the haploid cell line hap1 (fig. 9 c), and after pharmacological inhibition of TRPML1 channel with MLSI3 (Samie et al., 2013) during starvation (fig. 9 d).

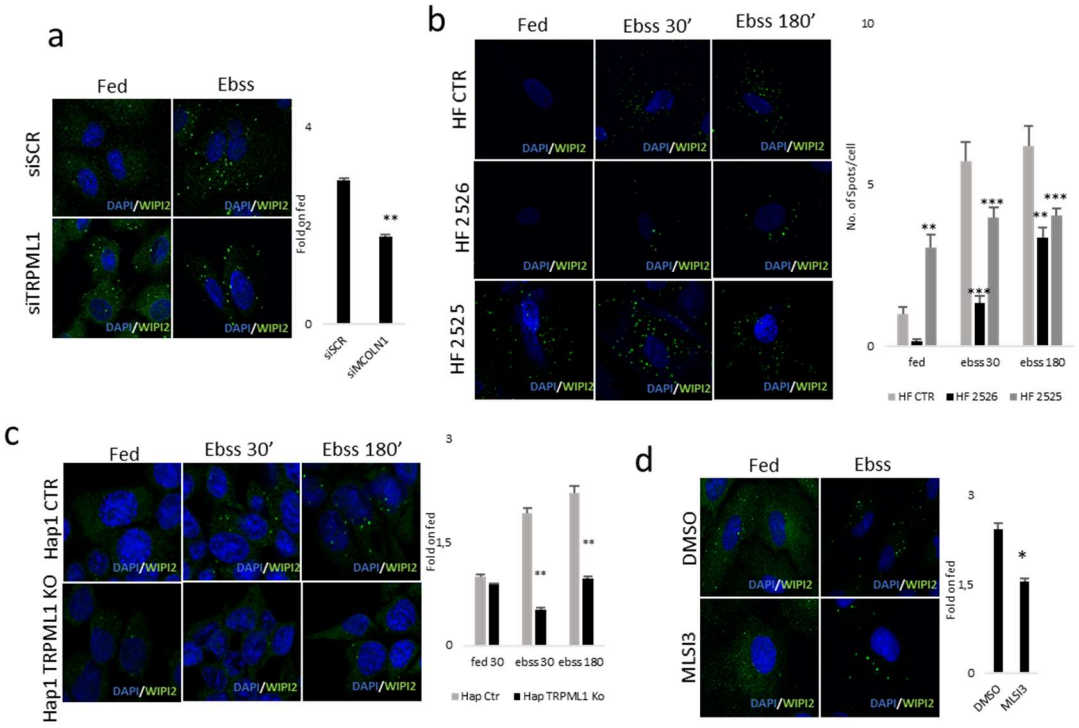

Figure 9: WIPI2 puncta are reduced in TRPML1 depleted cells. (a) Arpe19 cells silenced 72 hours or with a siRNA targeting a scramble sequence or one targeting TRPML1. Cells were then starved for 180 minutes with Ebss, in TRPML1 silenced cells WIPI2 puncta induction is reduced after starvation respect to scramble cells as also reported in the small bar plot on the right that represent the fold on the respective fed condition. (b) Immunofluorescence against endogenous WIPI2 on human fibroblasts wild type and MLIV (GM02526, GM02525). Cells were starved for 30 minutes and 180 minutes. In wild type cell, we observed a progressive increase in WIPI2 puncta formation by increasing the starvation time, MLIV cell lines, conversely, showed as the silenced one an impairment in the induction after both starvation time points. (c) Immunofluorescence against endogenous WIPI2 on hap1 cell line control and KO for TRPML1 with Crispr/Cas9 technology. Cells were starved for 30 minutes and 180 minutes. In control cell, we observed a progressive increase in WIPI2 puncta formation by increasing the starvation time, the KO cell line, conversely, showed an impairment in the induction after both starvation time points. (d) Arpe19 cells were treated overnight with 30µM of MLSI or DMSO. The day after cells were starved for 180 minutes with Ebss with DMSO or MLSI 30µM, in MLSI treated cells WIPI2 puncta induction is reduced after starvation respect to DMSO treated one, as also reported in the small bar plot on the right that represent the fold on the respective fed condition.

To confirm that the impairment on the induction of WIPI2 was caused by a defect in autophagosome biogenesis we perform a similar experiment using the lysosomal inhibitor Bafilomycin A1 (BafA1) (fig. 10). We observed that the number of WIPI2 spots in TRPML1 silenced cells was not increased upon BafA1 treatment both in fed and in starvation, whereas, in scramble silenced cells we observed a further increase in WIPI2 spots, indicating a defect in the initiation of autophagy.

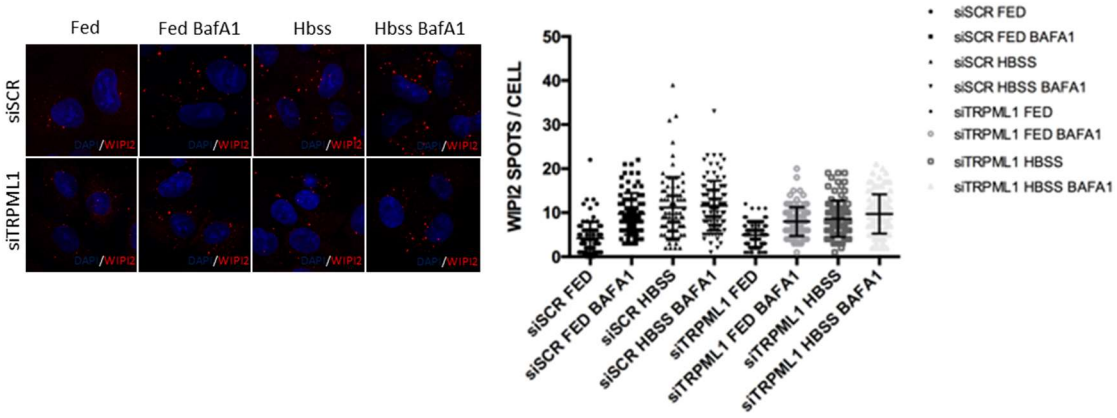

Figure 10: Arpe19 cells were silenced with a siRNA targeting TRPML1 or a scramble sequence (siSCR). After 72 hours of silencing cells were starved or leave in complete medium whit or without the adding of BafA1 for 4 hours. An immunofluorescence against endogenous WIPI2 was performed. The spots per cell were counted using ImageJ software. The plot on the right shows the mean value of WIPI2 spots/cell +/- sd.

In addition, we further validated our results by performing, in collaboration with the TIGEM electron microscopy (EM) facility, an immunogold using an anti-WIPI2 antibody in both human WT fibroblast and MLIV patient cells (fig. 11 a, b). Indeed, we observed decreased number of WIPI2-positive structures after starvation in MLIV patient cells compared with their WT counterparts. Interestingly, while WT fibroblasts presented WIPI2-staining localized in electron dense pre-autophagosomal structure (Yla-Anttila et al., 2009) (fig. 11 a, arrows), in MLIV these structures were less abundant (fig. 11 b). EM serial sections of the images showed aberrant structures in MLIV cells with a short finger-like protrusion emerging from the ER labelled with WIPI2 antibody (fig. 11 b, arrows).

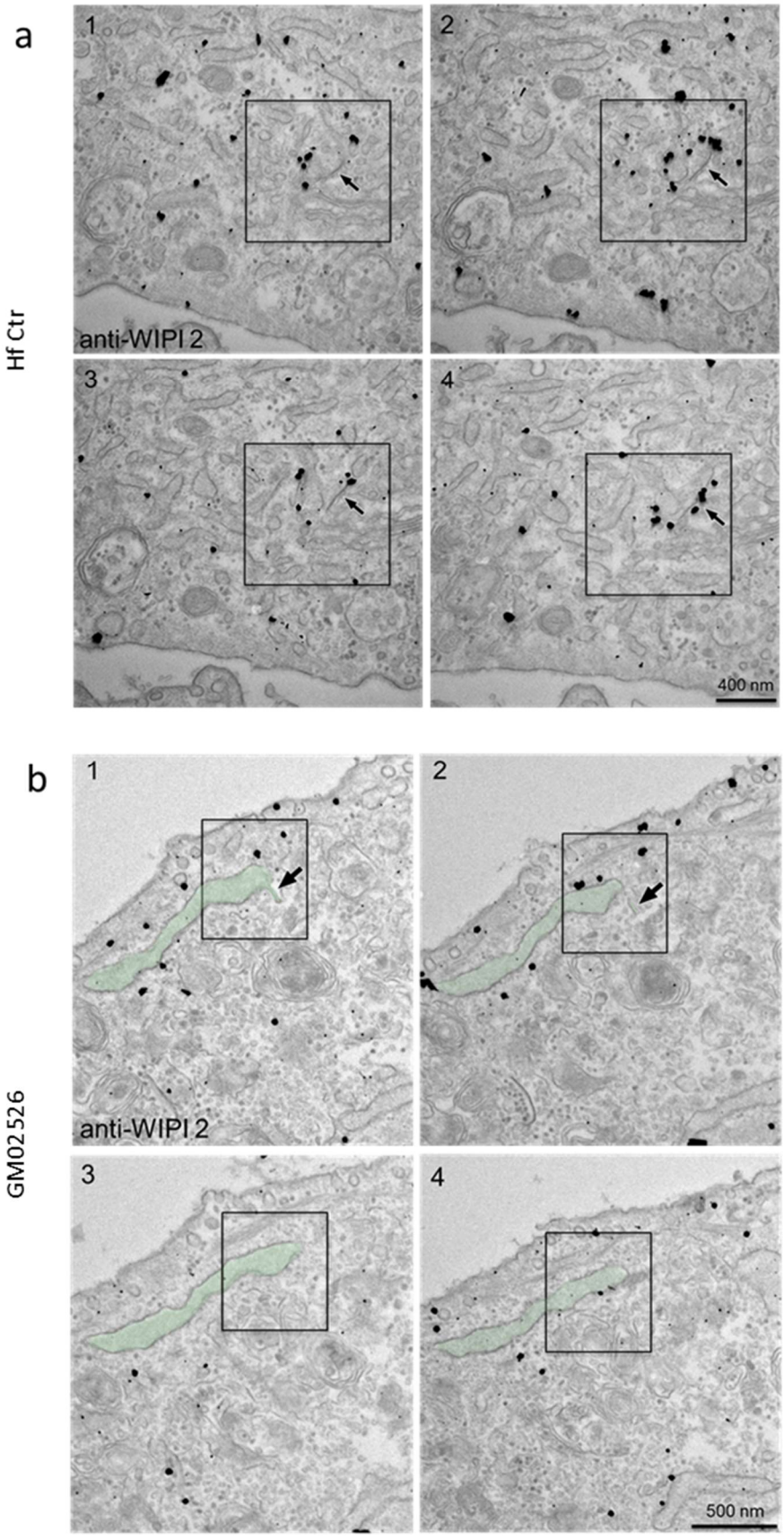

Figure 11: Electron microscopy on human and MLIV (GM02526) fibroblasts. (a) Human fibroblasts wild type, four serial sections are shown. WIPI2 resides at the phagophore structure (arrows). (b) Human fibroblasts MLIV (GM02526), four serial sections are shown. WIPI2 associates with membranes of endoplasmic reticulum. Arrow indicates aberrant phagophore-like structure.

The reduction of WIPI2 puncta formation in MLIV cells were not due to a decrease of WIPI2 mRNA or protein levels, since quantitative PCR or western blots against WIPI2, in normal nutrient and starvation conditions resulted in similar WIPI2 protein levels in MLIV and WT fibroblasts (fig. 12 a, b).

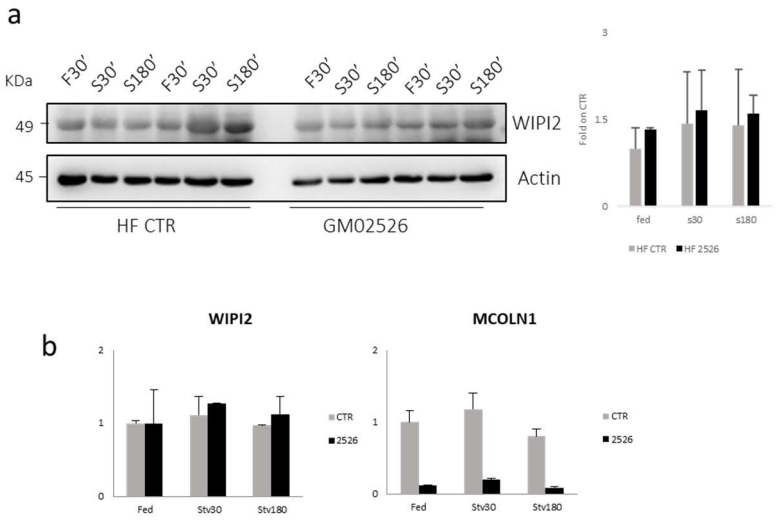

Figure 12:(a) Western blot against WIPI2 in total protein extract of human fibroblast control and MLIV (GM02526), no significant differences were observed in WIPI2 protein levels among the two cell lines and among the treatment as well. (b) Quantitative PCR on RNA from human fibroblast control and MLIV (GM02526). No significant differences were observed in WIPI2 mRNA levels among the two cell lines and among the treatment as well. As control we measured TRPML1 (MCOLN1) mRNA level and as expected was significantly downregulated.

Together with WIPI2 protein we have also performed immunofluorescence for endogenous LC3 which is used to recognise the mature autophagosomes. It has been reported that in steady state nutrient conditions LC3-puncta is already accumulated in MLIV patient fibroblasts, most likely due to a downstream delay in the autophagic flux (Vergarajauregui et al., 2008a). We confirmed this observation in MLIV fibroblasts (GM02526) (fig. 13 a) when compared with WT cells (Ctr). Interestingly, we also observed that while in WT cells LC3-puncta progressively increased during starvation, in MLIV cells the number of LC3 spots slightly increase, confirming a block in the induction of

autophagy during starvation. In addition, we confirmed the delay in autophagosome degradation looking at the number of LC3 and LAMP1 positive puncta, which indicates autophagosomes fused with lysosomes (fig. 13 b). Also for autophago-lysosome there is no increase upon starvation in TRPML1 silenced cells.

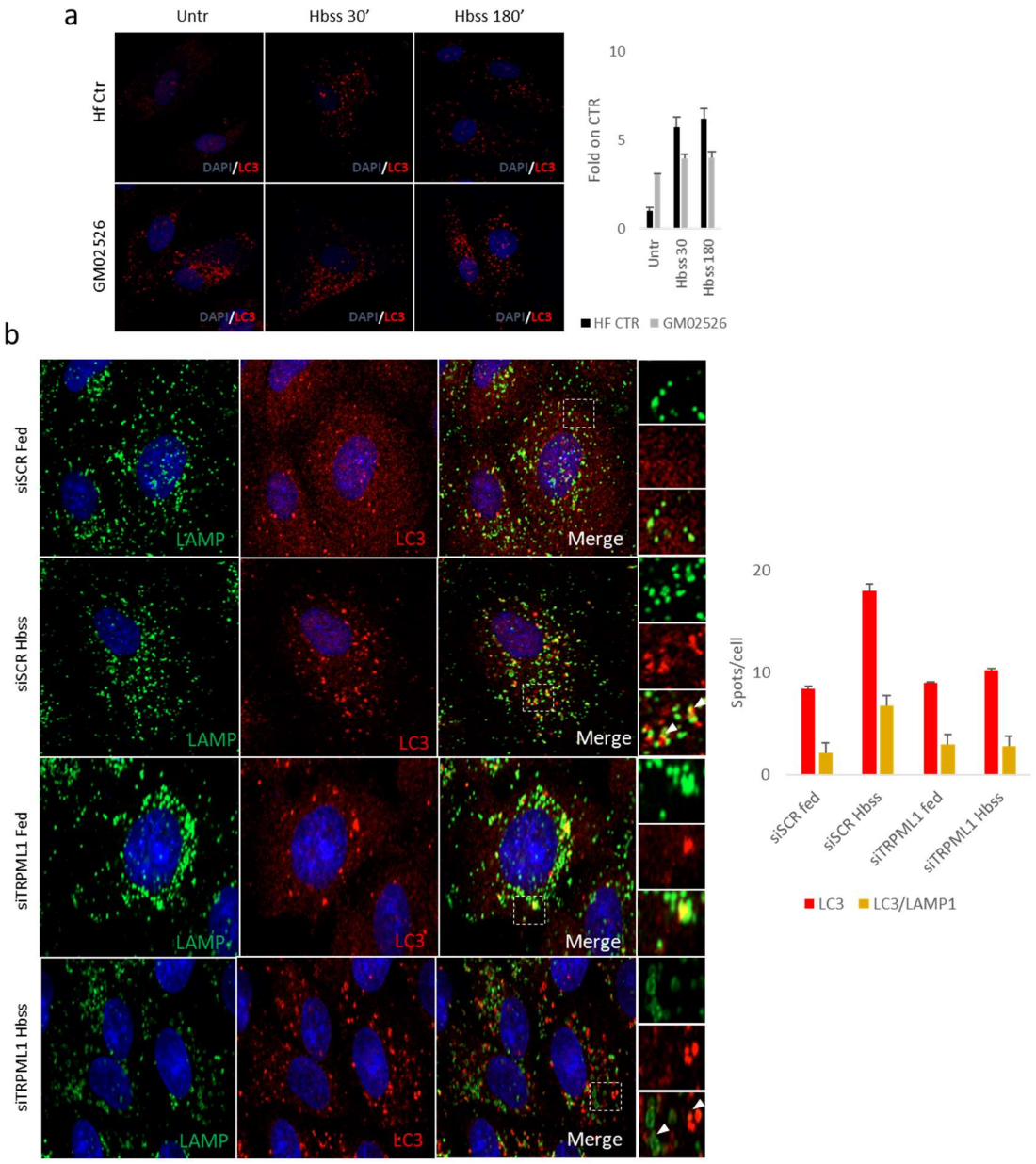

Figure 13: (a) Human fibroblasts wild type (Hf Ctr) and MLIV (GM02526) were starved for 30 and 180 minutes or left untreated. After treatment, an immunofluorescence against endogenous LC3 was performed. The bar plot on the right show the fold induction on untreated condition of Hf Ctr. (b) Arpe19 silenced 72 hours with a siRNA targeting TRPML1 or a scramble sequence, after silencing cells were feed or starved for 180 minutes. Cells were co-stained for endogenous LAMP1 and LC3. The bar plot shows the number of LC3 positive puncta (red bars) and the number of LC3/LAMP1 positive puncta (yellow bars).

To further confirm the latter results we quantified the number of nascent autophagosomes by transfecting human ARPE-19 cells with a plasmid carrying the specific autophagic reporter DFCP1-GFP. In contrast to WIPI2 that can binds PtdIns(3)P, but may also interacts with PtdIns(3,5)P2 (Tsuruta, 2016), the DFCP1 protein contains two FYVE domains that bind specifically PtdIns(3)P, and colocalizes with the ER pool of this lipid identified as omegasome (Axe et al., 2008). We found that genetic depletion or pharmacological inhibition of TRPML1 channel significantly reduced the induction of DFCP1-positive vesicles upon starvation, compared to WT cells (fig. 14 a, b). Thus, these results suggest that the induction of autophagosome biogenesis during starvation is impaired in cells depleted for TRPML1 and in human MLIV cells, and this effect is most likely due to delayed recruitment of PtdIns(3)P-binding proteins to autophagosome nucleation sites (fig. 9). In order to discard that transient DFCP1-GFP overexpression may alter the recruitment/sequestering of endogenous PtdIns(3)P to membranes, we perfomed similar experiments using stable HEK293 cells overexpressing DFCP1 GFP plasmid, this cell line was a gift of Dr. Ktistakis (Axe et al., 2008). In normal fed WT cells, we observed an increase in DFCP1 puncta formation upon starvation, whereas the silencing of TRPML1 significantly inhibits DFCP1-puncta during starvation, indicating that TRPML1 is involved in the recruitment of PtdIns(3)P-binding proteins DFCP1 and WIPI2 to the nascent autophagosome (fig. 14 c).

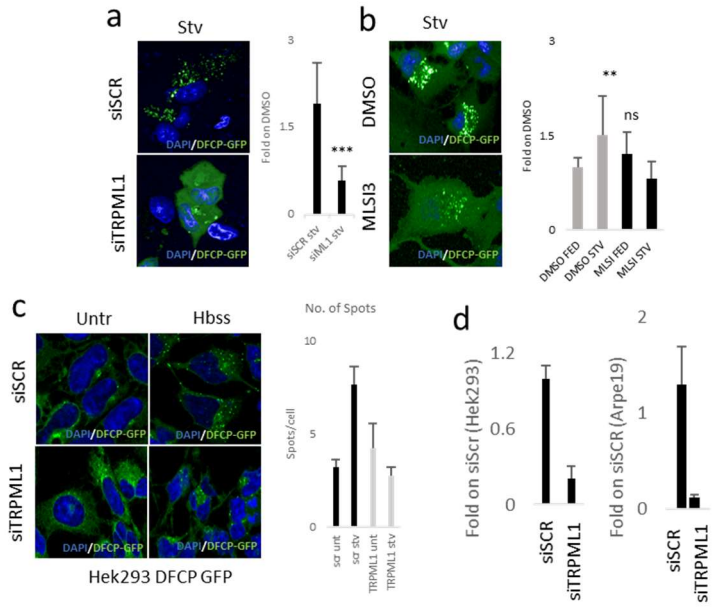

Figure 14: DFCP1 recruitment is TRPML1 mediated. (a) Arpe19 cells silenced 72 hours or with a siRNA targeting a scramble sequence or one targeting TRPML1, the last 16 hours were transfected with DFCP1 GFP plasmid. Cells were starved for 180 minutes and then number of DFCP1GFP structures were counted. A reduced number of vesicles were positive for DFCP1 GFP in cells depleted for TRPML1 (bar plot on right). (b) Arpe19 were treated overnight with 30μM of MLSI, at same time were transfected with DFCP1 GFP plasmid. Cells were starved for 180 minutes and then number of DFCP1GFP structures were counted. A reduced number of vesicles were positive for DFCP1 GFP in cells where TRPML1 activity was inhibited (bar plot on right). (c) Hek293 DFCP1 GFP cells were silenced 72 hours with a siRNA targeting a scramble sequence and one targeting TRPML1, then were starved 180 minutes. Number and size of DFCP1 GFP spots were counted and reported in the bar plots on right. (d) Quantitative PCR on Hek293 (left) and Arpe19 (right) to show knock down efficiency of TRPML1 silencing.

Then, we used a gain-function approach to investigate whether TRPML1 activation may activate the recruitment of WIPI2-positive autophagosomes in fed cells. First, we used pharmacological tools to activate TRPML1 by the treatment with the agonist MK6-83, kindly provided by Dr C. Grimm (Chen et al., 2014). We found that MK6-83 was able to promote endogenous WIPI2-puncta formation in two different cell lines in normal nutrient conditions (Hek293 and Arpe19) (fig. 15 a, b). Consistently, we also found that MK6-83 treatment induces LC3-puncta formation and elevation of autophagosomes colocalizing with lysosomes, indicating that direct activation of TRPML1 boost autophagosome-lysosomal fusion (fig. 15 c). Conversely, MLSI-mediated inhibition of TRPML1 inhibits autophagic flux and increases p62 accumulation (fig. 15 d). In addition, since MK6-83 can activates both TRPML1 and TRPML3 (Chen et al., 2014), we investigated

whether the WIPI2 puncta formation was selective towards TRPML1 by treating TRPML3 KO Hap1 cells with MK6-83. We found that MK6-83 treatment induces similar WIPI2 puncta in both WT and TRPML3 KO cells (fig. 15 e).

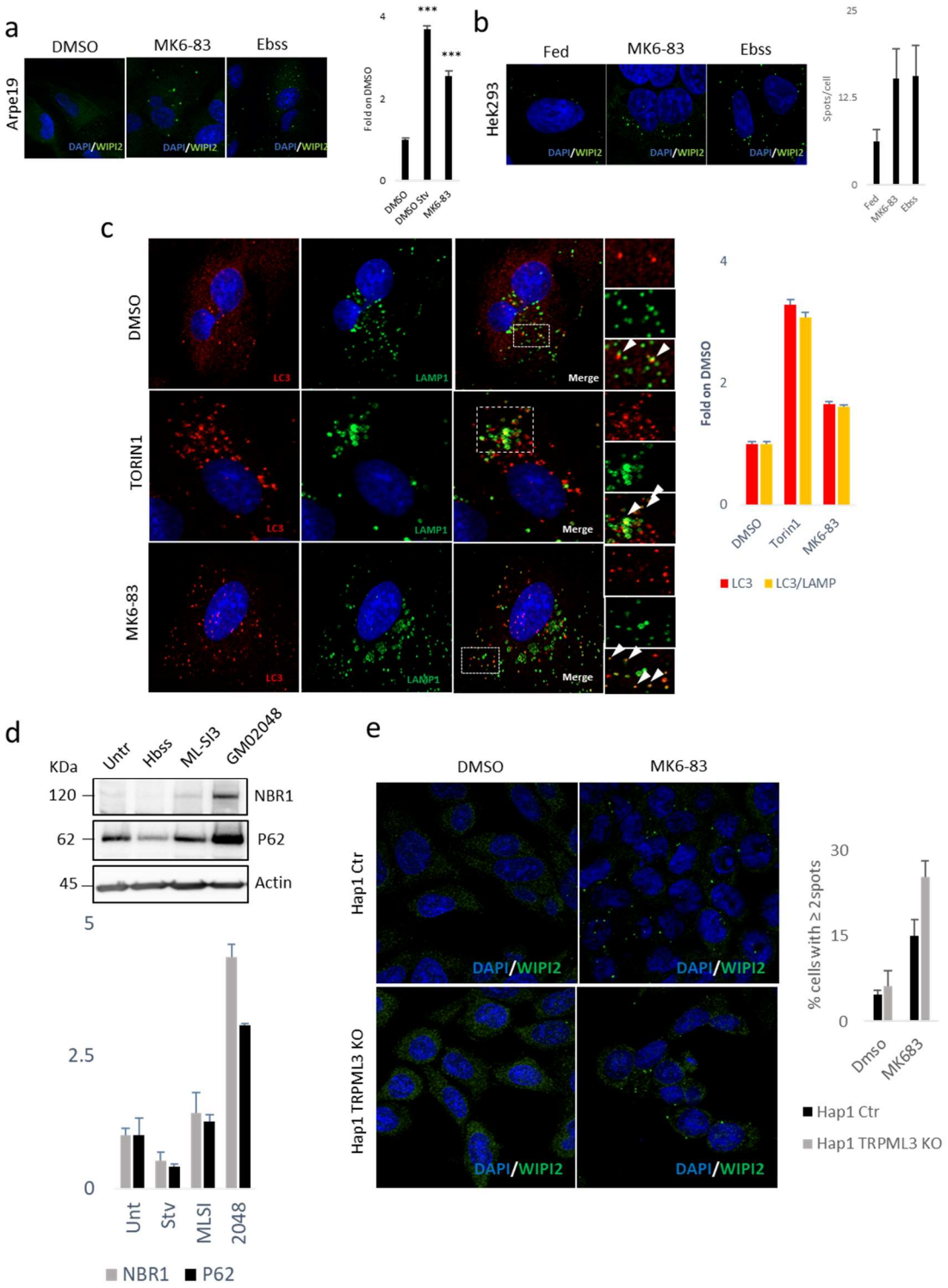

Figure 15: (a) Arpe19 cells were treated with 30µM of MK6-83 for 180 minutes, then an immunofluorescence against endogenous WIPI2 was performed, as positive control I used cells starved for 180 minutes. Number of spots were counted and normalized on cell number, in the bar plot on the right its reported the fold induction calculated on the DMSO. (b) Hek293 cells were treated with 30µM of MK6-83 for 180 minutes, then an immunofluorescence against endogenous WIPI2 was performed, as positive

control I used cells starved for 180 minutes. Number of spots were counted and normalized on cell number, in the bar plot on the right its reported the fold induction calculated on the DMSO. (c) Arpe19 cells were treated with 30μM of MK6-83 for 180 minutes, then an immunofluorescence against endogenous LAMP1 and LC3 were performed. DMSO and TORIN1 were used as negative and positive control respectively. Number of spots were counted and normalized on cell number, in the bar plot on the right its reported the fold induction calculated on the DMSO. (d) Western blot of insoluble fraction of human fibroblast control untreated or treated overnight with MLSI, 180 minutes of starvation and GM02048 (MLIV cell line) were used as positive and negative control for cellular clearance respectively. the western show the accumulation of two autophagic cargo NBR1 and P62. The bar plot shows the fold calculated on the untreated. (e) Hap1 control and TRPML3 KO were treated with MK6-83 for 3 hours. After fixation, an immunofluorescence against endogenous WIPI2 were performed. The plot on the right showed the percentage of cells that showed more than 2 WIPI2 puncta per cell. The experiment was performed twice.

Then, we overexpressed a vector carrying WT TRPML1 fused to the GFP (TRPML1-GFP) in human ARPE19 cells (fig. 16 a). Similarly to agonist-mediated TRPML1 activation, the overexpression of TRPML1-GFP promoted the formation of WIPI2-puncta while the overexpression of a TRPML1 non-conducting pore mutant (D471K/D472K; abbreviated TRPML1-DDKK) (Cao et al., 2017) was not able to increase the recruitment of WIPI2 to vesicle structures (fig. 8 b). Interestingly, most of the WIPI2-positive vesicles were closely to lysosomal localized TRPML1-GFP lysosomes, suggesting that PtdIns(3)P nucleation occurs in the vicinity of TRPML1 activation (fig. 16 b, c). Interestingly, a recent work from Biazik et al showed that in addition to ER, recycling endosomes and golgi, WIPI2-phagophores frequently form in close vicinity to late endosomes or lysosomes (Biazik et al., 2015). Thus, we used super resolution microscopy analysis to further confirm the closed vicinity of endogenous WIPI2-puncta to the lysosomes expressing TRPML1-GFP (fig. 16 c). Interestingly, TRPML1-mediated induction of WIPI2-puncta was also localized in the close proximity of the endoplasmic reticulum (ER), the major organelle involved in phagophore membrane source. Based on these results we reasoned that upon TRPML1 activation a local increase of lysosomal calcium may induce PtdIns(3)P recruitment in the proximity of the ER. Thus, we decided to silence the endoplasmic reticulum-localized Vesicle associated membrane proteins (VAMP)-Associated Proteins (VAPs) that have been implicated in tethering numerous different membrane contact sites (Eden, 2016).

We observed that upon VAPs (VAP-A/B) silencing we reduce the TRPML1-mediated WIPI2 puncta formation via MK6-83 treatment (fig. 16 d). These results suggest that TRPML1 activation induces phagophore formation in the very close vicinity of the ER most likely forming contact sites with this organelle.

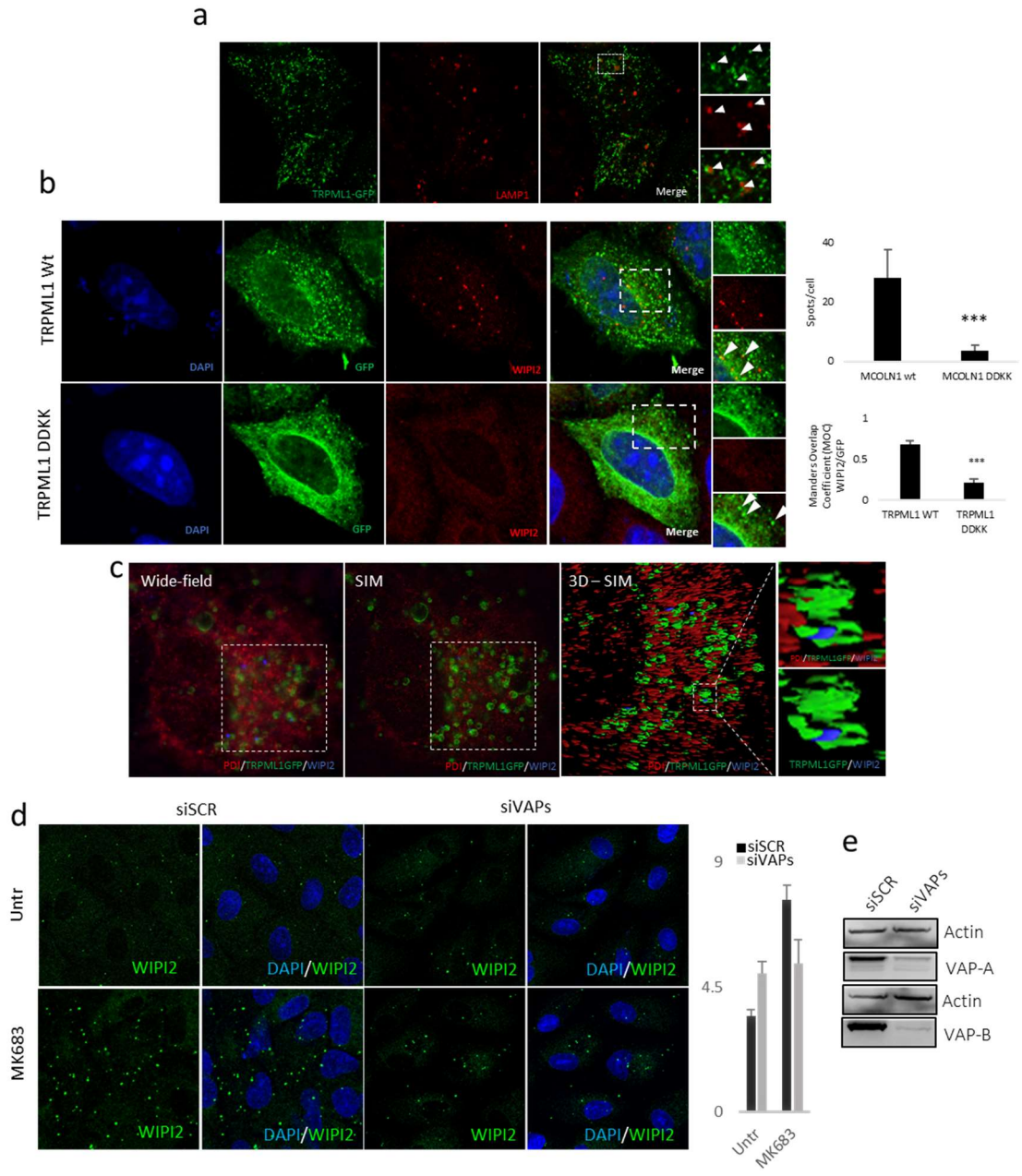

Figure 16: Genetic or pharmacological activation of TRPML1 promotes WIPI2 spots. (a) Arpe19 cells transfected with TRPML1 GFP and stained with endogenous LAMP1. White box and white arrow show the correct localization of TRPML1 on lysosomes. (b) Arpe19 cells were transfected 24 hours with TRPML1 GFP or TRPML1 DDKK GFP, then an immunofluorescence against endogenous WIPI2 were performed, on the right the first bar plot on the top show the number of WIPI2 spots in transfected cells, the second plot on the bottom show the Manders overlap coefficient (MOC) between WIPI2 and the GFP. (c) Arpe19 transfected with TRPML1 GFP were fixed and stained for endogenous endoplasmic reticulum marker PDI

(red) and WIPI2 (blue). Images were acquired with LSM880 super resolution using SIM, after acquisition a 3D reconstruction has been performed. (d) HeLa cells were treated 72 hours with an siRNA targeting VAP-A/B or with an siRNA scramble. Cells were left untreated or treated with MK6-83. An immunofluorescence against endogenous WIPI2 was performed. The bar plot on the right shows the number of spot per cell +/- standard deviation. (e) western blot of HeLa treated 72 hours with an siRNA targeting VAP-A/B or with an siRNA scramble, to show knock down efficiency.

TRPML1-mediated Autophagosome biogenesis requires a calcium-dependent pathway involving Calmodulin and CAMKKβ

Since TRPML1 is a lysosomal Ca^{2+} channel, and we already observed that a TRPML1 pore mutant was unable to induce WIPI2 puncta formation (figure 16 b), we investigated whether calcium chelation may impair WIPI2-puncta induction upon TRPML1 activation. We first, confirmed the requirement of Ca^{2+} during starvation-mediated autophagy induction (fig. 9). Hen, by using a fast calcium chelator, BAPTA-AM, we were able to completely block WIPI2 puncta formation upon starvation (fig. 17), while the use of a slower kinetic chelator, EGTA, was ineffectively inhibiting such formation (fig. 17). Then, we link these observations with TRPML1 activity, and therefore the co-treatment of MK6-83 agonist with BAPTA-AM completely block TRPML1-dependent recruitment of WIPI2 to autophagosomes. Altogether, we confirm the role of lysosomal calcium release, through TRPML1, with early autophagosome formation (fig. 17).

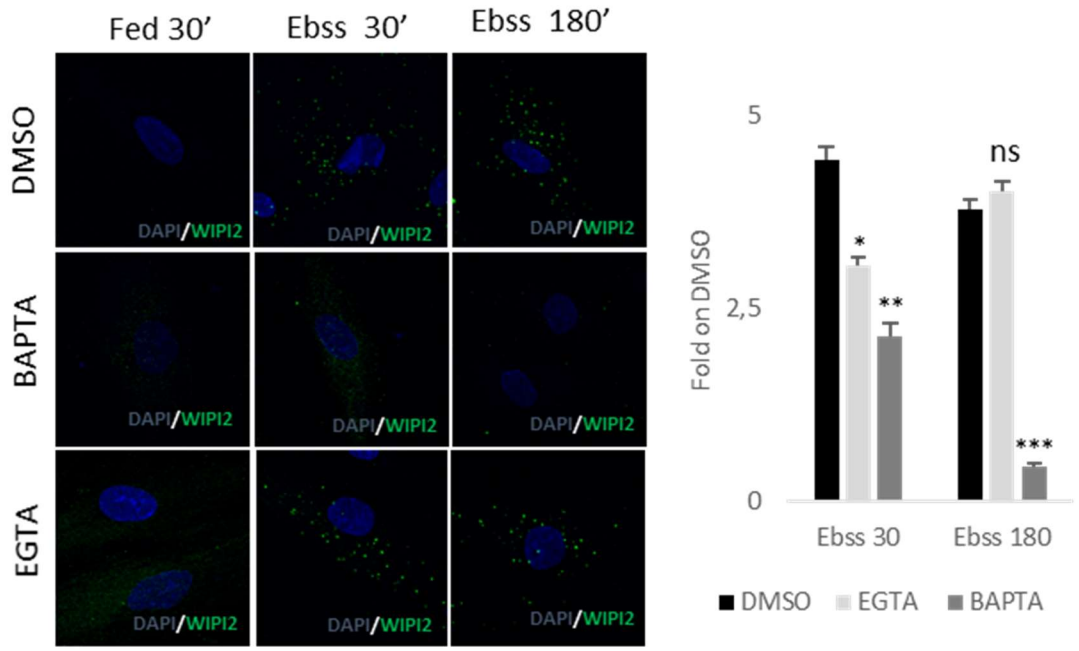

Figure 17: WIPI2 puncta formation is Ca^{2+}- and PI3K- Dependent. Human fibroblasts wild type was starved for 30 and 180 minutes with or without BAPTA or EGTA. An immunofluorescence against endogenous WIPI2 was performed. Number of spots were counted and normalized on cell number, in the bar plot on the right it is reported the fold induction calculated on the DMSO, the experiment was performed 3 times.

Ca^{2+}/calmodulin-dependent protein kinase kinase β(CaMKKβ) has been involved in the autophagic pathway (Hawley et al., 2005, Woods et al., 2005), thus we decide to use both STO-609, a selective inhibitor of CaMKKβ (Tokumitsu et al., 2002), and Calmidazolium (CMDZ) an inhibitor of calmodulin (CaM), which inhibits CaM-dependent phosphodiesterase (Gietzen, 1983). Starvation-mediated WIPI2 puncta formation was significantly reduced when cells are co-treated with STO-609 and CMDZ, respectively (fig. 18 a). Similarly, LC3 puncta formation was significantly reduced in the presence of STO-609 and CMDZ, suggesting that these calcium-dependent proteins are involved in the induction of autophagy upon nutrient deprivation conditions. We discard any effect of these drugs on mTOR pathway by measuring the phosphorylation of pS6 ribosomal protein by immunofluorescence (Fig. 18 b).

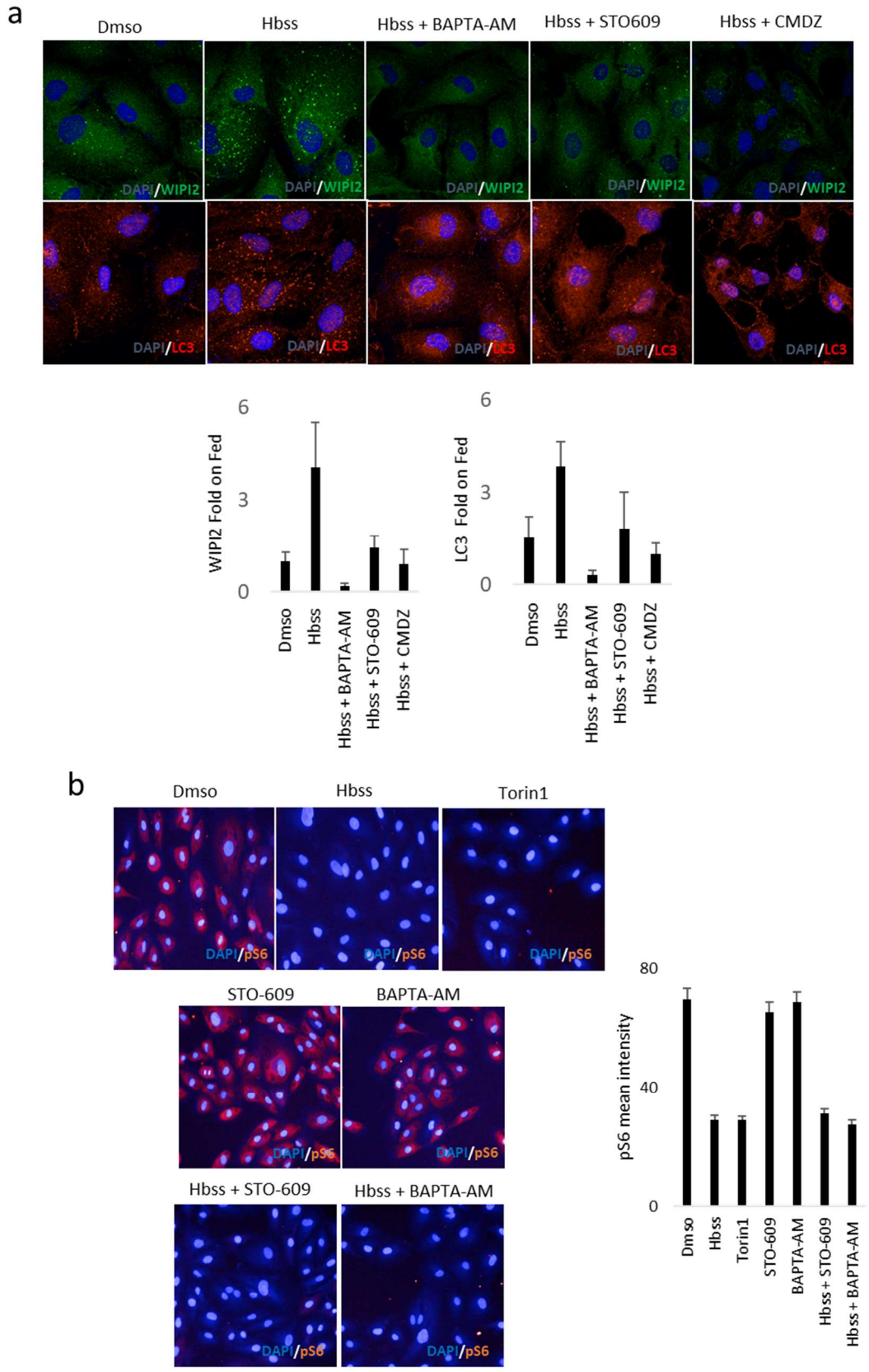

Figure 18: (a) Arpe19 cells were starved with or without STO-609 and CMDZ. An immunofluorescence against endogenous WIPI2 and LC3 was performed. In the lower panel of the figure bar plots shows the fold on Fed condition. (b) Arpe19 were treated with STO6-09 and BAPTA-AM in complete medium or starved in co-treatment with STO6-09, BAPTA-AM. Dmso was used as control of mTORC1 activity, Torin1 and Hbss were used as control for mTORC1 inactivation. An immunofluorescence against pS6 ribosomal protein was performed, the mean intensity was measured and reported in the bar plot on the right.

Since it has been proposed that CaMKKβ induces autophagy throught the phosphorylation of AMPK on threonine 172 (Woods et al., 2005), we asked whether TRPML1 calcium release could be involved in Ca^{2+}- mediated AMPK activation via phosphorylation of T172. Indeed, we found that pharmacological activation of TRPML1 channel activity with MK6-83 induced phosphorylation of AMPK on threonine 172 (T172) in a dose-response manner (fig. 19 a). Furthermore, using the concentration of MK6-83 which induces the highest AMPK phosphorylation, we found that while AMPK is phosphorylated, mTORC1 substrates were not altered (figure 19 a, b). In addition, the acute silencing of TRPML1 inhibits AMPK phosphorylation upon MK6-83 activation, confirming the selectivity of TRPML1-mediated activation of AMPK phosphorylation (fig. 19 a). Together, we propose that TRPML1-mediated induction of autophagosome formation requires Calmodulin and CaMKKβ activation, and the subsequent phosphorylation of AMPK.

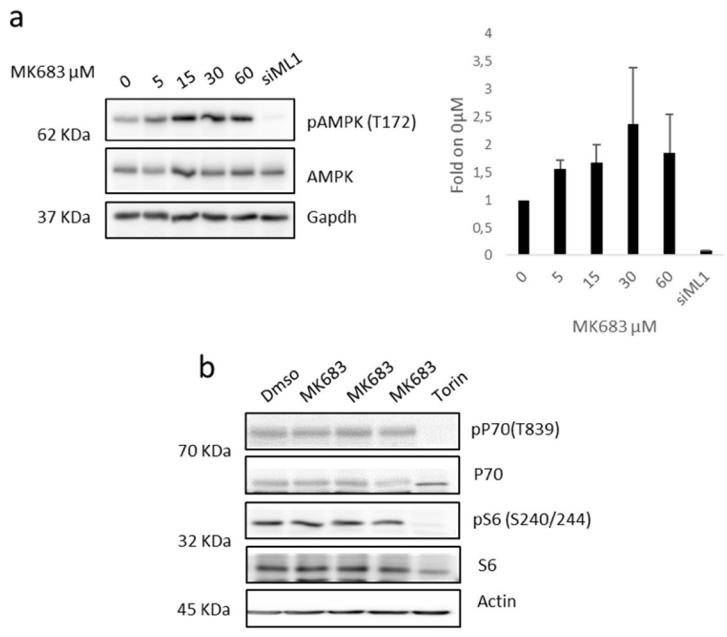

Figure 19: Pharmacological activation of TRPML1 induce AMPK phosphorylation. (a) Western blot showing Arpe19 total protein extract treated with increasing concentration of MK6-83 (from 0 to 60µM). To test the specificity of MK6-83 a sample silenced 72 hours for TRPML1 was used as negative control. Dose response effect of MK6-83 on AMPK phosphorylation was showed in the bar plot on the right. (b) Western blot showing Arpe19 total protein extract treated with 30µM of MK6-83, Torin1 treatment was used as control for mTORC1 inactivation.

PIK3C3 complex is assembling but is less active

The recruitment of WIPI2 and DFCP1 to the nascent autophagosome requires the generation of PtdIns(3)P by the autophagic protein complex PIK3C3 (Marat and Haucke, 2016). Moreover, the recruitment of WIPI2 and DFCP1 is sensitive to PI3K inhibitors, such as wortmannin (Powis et al., 1994). Indeed, we found that wortmannin was able to block WIPI2 puncta formation in cells treated with the TRPML1 activator MK6-83 (fig. 20), suggesting that the induction of autophagosome formation during TRPML1 activation is PIK3-dependent.

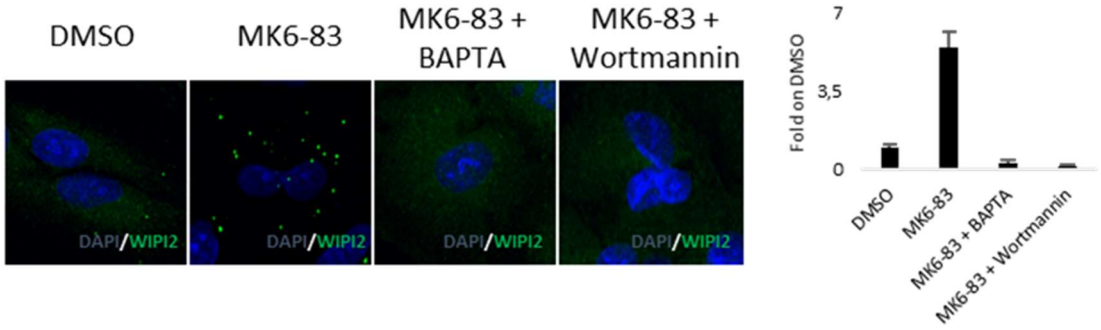

Figure 20: WIPI2 puncta formation is Ca2+- and PI3K- Dependent. Arpe19 cells were treated with 30µM of MK6-83 for 180 minutes in co-treatment with BAPTA or wortmannin. An immunofluorescence against endogenous WIPI2 was performed. Number of spots were counted and normalized on cell number, in the bar plot on the right its reported the fold induction calculated on the DMSO.

Then, we investigated whether the formation of the autophagic PIK3C3 protein complex might be altered in the absence of TRPML1. Thus, we decided to perform a proteomic approach by immunoprecipitating the catalytic subunit VPS34 in both Hap1 WT and Hap1 depleted of TRPML1 cells. Proteomic results clearly showed that there were not significant differences in the formation of PIK3C3 complex in TRPML1 KO cells, since all the major members (Beclin1, and PIK3R4) were present together with UV irradiation resistance-associated gene (UVRAG), which has been proposed to positively regulates autophagic flux (Liang et al., 2006) (Fig. 21 a; tab. 2 and 3). Indeed, we validated these results by immunoprecipitation of the PIK3C3 complex in both cell lines (fig. 21 b, c). Then,

we asked whether TRPML1 inhibition may reduce the activity of the PIK3C3 by monitoring its activity. The experiment was performed in both acute silenced of Arpe19 cells using TRPML1 siRNAs, and in WT or TRPML1 KO Hap1 cells. Upon PIK3C3 immunoprecipitation we determine the amount of PtdIns(3)P produced. In TRPML1 silenced cells the amount of PtdIns(3)P produced was lower if compared with the scramble silenced cells (fig. 21 d). Similarly, in Hap1 TRPML1 KO cells the PtdIns(3)P levels were not detectable compared with WT cells (fig. 21 e). Detection of similar PIK3C3 protein levels by immunoblotting of the same immunoprecipitates confirm the presence of PIK3C3 in the different samples (fig. 21 d, e). Thus, we conclude that TRPML1 may modulate WIPI2 and DFCP1 recruitment to the nascent autophagosome by regulating the activity of the autophagic protein complex PIK3C3.

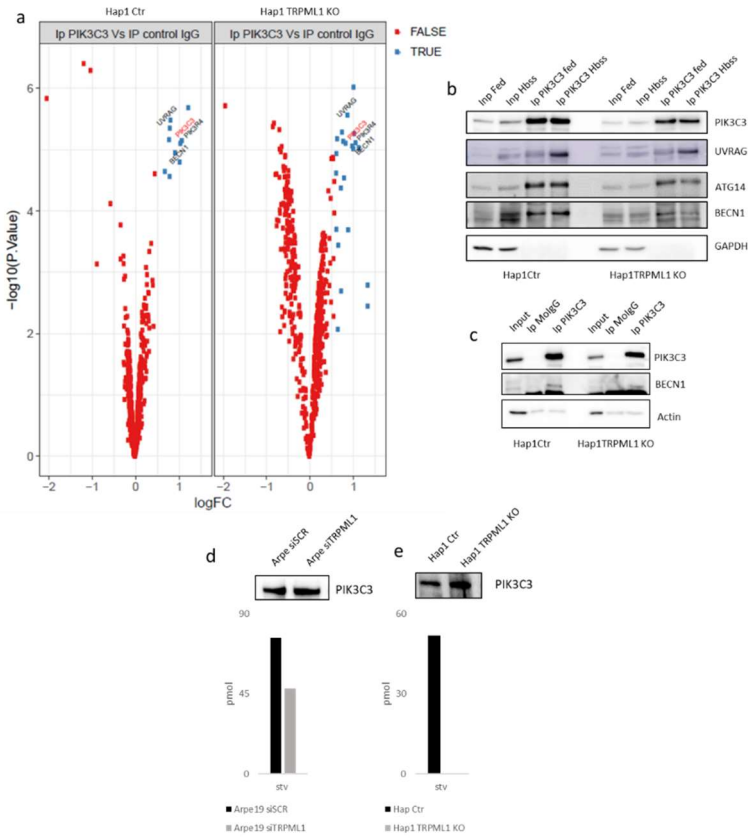

Figure 21: Proteomic analysis on PIK3C3 and PIK3C3 kinase assay. (a) volcano plots show enriched protein compared with control mouse IgG, red spots represent non-specific binding (protein equally present in the mouse IgG), blue spots represent the specific protein enriched. In the plot, the immunoprecipitated protein is written in red, the other member of PIK3C3 complex are written in black, a complete list of all hits is reported in table 1 and 2. (b) western blot showing immunoprecipitation of PIK3C3 in Hap1 Ctr and TRPML1

KO, the immunoprecipitation was performed in fed and during starvation (c) western blot showing immunoprecipitation of PIK3C3 in Hap1 Ctr and TRPML1 KO, the immunoprecipitation was performed only in starvation, in this blot there is also a lane for the mouse IgG for both cell lines.

TRPML1 is required for the localization of ULK1 complex on the isolation membrane

PIK3C3 and its enzymatic product PtdIns(3)P is required, directly or indirectly, for the recruitment of multiple autophagy components (WIPI1, ZFYVE1/DFCP1, ATG5 and LC3) to forming autophagosomes (Polson et al., 2010, Matsunaga et al., 2010). It has been demonstrated that the recruitment of PIK3C3 is mediated by the ULK1 complex. Together the complexes are necessary for the correct autophagy initiation. The ULK1 complex is composed by ULK1, ATG13 and FIP200 and plays a central role in starvation-induced autophagy, it integrates signals from upstream sensors such as mTOR and AMPK and transduces them to the downstream autophagy pathway (Wong et al., 2013). ATG13 is required for the correct localization of the ULK1 complex on the phagophore membrane (Karanasios et al., 2016), thus we used stably ATG13 HEK293 to follow the ULK1 complex during starvation in both normal or TRPML1 depleted cells. In WT cells in normal nutrient conditions ATG13 GFP was mainly distributed all around the cytoplasm, whereas during starvation ATG13 was recruited to a vesicular compartment (Fig. 22). Conversely and in agreement with its role in autophagy initiation, TRPML1 depletion significantly reduced ATG13-GFP puncta formation during starvation (fig. 22), suggesting that TRPML1 signalling activates autophagy initiation through the activation of the ULK1-complex.

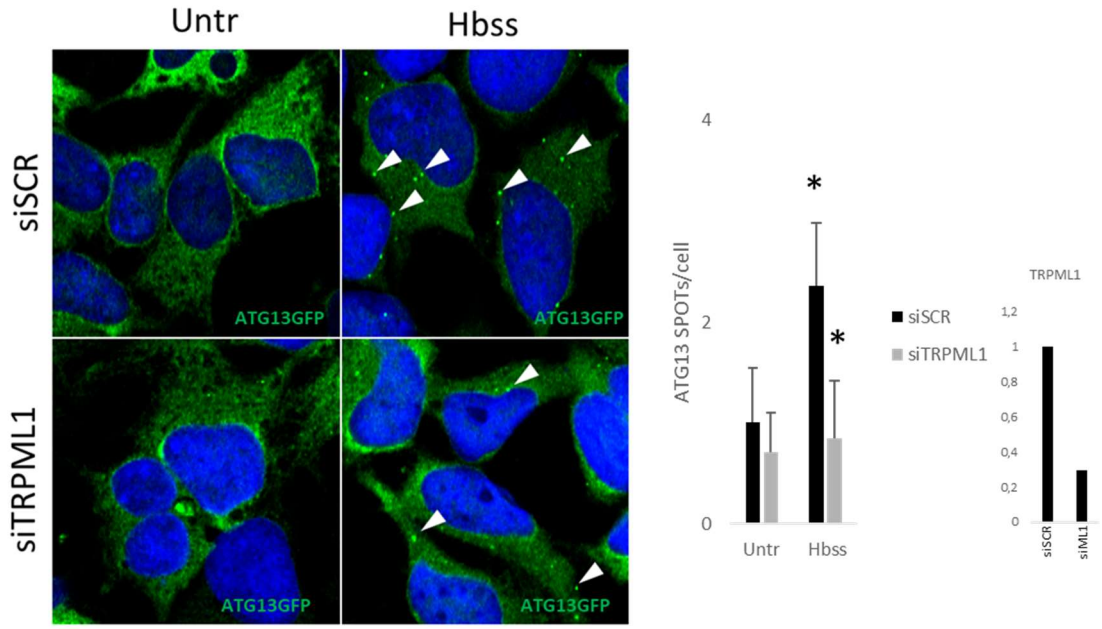

Figure 22: Hek293 ATG13 GFP cells were silenced 72 hours with a siRNA targeting a scramble sequence and one targeting TRPML1, then were starved 180 minutes. Number of ATG13 GFP spots were counted and normalized on cell number as showed in the bar plots on right. An additional bar plot is added and its showing silencing efficiency of TRPML1 by quantitative PCR.

Conclusion

Although both calcium signaling and the lysosomal calcium channel TRPML1 have been already involved in autophagy, these data have been controversial and fragmented in many aspects. In this work we have described how TRPML1 calcium release is crucial for TFEB activation via calcineurin, promoting the transcription of autophagic and lysosomal genes (Medina et al., 2015). This pathway may be crucial for the sustaining of autophagy during autophagy. In addition, here we have described a novel role for TRPML1 mediated lysosomal calcium release in the modulation of autophagy initiation during starvation. Thus, by using both loss-of-function and gain-of-function approaches we showed that TRPML1 is required for the recruitment of PtdIns(3)P-binding proteins DFCP1 and WIPI2 on the nascent autophagosome membrane. In addition and in agreement with a local increase on lysosomal calcium release upon TRPML1 activation, nascent autophagosomes forms in the close proximity of lysosomes and ER regions, suggesting

that PtdIns(3)P nucleation occurs in the vicinity of TRPML1 activation. Hence, silencing of VAPs, implicated in tethering of numerous different membrane contact sites with ER, consistently reduce TRPML1-mediated WIPI2 puncta formation upon MK6-83-mediated activation of TRPML1. Looking at the potential pathways activated during TRPML1-mediated induction of autophagosome formation we found that this process requires both calmodulin and CaMKKβ. We propose that CaMKKβ induces AMPK phosphorylation and therefore the phosphorylation of downstream ULK1 complex, an essential complex during autophagy initiation. Indeed, by looking at the ULK1 protein partner ATG13, we found that the silencing of TRPML1 inhibits ATG13-recruitment to vesicles during starvation. WIPI2 puncta formation requires the generation of PtdIns(3)P by PIK3C3, and we found that although the assembly of this complex is not altered in cells depleted of TRPML1, its activity was significantly reduced compared with WT cells. Therefore, we propose a working model where we hypothesize that during starvation TRPML1 releases lysosomal calcium that activates a calcium-dependent pathway involving CaMKKβ/AMPK signalling that promotes the induction of two essential protein complexes involved in autophagy initiation such as ULK1 and PIK3C3 complexes (fig. 23). In addition, this signaling may be important in the pathology of MLIV disease, is impaired in MLIV fibroblast, and open novel therapeutic opportunities to rescue autophagy induction by using small molecules or calcium ionophores that may bypass TRPML1 disfunction. Therefore, calcium elevating agents such as curcumin has been used in LSDs like NPC disease to rescue lipid accumulation (Lloyd-Evans et al., 2008). Interestingly, TRPML1 activity is inhibited in NPC cells due to the accumulation of sphingosine within lysosomes. Thus, further characterization of autophagy initiation in NPC may reveal similar impairment in the formation of phagophores that can be rescued by promoting downstream effectors of the TRPML1-dependent pathway described here.

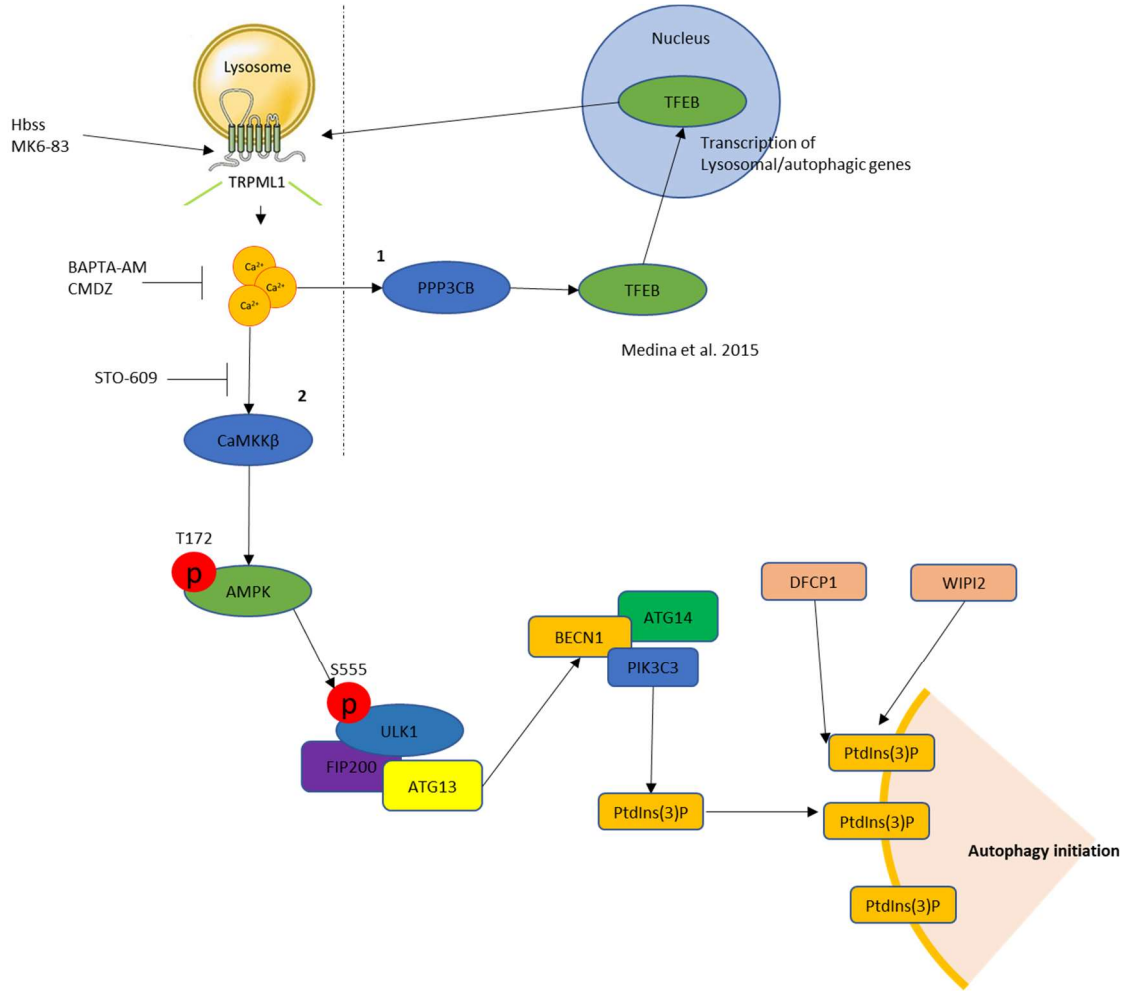

Figure 23: Supposed working model. Calcium release via TRPML1 (mediated by Hbss or MK6-83) act on several processes. (1) Lysosomal calcium via TRPML1 activate PPP3CB which dephosphorylate TFEB that translocate into the nucleus activating the transcription of lysosomal/autophagic genes and in turn modulate TRPML1 too (Medina et al., 2015). (2) Calcium release via TRPML1 could activate CaMKKβ which could act on AMPK that phosphorylate ULK1 that activate autophagic flux via PIK3C3 complex which produce PtdIns(3)P that in turn recruit its effector WIPI2 and DFCP1 required for autophagy initiation.

Methods

Drugs and cellular treatments

The following drugs were used to perform the assays: Torin1 (1uM, otherwise indicated) from Tocris Bioscience; BAPTA – AM (10uM) from Invitrogen; EGTA – AM (5uM) from Santa Cruz biotechnology; MK6-83 (30uM) a gift of Dr. C. Grimm; Bafilomycin A1 (400n) from SIGMA; STO-609 (20uM) from Cayman Chemical; CMDZ (10uM) from Cayman Chemical; wortmannin (5uM) from SIGMA; the starvation medium was prepared with HBSS (Invitrogen), 10mM HEPES (SIGMA).

Cell culture, plasmids and siRNA transfection

Arpe 19, Hek 293 were purchased at ATCC and cultured in DMEM F12 or DMEM supplemented with 10% fetal bovine serum, 200uM L – glutamine, 100uM sodium pyruvate, 5% CO_2 at 37°C. HAP1 (TRPML1 KO; TRPML3 KO; Ctr) were purchased at Horizon and cultured in IMDM supplemented with 10% fetal bovine serum, 200uM L – glutamine, 100uM, , 5% CO_2 at 37°C. Human patient fibroblast CTR, GM02526, GM02525 were purchased at Coriell institute and cultured in DMEM supplemented with 15% fetal bovine serum, 200uM L – glutamine, 5% CO_2 at 37°C. Hek293 DFCP GFP and Hek 293 ATG13 GFP were a gift of Dr Ktistakis and were cultured in DMEM supplemented with 10% fetal bovine serum, 200uM L – glutamine, 100uM sodium pyruvate, 0.8 mg/mL of G418 , 5% CO_2 at 37°C. Cells were silenced with 50nM of siRNA against TRPML1 (sequence: CCUUCGCCGUCGUCUCAAA); VAP-A (sequences: CCACAGACCUCAAAUUCAA; GGCAAAACCUGAUGAAUUA; CCUGAGAGAUGAAGGUUUA; CAAGGAAACUAAUGGAAGA) and VAP-B (sequences: GUAAGAGGCUGCAAGGUGA; CCACGUAGGUACUGUGUGA; UGUUACAGCCUUUCGAUUA; GUAAUUAUUGGGAAGAUUG) for 72 hours using Lipofectamine RNAimax from Invitrogen according to the protocol from manufacture. The plasmid DFCP1 – GFP was a gift of Dr. Carmine Settembre (TIGEM), the plasmid TRPML1 DDKK GFP was a gift of Dr. Xu (Cao et al., 2017). TRPML1 GFP was generated sub cloning the TRPML1 CDS (OriGene) in the PE GFP C3 from Invitrogen between XhoI and EcoRI.

Antibodies and western blotting

For western blots, the following antibodies were used: B-Actin (AC-15, cat. A5441, 1:4000), NBR1 (cell signalling cat. 9891, 1:1000), p62 (BD cat. 610833, 1:1000), WIPI2 (Abcam cat. ab105459, 1:1000), LC3 (Novus NB100-2220, 1:1000), ULK1 (cell signalling cat. 8054 1:1000), Phospho-ULK1 (Ser757) (cell signalling cat. 6888 1:1000), Phospho-

ULK1 (Ser555) (cell signalling cat. 5869 1:1000), p70 S6 Kinase (cell signalling cat. 2708 1:1000), Phospho-p70 S6 Kinase (Thr389) (cell signalling cat. 9205 1:1000), S6 Ribosomal Protein (cell signalling cat. 2317 1:1000), Phospho-S6 Ribosomal Protein (Ser240/244) (cell signalling cat. 5364 1:1000), Phospho-AMPKα (Thr172) (cell signalling cat. 2535 1:1000), AMPKα (cell signalling cat. 5831 1:1000), VAP-A and VAP-B was provided by Dr. Antonella De Matteis laboratory (TIGEM).

Total cell lysate was prepared by solubilization in TRIS HCl 10mM pH 8.0 and 0.2% SDS supplemented with protein and phosphatases inhibitor (SIGMA). To generate soluble and insoluble fraction the protocol used was described in Vergarajauregui S. et al. 2008 (Vergarajauregui et al., 2008a). Protein concentration was determined by the Bradford method.

After SDS-PAGE and immunoblotting the protein recognised by the specific antibody were visualized by chemiluminescence methods (Luminata Crescendo Western HRP substrate, Millipore) using peroxidase-conjugated anti-rabbit or anti-mouse secondary antibodies (Calbiochem). Membranes were developed using a Chemidoc UVP imaging system (Ultra-Violet Products Ltd) and densitometric quantification was performed in unsaturated images using ImageJ (NIH).

Immunofluorescence

For immunofluorescence, the following antibodies were used: WIPI2 (Abcam cat. ab105459, 1:1000), LC3 (cell signalling cat. 2775, 1:100), LAMP1 (Santa Cruz cat. sc-20011, 1:400), PDI (cell signalling cat. 3501s, 1:200), pS6 ribosomal protein (cell signalling 9865s 1:400)

Cells were fixed with ice cold methanol for 5 minutes on ice and permeabilized in 0.1% (w/v) saponin, 0.5% (w/v) BSA and 50 mM NH_4Cl in PBS (blocking buffer). Cells were

incubated with the indicated primary antibodies for 1 hour and subsequently incubated with secondary antibodies. For confocal imaging, the samples were examined under a Zeiss LSM 800 confocal microscope. Optical sections were obtained under a ×63 immersion objective at a definition of 1024 × 1024 pixels (average of eight or sixteen scans), adjusting the pinhole diameter to 1 Airy unit for each emission channel to have all the intensity values between 1 and 254 (linear range). For image analysis Columbus software (Columbus 2.6.0.127073 © Copyright 2008-2017 PerkinElmer) was used.

For super resolution images, samples were examined under a Zeiss LSM 880 super resolution microscope. Optical sections were obtained under a ×63 immersion objective 1.4 oil DIC. To perform 3D reconstruction, we acquired images with pixel size of 0.064µm (x and y), z-step size 0.21 µm (12 images for z-stack). All post processing and 3D reconstruction of the image were performed using ZEN software (Zeiss).

Immuno-electron microscopy

Cells were fixed in a mixture of 4% paraformaldehyde and 0.05% glutaraldehyde prepared in 0.2 M Hepes. Then the cells were washed and incubated with the blocking/ permeabilizing mixture (0.5% BSA, 0.1% saponin, 50 mM NH4Cl) for 30 min and subsequently with the primary antibody against WIPI2, diluted 1:100 in blocking/ permeabilizing solution, overnight. The following day the cells were washed and incubated with the secondary antibody, the anti-rabbit Fab' fragment coupled to 1.4-nm gold particles, diluted 1:50 in blocking/ permeabilizing solution, for 2 h. After this incubation with the antibodies, the gold-enhancement reaction has to be performed to increase the size of the 1.4-nm gold particles. Then samples were post-fixed in a mixture of osmium tetroxide and potassium ferrocyanide, dehydrated in ethanol and acetone and embedded in epoxy resin as described previously (Polishchuk et al., 2014). Thin 60 nm serial sections were cut using a Leica EM UC7 ultramicrotome. EM images were acquired

using a FEI Tecnai-12 electron microscope (FEI, Eindhoven, Netherlands) equipped with a VELETTA CCD digital camera (Soft Imaging Systems GmbH, Munster, Germany).

RNA extraction and quantitative PCR.

Total RNA was extracted from cells using RNeasy Plus Mini Kit (Qiagen). Reverse transcription was performed using QuantiTect Rev Transcription Kit (Qiagen). Real-time quantitative Reverse Transcription PCR (qRT-PCR) was performed using the LightCycler® System 2.0 (Roche Applied Science). HPRT was used for qRT-PCR as reference gene. The parameters of real-time qRT-PCR amplification were according to Roche recommendations. The following primers were used in this study: HPRT fw: tggcgtcgtgattagtgatg, rev: aacacccttttccaaatcctca; TRPML1 fw: gagtgggtgcgacaagtttc, rev: tgttctcttcccggaatgtc; WIPI2 fw: tacctgccttcccaagtgac, rev: agcgagcagatgtttttgtg.

DFCP1 GFP Assay

Arpe19 cells were transfected with TRPML1 or scramble control siRNA using RNAiMax. 48h later the cells transfected with the DFCP1 - GFP construct using Lipofectamine LTX and Plus (Invitrogen), and 24h later serum starved and fixed with ice cold methanol for 5 minutes. Imaging was performed with a 63x Plan Apochromat NA 1.4 DIC oil immersion objective on an LSM 800 confocal microscope (Zeiss). For image analysis Columbus software (Columbus 2.6.0.127073 © Copyright 2008-2017 PerkinElmer) was used.

PIK3C3 Immunoprecipitation, proteomic and kinase activity

After plating cells were starved for 1 hour to increase PIK3C3 complexes. After starvation cells were washed one in ice cold PBS and then twice with Buffer A (20mM TRIS-HCl pH 7.5; 137mM NaCl; 1mM $MgCl_2$; 1mM $CaCl_2$; 100mM NaF; 10mM Na pyrophosphate; 100uM Na_3VO_4). Cells were lysed 20 minutes in Buffer A supplemented with 1% NP-40; 10% Glycerol and protease and phosphatase inhibitor (buffer recipe from Echelon). After

10 minutes of centrifugation at max speed 4°C, supernatant was collected and quantified as described in antibodies and wester blotting. 2mg of protein extract was incubated o/n at 4°C with 2ug of PIK3C3 antibody (Santa Cruz cat. SC365404). Subsequently 40uL of protein A/G agarose conjugated (Santa Cruz cat. SC2003) was incubated for 2h at 4°C. Once the immunoprecipitation was completed the PIK3C3 enzyme bound to the agarose beads was used for western blot analysis, proteomic and PIK3C3 kinase assay. For western blot and proteomic, the enzyme was eluted by adding sample buffer 2X and boiled 5 minutes at 95°C, then was separated on acrylamide gel. For proteomic analysis, we send the gel to EMBL facility in Hidelberg. For PIK3C3 kinase activity we use Cell III PI3-Kinase Kit from echelon (cat. K-3000) and we follow kit instruction.

Tables

Table 2: Complete proteomic hits list. This table shows the protein enriched in the Ip of PIK3C3 in Hap1 Ctr cells and was obtained normalizing the results with an Ip of Mouse IgG in the same cell lines. A linear modeling approach was used to analyze the data using the limma package in R/Bioconductor.

Gene name	Description	logFC	P.Value
DLST	Dihydrolipoyllysine-residue succinyltransferase component of 2-oxoglutarate dehydrogenase complex, mitochondrial	1.23E+00	2.07E-06
EIF2AK2	Interferon-induced, double-stranded RNA-activated protein kinase	8.21E-01	3.30E-06
UVRAG	**UV radiation resistance-associated gene protein**	**8.07E-01**	**4.46E-06**
OGDH	2-oxoglutarate dehydrogenase, mitochondrial	7.91E-01	6.90E-06
PIK3C3	**Phosphatidylinositol 3-kinase catalytic subunit type 3**	**1.08E+00**	**7.15E-06**
PIK3R4	**Phosphoinositide 3-kinase regulatory subunit 4**	**1.05E+00**	**7.91E-06**
CBFA2T2	Protein CBFA2T2	9.27E-01	1.12E-05
BECN1	**Beclin-1**	**1.04E+00**	**1.60E-05**
EML3	Echinoderm microtubule associated protein like 3, isoform CRA_e	6.93E-01	2.27E-05
GBF1	Golgi-specific brefeldin A-resistance guanine nucleotide exchange factor 1	8.05E-01	2.75E-05

Table 3: Complete proteomic hits list. This table shows the protein enriched in the Ip of PIK3C3 in Hap1 TRPML1 KO cells and was obtained normalizing the results with an Ip of Mouse IgG in the same cell lines. A linear modeling approach was used to analyze the data using the limma package in R/Bioconductor.

Gene name	Description	logFC	P.Value
EIF2AK2	Interferon-induced, double-stranded RNA-activated protein kinase	1.02E+00	9.60E-07
UVRAG	**UV radiation resistance-associated gene protein**	**8.80E-01**	**2.73E-06**
TAF15	TATA-binding protein-associated factor 2N	7.53E-01	5.20E-06
DLST	Dihydrolipoyllysine-residue succinyltransferase component of 2-oxoglutarate dehydrogenase complex, mitochondrial	1.04E+00	5.47E-06
DKC1	H/ACA ribonucleoprotein complex subunit 4	6.42E-01	6.65E-06
OGDH	2-oxoglutarate dehydrogenase, mitochondrial	7.82E-01	7.36E-06
PIK3C3	**Phosphatidylinositol 3-kinase catalytic subunit type 3**	**1.07E+00**	**7.70E-06**
EML3	Echinoderm microtubule associated protein like 3, isoform CRA_e	8.38E-01	7.87E-06
GBF1	Golgi-specific brefeldin A-resistance guanine nucleotide exchange factor 1	9.88E-01	8.74E-06
BECN1	**Beclin-1**	**1.14E+00**	**9.32E-06**
PIK3R4	**Phosphoinositide 3-kinase regulatory subunit 4**	**1.01E+00**	**9.65E-06**
NOP58	Nucleolar protein 58	6.25E-01	1.16E-05
CAPRIN1	Caprin-1	6.19E-01	2.42E-05
NOP56	Nucleolar protein 56	8.00E-01	2.89E-05
CBFA2T2	Protein CBFA2T2	7.31E-01	4.23E-05
MATR3	Matrin-3	6.25E-01	2.00E-04
RASAL2	Ras GTPase-activating protein nGAP (Fragment)	8.96E-01	2.03E-04
LMNB1	Lamin-B1	6.67E-01	3.62E-04
HIST1H3A	Histone H3.1	1.35E+00	1.62E-03
RTCB	tRNA-splicing ligase RtcB homolog	7.36E-01	2.02E-03
HIST1H4A	Histone H4	1.34E+00	3.57E-03
HNRNPC	Heterogeneous nuclear ribonucleoproteins C1/C2	6.59E-01	8.50E-03

Chapter 2

TRPML1 as target for treating lysosomal storage diseases: a high content screening approach

Abstract

In this work, we have investigated the role of TRPML1-mediated lysosomal signaling in the modulation of the autophagic and lysosomal pathways. We have found that TRPML1 modulates autophagy at the transcriptional level by inducing TFEB at the initial steps of autophagosome formation during starvation. Since mutations in TRPML1 cause a severe human LSD, called mucolipidosis type IV (Sun et al., 2000, Bassi et al., 2000, Bargal et al., 2000), our findings might be of interest to develop novel therapeutic approaches to identify correctors of cellular defects related with this disease. Thus, we investigated two different approaches; 1) Identify TFEB inducers in MLIV cells from a collection of FDA drugs able to promote TFEB nuclear translocation in WT cells, and; 2) Develop a primary high content screening assay aimed at identifying FDA-compounds promoting the clearance of cholesterol in human MLIV cells. Together, these two screening assays resulted in the identification of 9 compound hits able to restore TFEB signalling and promote lipid storage clearance in human fibroblast from MLIV patients.

Introduction

Lysosomes are membrane-bound organelles that contain an acidic lumen and several hydrolases that are devoted to the degradation of specific substrates. In addition, the lysosomal membrane contains proteins that are involved in the transport of substances into and out of the lumen, acidification of the lysosomal lumen and fusion of the lysosome

with other cellular structures. In addition to the central role of lysosomes in the degradation of extracellular and intracellular substrates, lysosomes can also secrete their content by fusing with the plasma membrane (lysosomal exocytosis), and recently the lysosome has been implicated in nutrient sensing and in signalling pathways that are involved in cell metabolism and growth (Settembre et al., 2012, Settembre et al., 2013). Lysosomal dysfunction has been associated with several human diseases, as well as with the process of ageing, which may be associated with a decline in lysosomal function and a progressive accumulation of intracellular material (for example, lipofuscin and ubiquitin). Thus, genetic defects in specific lysosomal components lead to the accumulation of substrates that are not degraded in the lysosomal lumen, followed by progressive lysosomal dysfunction in several tissues and organs. These disorders are known as lysosomal storage diseases (LSDs). Approximately 60 different types of LSDs have been recognized. Historically, LSDs have been classified on the basis of the type of material that accumulates in the lysosomes, such as mucopolysaccharides, sphingolipids, glycoproteins, glycogen and lipofuscins. LSDs often show a multisystemic phenotype that is associated with severe neurodegeneration, mental decline, cognitive problems and behavioural abnormalities. More than 20 loss-of-function (LOF) mutations of TRPML1 have been associated with a LSD called mucolipidosis type IV (MLIV) which is characterized by psychomotor retardation and achlorhydria (Xu and Ren, 2015, Altarescu et al., 2002). The symptoms typically manifest in the first years of life, and there is still no cure to treat patients affected by this disorder. MLIV-affected cells show accumulation of aberrant lysosomes filled with auto-fluorescent lipid material, including cholesterol (Li et al., 2016). In addition, lysosomal dysfunction results in a partial block of autophagy that is characterized by the accumulation of autophagic markers such as LC3 and p62 (Vergarajauregui et al., 2008a). Interestingly, both the accumulation of lipids as well as

disturbed lysosomal Ca^{2+} homeostasis have been described in different LSDs and in some cases, have been proposed to involve TRPML1. Indeed, it has been demonstrated that in Niemann-Pick type A-C disease, the prolonged accumulation of cholesterol, sphingomyelins, sphingosine and glycosphingolipids leads to the progressive impairment of TRPML1 function suggesting that defective TRPML1 activity may be part of the pathogenic mechanisms in many LSDs (Xu and Ren, 2015) (Shen et al., 2012).

In chapter 1 of my thesis we have demonstrated the existence of a signalling that starts at the lysosomes in which Ca^{2+} release via TRPML1 plays a major role in lysosomal adaptation to starvation by activating the Ca^{2+}-dependent phosphatase calcineurin that de-phosphorylates TFEB inducing its nuclear translocation (Medina et al., 2015). Most importantly, it has been showed that TFEB overexpression promotes cellular clearance in different LSDs by inducing lysosomal exocytosis, a process that also requires TRPML1-dependent Ca2+ release (Medina et al., 2011). Indeed, TFEB overexpression increases the number of the lysosomes in the proximity of the plasma membrane and promotes their fusion upon a rise in calcium concentration (Medina et al., 2011). Thus, the identification of compounds which promote clearance in MLIV cells by using cell-based High Content (HC) screening of drugs (including FDA-approved molecules) may represent a novel therapeutic approach to clear lysosomal storage in Mucolipidosis type IV.

Results and discussion

1. (HC)-screening TFEB relocator molecules in MLIV patient fibroblasts

We have recently described a new lysosomal signaling involving TRPML1 during nutrient starvation. By using a siRNA-mediated High Content screening to identify the phosphatase(s) that dephosphorylates and activates TFEB, we have found that inhibition of the Ca^{2+}-activated serine/threonine phosphatase calcineurin prevents the nuclear translocation of TFEB in starved cells. Moreover, by using a genetically-encoded

lysosomal Ca_{2+} sensor fused to TRPML1 (GCaMP-ML1), we found that upon nutrient starvation the activity of this channel increases, suggesting that starvation triggers the release of microdomains of Ca^{2+} from the lysosome (Medina et al., 2015). In agreement with these data, TRPML1 overexpression or agonist-mediated activation of TRPML1 induce TFEB nuclear translocation (*see Chapter 1 Fig. 10 a, b*). Thus, starvation specifically induces lysosomal Ca^{2+} release through TRPML1 generating a Ca^{2+} microdomain that is responsible for calcineurin activation and TFEB de-phosphorylation in the proximity of the lysosomal membrane (Medina et al., 2015). As TFEB transcriptionally regulates autophagy and lysosomal exocytosis, we investigated whether the modulation of this newly identified lysosomal signaling pathway, involving TRPML1, modulates these functions. We found that TRPML1 overexpression induces autophagy as measured by the elevation of the autophagic marker LC3 (*see Chapter 1 Fig. 16 b, c*) and induces cellular clearance in multiple sulfatase deficiency (MSD), a neurodegenerative LSD (Medina et al., 2015) (Medina et al., 2011). Conversely, human MLIV-affected fibroblasts presented a reduction in starvation- mediated TFEB nuclear translocation, impaired lysosomal exocytosis (Medina et al., 2011) and accumulated autophagic substrates such as p62 and NBR1 (Vergarajauregui et al., 2008a). Our previous data demonstrated that TRPML1 could be targeted to promote clearance through the activation of TFEB (Medina et al., 2011). In an MLIV disease context this cannot happen and alternative strategies need to be investigated. By combining a TFEB nuclear translocation assay and (HC) imaging we previously collected compounds able to induce TFEB nuclear translocation in HeLa cells. The next step was to assay them again to understand which of them have a mechanism of action that relies on TRPML1 activity. To do so, we developed a (HC) imaging assay to follow endogenous TFEB localization in both WT and MLIV human fibroblasts.

In order to identify whether previously identified compounds inducing TFEB nuclear translocation may promote the same nuclear translocation in TRPML1 depleted cells, we screened 150 TFEB relocators in human MLIV fibroblasts. We screened for the ability of these 150 compounds to induce endogenous TFEB nuclear translocation in both WT and GM02526 MLIV patient cells after 3 hours of treatment. The plates were analysed using Columbus software (© Copyright 2008-2017 PerkinElmer). We projected a script which, with the help of macros, segmented the cells in two regions (cytoplasm and nucleus). In figure 1 there is an example of the macro used for this analysis and in table 2, in Tables paragraph at the end of this chapter, is reported the complete script sequence (Fig. 24, tab. 4).

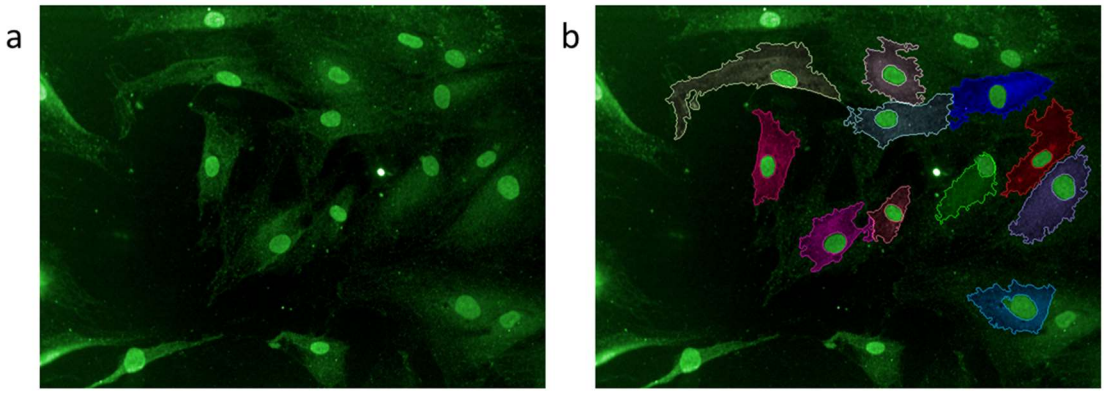

Figure 24: Example of Columbus macro. (a) Human fibroblasts treated with Torin1, cells were then stained with endogenous TFEB (in green). (b) Same figure showed in panel a, with different colors are highlighted cells identified by Columbus software. The object (cells) touching the edges of the field where excluded from the analysis.

The mean fluorescence of nuclear and cytoplasmic regions was calculated by the software. The selection of the Hits was based on the percentage of the cells that showed a high nuclear TFEB fluorescent intensity 3 standard deviation above the positive control represented by Torin1. Interestingly, we found that only 2 (compound 28 and compound 31) out of 150 compounds were able to induce endogenous TFEB nuclear translocation

independently of the presence of MCOLN1 (fig. 25), confirming the major role of TRPML1 in the regulation of TFEB and therefore lysosomal function.

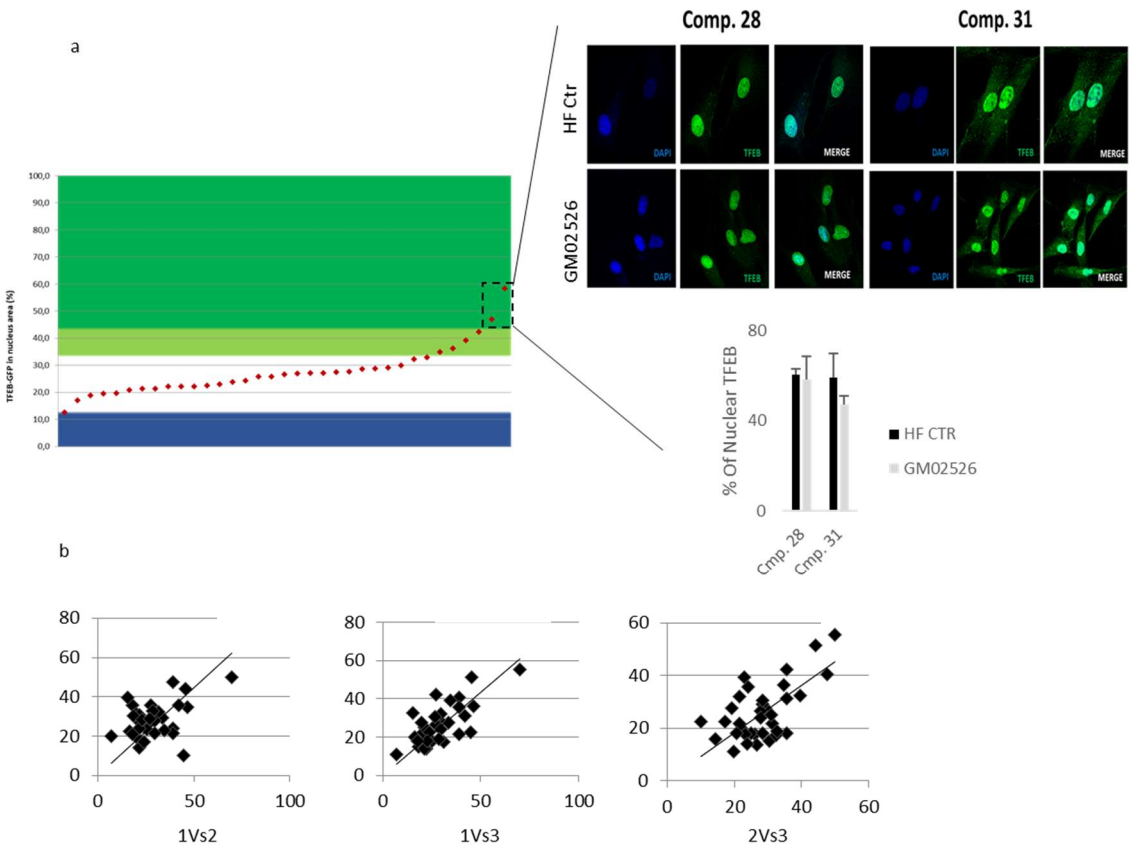

Figure 25: (HC)-screening of 150 TFEB relocator molecules in MLIV cells. (a) distribution of the mean value of % of nuclear TFEB, in the dotted box the two HITs are highlighted, the two Hits were selected since their value of % of nuclear TFEB was above 3 standard deviation. (b) The screening was performed in triplicate and the plots showed the correlation analysis among the 3 replicas.

Since TFEB nuclear translocation is also regulated by the activity of mTORC1 complex, we asked whether the TFEB nuclear translocation induced by these two hits may be the result of mTORC1 inhibition. However, compound testing in a high content assay measuring the phosphorylation of a second level mTORC1 substrate, the ribosomal protein S6 (S6), did not show any reduction in such phosphorylation (fig. 26), indicating that these compounds induce TFEB nuclear translocation in both a MCOLN1 and mTORC1 independent manner.

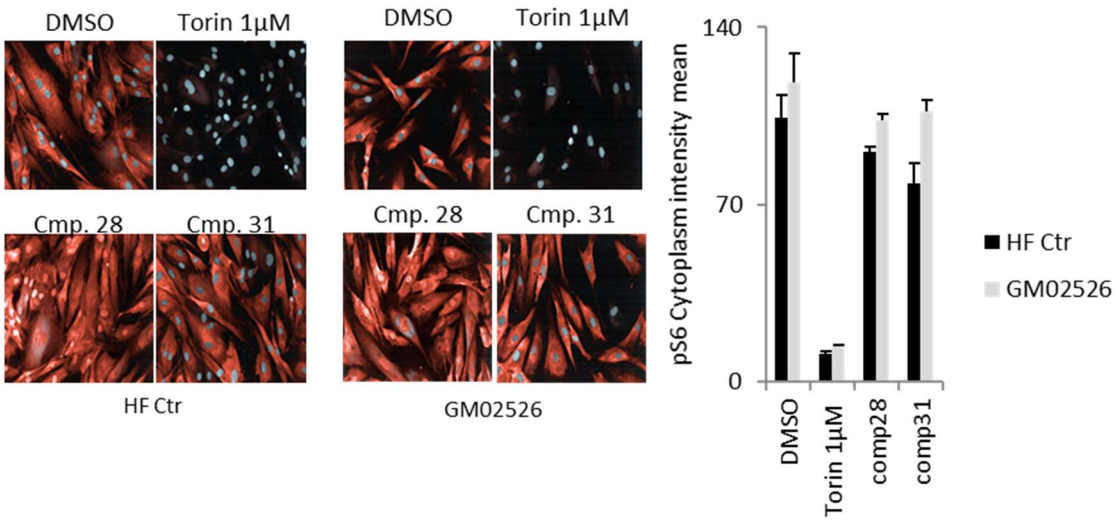

Figure 26: mTOR activity is not altered by compound 28 and 31 treatments. This figure showed immunofluorescence against endogenous phosphorylated residues of S6 ribosomal protein (S235/236) conjugated with a 594nm secondary antibody. Is clear from the image that the huge effect on mTOR inhibition was given by Torin1 which was used as positive control. The plot on the right showed the quantification of fluorescent intensity inside cytoplasm, the experiment was performed in triplicate.

Furthermore, since our main purpose was the identification of compounds able to promote cellular clearance in human MLIV fibroblasts, we analysed relevant pathological features observed in cells, such as autophagy impairment, lipofuscin accumulation and cholesterol storage (Vergarajauregui et al., 2008a, Soyombo et al., 2006). Thus, we first confirmed that autophagic substrates such as P62 accumulate in human MLIV fibroblast (Vergarajauregui et al., 2008a). Interestingly, we also found that another autophagic substrate, NBR1 (Kirkin et al., 2009), accumulates in the insoluble fractions of MLIV protein extracts (fig. 27 a). In addition, by using flow cytometry, we found that MLIV fibroblasts also show an elevation of auto fluorescence, suggesting that our cellular model is accumulating lipofuscin (fig. 27 b).

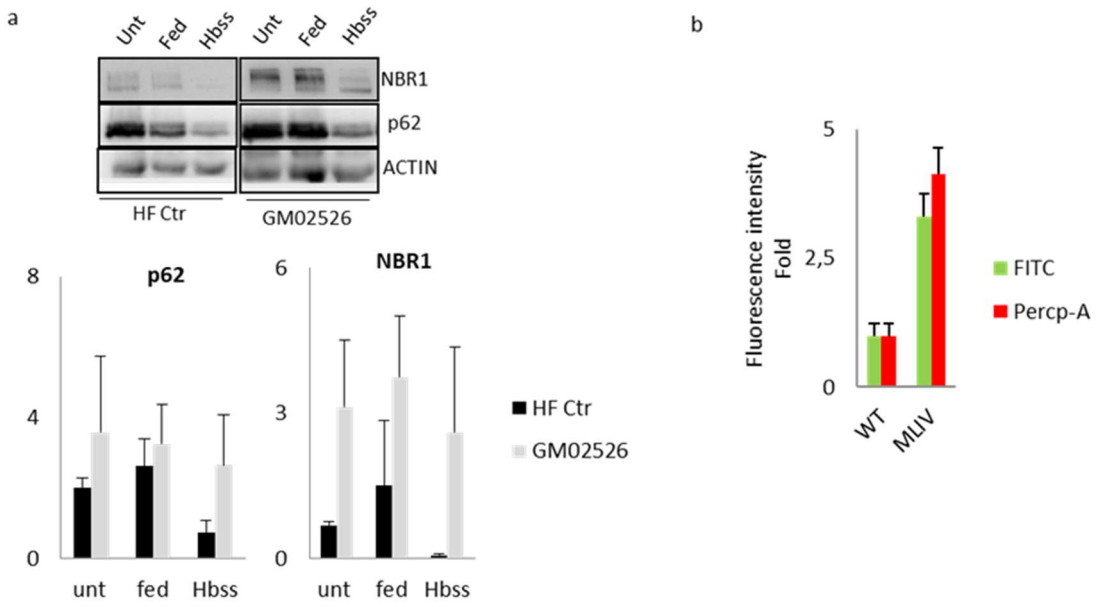

Figure 27: Development of secondary assays. (a) Western blots of insoluble fraction of human fibroblast ctr and GM02526, the bar plot represents the quantification of 3 independent experiment. (b) Bar plot showing the increase of auto fluorescent material stored in MLIV cells (GM02526) compared with WT cells. Using the BD FACS Aria III cells were excited with 488nm laser then the emission with 2 different filters was measured. In green is reported the emission with FITC (530/30nm) in red the emission with PerCP-A (695/40nm). The plot showed the average of mean fluorescent intensity from 3 different experiment.

MLIV is characterised not only by the accumulation of autophagic cargo but also lipids. Indeed, by using a novel reporter of cholesterol accumulation PFO-GST (Kwiatkowska et al., 2014) in human MLIV cells (GM02526 and GM02527) and WT, we also found a significant increase of such lipid in disease cells compared with WT counterpart. We used the latter results to develop a second (HC)-screening assay to test the ability of our compounds to reduce cholesterol storage in MLIV cells (see sub-paragraph 2). As positive control, we used the cholesterol-depleting compound cyclodextrin, that has been shown to reduce cholesterol accumulation in Niemann Pick C patient cells (Rosenbaum et al., 2010). Starting from this characterization we decided to test the selected Hits in these secondary assays. First of all, we tested the ability of the 2 compounds to induce autophagic substrate clearance (p62 and NBR1 cargo (Lamark et al., 2009)) and we found

that only the compound 28 was able to reduce both p62 and NBR1 accumulation at different time-points in human GM02526-MLIV fibroblasts (fig. 28).

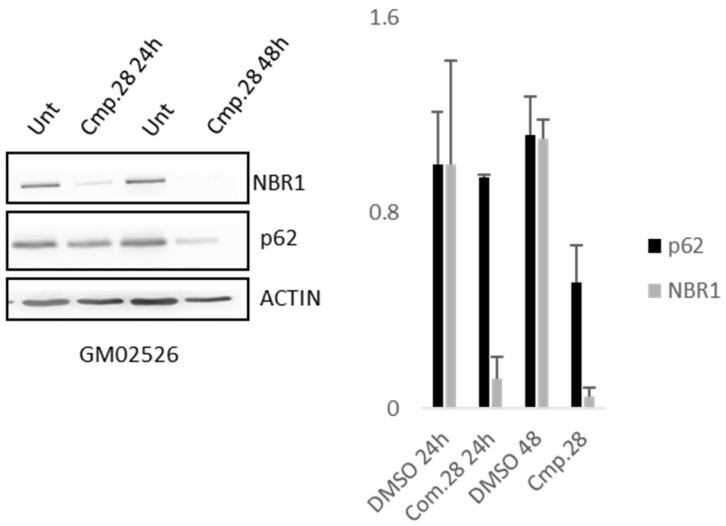

Figure 28: Compound 28 ameliorates autophagic phenotype of MLIV cells. (a) Western blot showing the decrease of autophagic cargo p62 and NBR1 after cmp.28 treatment (24 and 48 hours) on insoluble fraction from GM02526 patient cell line. The bar plot on the right showed the quantification of 3 different experiment.

Furthermore, we tested also the compound 28 for cholesterol clearance in two different MLIV patient fibroblast cell lines (GM02526 and GM02527). While with cyclodextrin we observed a clear cholesterol reduction, the efficacy of compound 28 was not so elevated as the clearance effect on p62 and NBR1 accumulation (fig. 29).

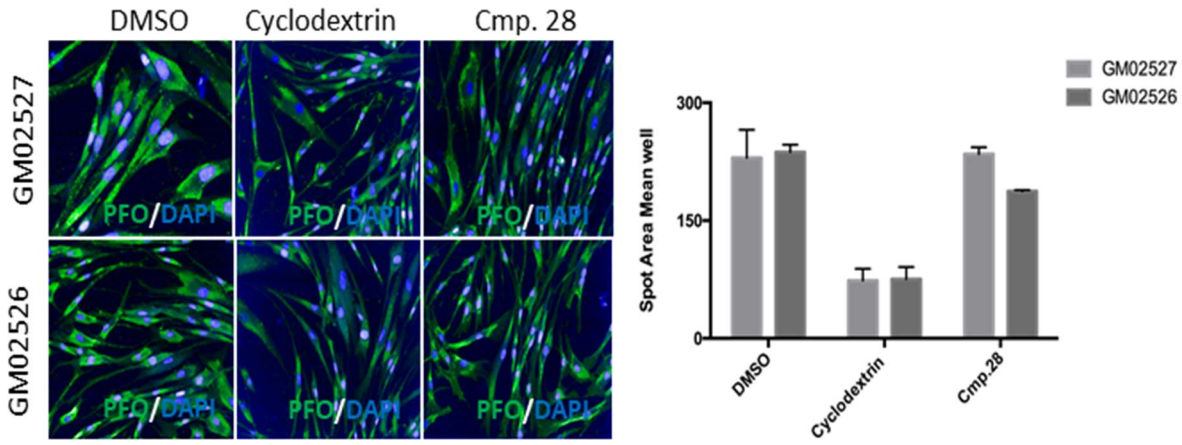

Figure 29: Cmp.28 partially decreases cholesterol accumulation in GM02526 cell line. To emphasize the cholesterol staining the cells were pretreated with U18666A. Immunofluorescence with PFO-GST to stain the cholesterol accumulation in MLIV cells. The experiment was performed in triplicate.

While performing our secondary assay we observed some toxicity for compound 28. Thus, in collaboration with bioinformatic core at TIGEM we tried to identify potential analogues by using a new computational approach called MANTRA which exploits similarities between drug-induced transcriptional profiles already available in public databases (Carrella et al., 2014). We run the analysis to screen for drugs presenting a similar transcriptional profile to the one generated by compound 28 (fig. 30 a). Among the network of drugs with a significant "proximity" to Compound 28 hit we generated a sub-library of 121 compounds. We screened this new sub-library formed by compound 28 analogues for TFEB nuclear translocation. We screened both wild type and MLIV fibroblast and finally we selected the common Hits. We identified 2 out of 121 which promote TFEB nuclear translocation in both cell lines (fig. 30 b, c, d). Together, we have identified compound 28 which was able to induce TFEB nuclear translocation and clearance of autophagic substrates in MLIV cellular models. In addition to act in the absence of TRPML1, this compound hit is not inducing TFEB nuclear translocation through the inhibition of mTOR. In addition, by looking among compound 28 analogues we identified other two compounds which could exploit the same effect of compound 28 but

with less toxicity. Further analysis of the signaling activated by these compounds is needed to identify the potential mechanism of action.

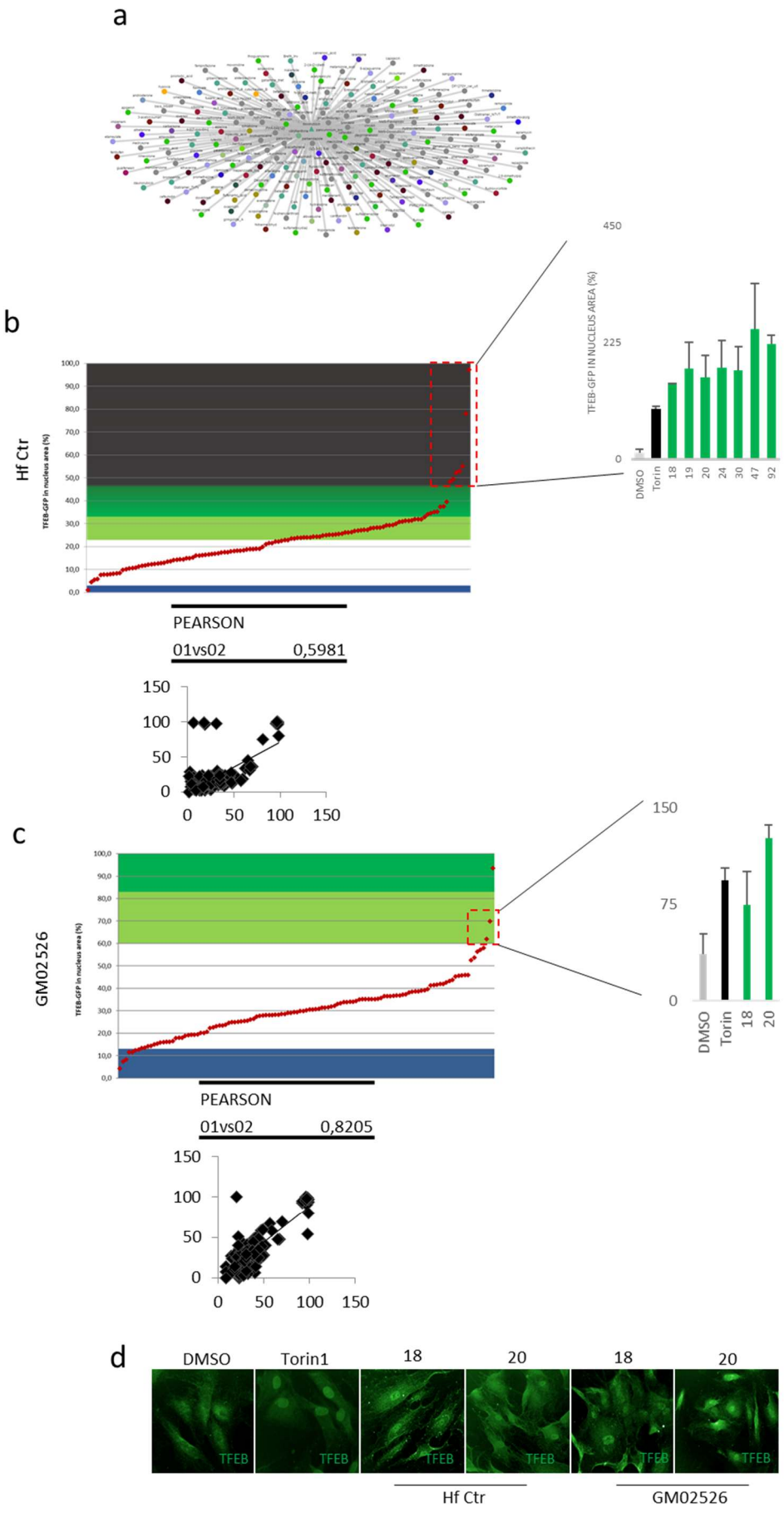
a
b
Hf Ctr
TFEB-GFP in nucleus area (%)
PEARSON
01vs02 0,5981
TFEB-GFP IN NUCLEUS AREA (%)
DMSO
Torin
18
19
20
24
30
47
92
c
GM02526
PEARSON
01vs02 0,8205
d
DMSO
Torin1
18
20
TFEB
Hf Ctr
GM02526

Figure 30: (a) Transcriptional network generated with MANTRA starting from compound 28. (b) Analogues of compound 28 were tested on human wild type fibroblasts (Hf Ctr) for 3 hours, the plot shows the distribution of the mean value of % of nuclear TFEB, in the dotted box the 7 HITs are highlighted, Hits were selected since their value of % of nuclear TFEB was above 3 standard deviation from DMSO. (c) Analogues of compound 28 were tested on MLIV fibroblasts (GM02526) for 3 hours, the plot shows the distribution of the mean value of % of nuclear TFEB, in the dotted box the 2 HITs are highlighted. Hits were selected since their value of % of nuclear TFEB was above 1 standard deviation from DMSO. (d) Representative images of compound 18 and 20 which promote TFEB nuclear translocation in both cell lines. Dmso and Torin1 have been used as negative and positive control respectively for TFEB translocation.

2. *(HC)-screening of whole FDA library to identify compounds that reduce cholesterol accumulation in MLIV fibroblasts*

The second primary (HC)-screening assay was based on a cholesterol reduction assay. It has been reported that MLIV fibroblasts accumulate cholesterol within lysosomes (Soyombo et al., 2006), thus we decided to design a cellular based assay focused on cholesterol reduction. To stain cholesterol we used a novel approach based on the use of the protein toxin of microbial origin perfringolysin O conjugated with GST (PFO-GST) (kindly provided by Dr. Sobota from the Nencki Institute of Experimental Biology) (Kwiatkowska et al., 2014). PFO-GST specifically recognizes free cholesterol avoiding the drawbacks of other dyes such as filipin. PFO-GST labelling can be performed in fixed samples making this approach highly suitable for (HC)-screening. In addition, the cells could be permeabilized and co-stained with other markers such as LAMP1, and therefore we can measure the quantity of cholesterol accumulation within the lysosome. As part of the assay validation, we used this approach in two MLIV patient cell lines (GM02526 and GM02527) as well as in control fibroblasts. We designed a specific script to quantify PFO-GST staining (fig. 31) and analysed several parameters to select the one that offers the best signal window to perform a screening (fig. 31 a). First of all, we evaluate the fluorescent intensity of 488nm channel in the whole cytoplasm, without having huge variation among cell lines and treatments, thus we decided to measure the fluorescence intensity restricted to the spot region (highlighted in red in figure 31). The complete script

sequence is reported in table 3 in Tables paragraph at the end of this chapter (fig. 31, Tab. 5).

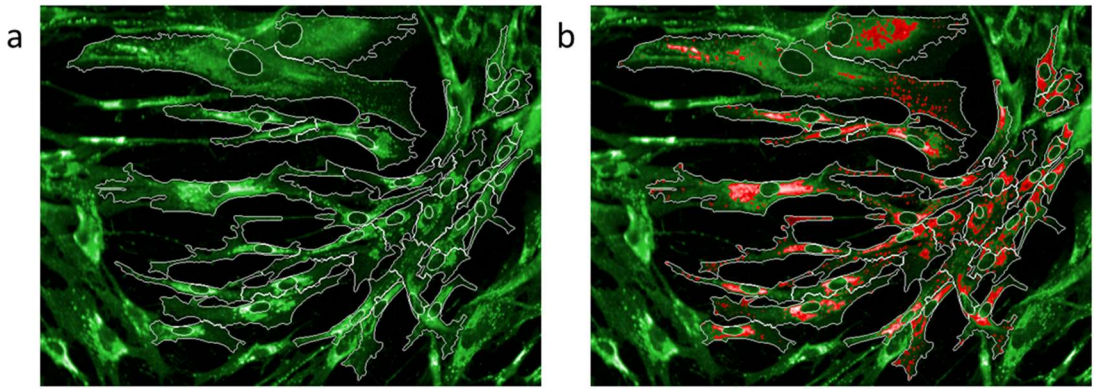

Figure 31: Example of Columbus macro. (a) Human fibroblasts GM02527 stained with PFO-GST with white line are highlighted cell regions (nucleus and cytoplasm). (b) same image reported in panel a. In red is highlighted area occupied by cholesterol storage. The object (cells) touching the edges of the field where excluded from the analysis.

To further increase the signal window, we pre-treated the cells with U18666A, this drug inhibits three membrane-bound enzymes in sterol synthesis that catalyse very different reactions (a ring-forming cyclase, an isomerase, and a reductase), furthermore, it blocks the egress of cholesterol and other molecules from lysosomes and the movement of cholesterol from the plasma membrane to the endoplasmic reticulum. For all these reasons, it represents a versatile chemical tool used to address questions on control of cholesterol biosynthesis and intracellular trafficking of cholesterol (Cenedella, 2009, Liscum and Faust, 1989). As positive control of cholesterol clearance, we used cyclodextrin that has been reported to reduce cholesterol storage in Niemann pick type C disease cells (fig. 32 b) (Liu, 2012).

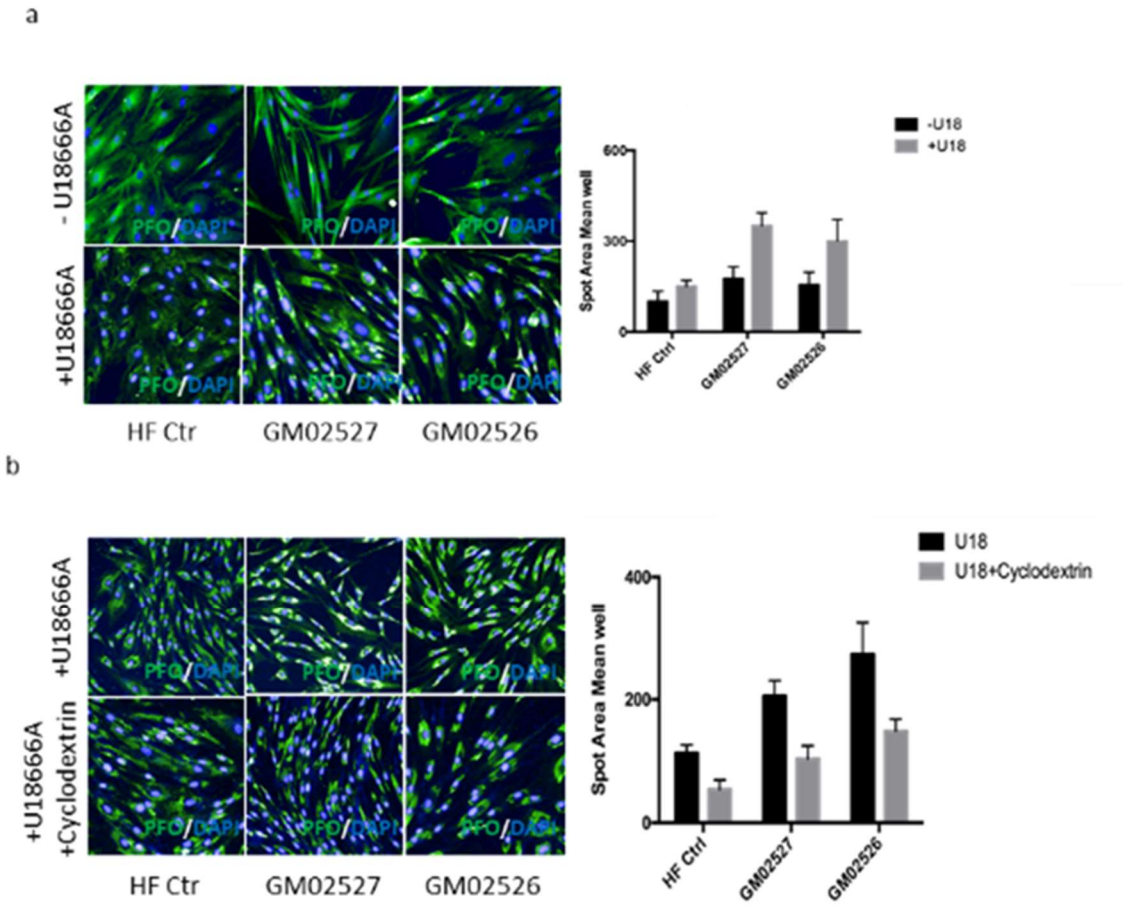

Figure 32: Selection of (HC)-screening parameters. (a) Immunofluorescence on control fibroblast (HF Ctr) and MLIV (GM02527, GM02526) untreated or pretreated with the cholesterol accumulating-drug U18666A and stained with recombinant PFO-GST. The plot on the right showed the intensity of 488nm emission in the area of the spot, the experiment was performed in triplicate b – Cyclodextrin reduces cholesterol accumulation in both WT and MLIV fibroblasts. The plot on the right showed the intensity of 488nm emission in the area of the spot, the experiment was performed in triplicate.

After the validation and selection of our cholesterol assay parameters, we have screened the full Prestwick Chemical Library®, composed by a collection of 1280 FDA-approved drugs, in the MLIV cell line GM02527. The screening was performed in triplicate, each plate was treated 16 hours with U18666A, then the drugs were added for 48 hours. We obtained 9 total HITs. Subsequently, FDA101 was discarded since visual inspection of the acquired images revealed that this drug is auto-fluorescent in both the 405nm and 488nm channels. Figure 33 and figure 34 show some images coming from the screening and a complete list of the selected HITs is available in table 1 at the end of this chapter in

Table paragraph (Fig. 33 and 34, and table 6). These hits will need further validation to understand the potential mechanism of action reducing lipid accumulation.

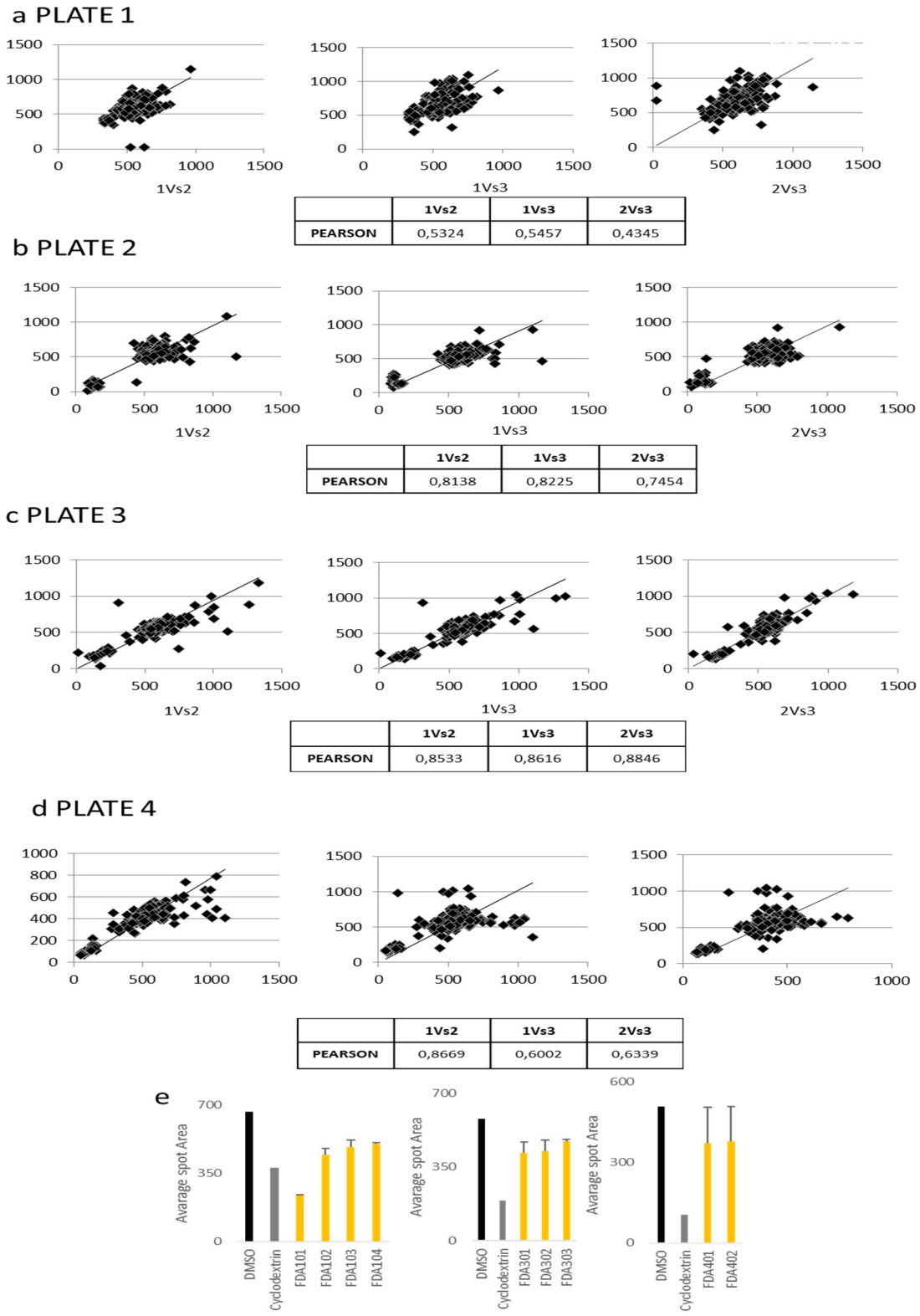

	1Vs2	1Vs3	2Vs3
PEARSON	0,5324	0,5457	0,4345

	1Vs2	1Vs3	2Vs3
PEARSON	0,8138	0,8225	0,7454

	1Vs2	1Vs3	2Vs3
PEARSON	0,8533	0,8616	0,8846

	1Vs2	1Vs3	2Vs3
PEARSON	0,8669	0,6002	0,6339

Figure 33: Screening output. (a, b, c, d) Plot showing the correlation among the 3 replicas of the screening for each plate. (e) bar plot representing the compound effect in reducing cholesterol spot area. In black and grey are reported respectively the DMSO and the cyclodextrin treated cells, whereas with yellow bar are showed the hits coming from each plate.

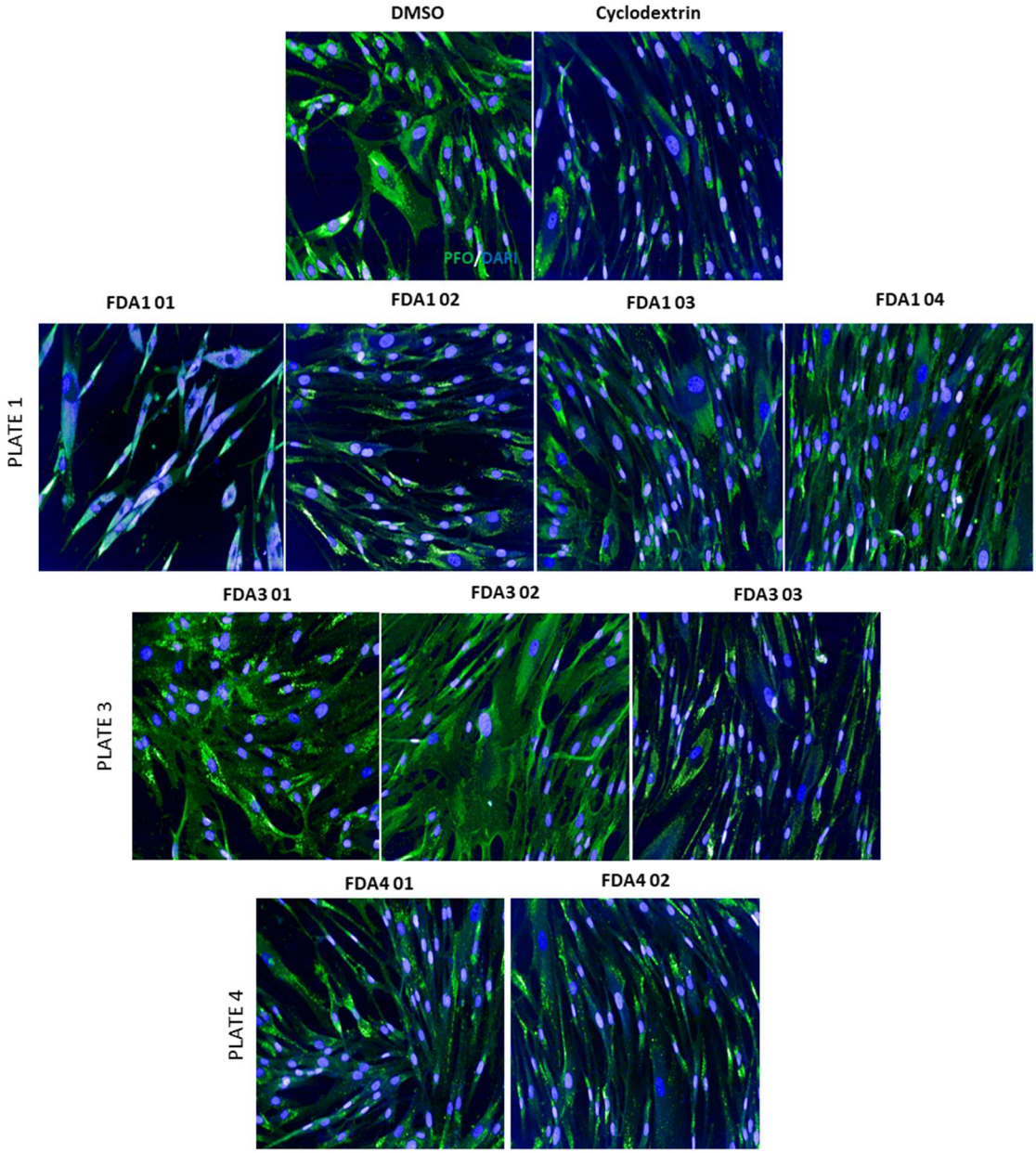

Figure 34: Screening output, representative images. GM02527 MLIV fibroblast stained with PFO-GST (in green) and DAPI (blue). On the top are reported the DMSO and the cyclodextrin treated cells and then follows representative image of the selected hits.

Conclusion

We have used the knowledge resulted from the first chapters of this work to develop strategies to screen for FDA compounds able to ameliorate the cellular phenotype of human MLIV fibroblasts. By screening TFEB inducers on MLIV cells we identified that only one drug, Compound 28, out of 150 tested was able to induce TFEB nuclear translocation in cells depleted of TRPML1. Moreover, this compound hit also was able to promote the

clearance of autophagic substrates such as p62 and NBR1 that accumulates in MLIV cells. During our experiments, we have observed that this drug affects cell viability, thus, we tried to identify potential analogues by using a new computational approach developed by our Bioinformatic core at TIGEM called MANTRA that exploits similarities between drug-induced transcriptional profiles already available in public databases (Carrella et al., 2014). Starting from this analysis we generated a sub-library composed by 121 compounds which showed similar transcriptional profile to the one generated by compound 28. We tested this library for TFEB nuclear translocation in wild type and MLIV fibroblasts and we selected 2 out of 121, these compounds will be tested in the next future by their ability to reduce pathological accumulation of autophagic substrates and lipids (using the developed clearance assays described in results sub paragraph 1). In addition, since compound 28 induces clearance in a TRPML1- and mTOR-independent manner, we will investigate other clearance mechanisms that may be involved on the activity of compound 28 and their analogues such as alternative pathways for autophagy induction or lysosomal exocytosis (Medina et al., 2011). Since lysosomal exocytosis requires calcium, we plan to use calcium chelators such as BAPTA-AM together with compound 28 to block compound 28-mediated activity (i.e. induction of TFEB nuclear translocation). In addition, we will test whether compound 28 induces lysosomal exocytosis using a specific assay that measure the appearance of the lysosomal membrane protein LAMP1 in the plasma membrane.

As a second approach to repurpose FDA drugs promoting clearance in MLIV cells, we developed a new (HC)-screening cholesterol clearance assay. We have isolated 8 compounds hits that consistently reduce cholesterol accumulation in MLIV fibroblast. These hits will be confirmed by their ability to reduce cholesterol in a dose-response manner to determine selectivity and potency (EC50s). Then, similarly to the previous

paragraph (results sub paragraph 1) we will use secondary assays to investigate whether they are able to reduce pathological parameters such as accumulation of autophagic substrates and lipofuscin storage. Moreover, we will investigate whether these compounds act through the activation of clearance pathways such as autophagy and/or lysosomal exocytosis. Together these (HC)-screenings allowed us to identify 12 potential compounds that could be repurposed to new therapeutic applications. They restore TFEB signalling and promote lipid storage clearance in human fibroblast from MLIV patients or for other lysosomal storage disease in which TRPML1 activity have been compromised like Nieman-Pick Type C disease (NPC). All the results presented in this chapter required additional work, in particularly regarding the mechanism of action, but represent a powerful and promising starting point that take advantage from using already approved compounds which made them closer respect to unknown compounds for a potential cure for MLIV and other LSDs.

Methods

Drug treatments

For the (HC)-screening assay all the drug treatments were performed using a robotic liquid handling station, Hamilton STARLet. The original compound plates 10mM (Prestwick chemical library or 150 TFEB relocator drugs composed by Prestwick and Selleck chemical libraries) in DMSO were diluted to a final concentration of 100µM in culture medium without serum. From this plate, 5µl were added directly on cells that have been plated the day before in 45µl. All drug treatments were performed in 384 well plate using a final concentration of 10µM.

Cell culture

HeLa TFEB GFP were previously described (Settembre et al., 2012) and cultured in RPMI supplemented with 10% fetal bovine serum, 200uM L – glutamine, 100uM sodium

pyruvate, 1mg/ml G418, 5% CO_2 at 37°C. Human fibroblasts from Mucolipidosis type IV (MLIV) patients were purchased from the Coryell Institute: GM02526 (Genotype Δ6432/486-2 A→G), GM02527 (Genotype 486-2 A→G/486-2 A→G), GM02048 (Genotype Δ6432/486-2 A→G) and cultured in DMEM supplemented with 15% fetal bovine serum, 200uM L – glutamine, 5% CO_2 at 37°C.

Antibodies and western blotting

For western blots, the following antibodies were used: B-Actin (AC-15, cat. A5441, 1:4000), NBR1 (cell signalling cat. 9891, 1:1000), p62 (BD cat. 610833, 1:1000). Total cell lysate was prepared by solubilization in TRIS HCl 10mM and 0.2% SDS supplemented with protease and phosphatase inhibitor (SIGMA). Soluble and insoluble fraction were generated as previously described (Vergarajauregui et al., 2008a). Protein concentration was determined by the Bradford method.

After SDS-PAGE and immunoblotting the protein recognised by the specific antibody was visualized by chemiluminescence methods (Luminata Crescendo Western HRP substrate, Millipore) using peroxidase-conjugated anti-rabbit or anti-mouse secondary antibodies (Calbiochem). Membranes were developed using a Chemidoc UVP imaging system (Ultra-Violet Products Ltd) and densitometric quantification was performed in unsaturated images using ImageJ (NIH).

Immunofluorescence

For immunofluorescence, the following antibodies were used: TFEB (cell signalling cat. 4240, 1:200), p-S6 ribosomal protein (S235/236) – Alexa 594 (cell signalling cat. 9865s 1:200). Cells were fixed with PFA for 10 minutes on ice and permeabilized in 0.1% (w/v) saponin, 0.5% (w/v) BSA and 50mM NH_4Cl in PBS (blocking buffer). For TFEB staining the blocking buffer was prepared with Triton X-100 0.05%. Cells were incubated with the

indicated primary antibodies for 1 hour and subsequently incubated with secondary antibodies. Images were acquired using Opera system from PerkinElmer and for image analysis was used Columbus software (Columbus 2.6.0.127073 © Copyright 2008-2017 PerkinElmer).

PFO-GST assay

On experiment day, cells were seeded in 384 well-plate, after 8 hours from seeding 4µg/ml of U18666A were added to cells for 16 hours. After U18666A pre-treatment the cells were treated for 48 hours as described in subparagraph "Drug treatments" of this chapter. Cells were then fixed in 3% paraformaldehyde (PFA) for 30 minutes at room temperature. PFA was quenched with an incubation with 0.1M glycine solution in PBS for 5 minutes at room temperature. Cells were then permeabilized with 0.05% Triton X-100 in PBS for 10 minutes and blocked 30 minutes in 3% fish gelatine (this last step was repeated twice). PFO-GST was prepared 5µg/ml in 0.2% fish gelatine and added on cells for 45 minutes. After 3 washes the antibody against GST (Rockland) was added for 1 hour, subsequently after 3 washes the secondary antibody Alexa 488 was added for 45 minutes. Images were acquired using Opera system from PerkinElmer and for image analysis was used Columbus software (Columbus 2.6.0.127073 © Copyright 2008-2017 PerkinElmer).

Auto fluorescence measurement by FACS

Cells were seeded in a 6 well plate, after seeding the cells were detached and resuspended in FACS buffer (2mM EDTA, 1% FBS, 0.1% Trypsin). Before FACS analysis the cells were filtered with a pre-separation filter with a cut off of 20/30µm. The instrument used was BD FACS Aria III. The cells were loaded into the instrument using a nozzle of 130µm and the auto florescence of the cells was read using excitation laser 488nm and 2 emission filter PerCP (695/40nm) and FITCH (530/30nm). The auto fluorescence intensity of MLIV fibroblast was determined normalizing both the emission on control fibroblast.

Tables

Table 4: List of the positive HITs obtained from the (HC)-screening of Prestwick Chemical Library®

DRUGS	Avarage spot Area	Std dev	Vitality
FDA101	237,38	2,98	69%
FDA102	442,73	34,39	103%
FDA103	484,23	34,36	106%
FDA104	498,48	9,48	100%
FDA301	416,42	51,50	97%
FDA302	426,49	51,97	110%
FDA303	469,76	11,84	83%
FDA401	369,71	135,10	76%
FDA402	378,23	129,35	62%

Table 5: Script sequence used for the (HC)-screening of results sub-paragraph 1. In the table below are listed in sequence all the steps and parameters used to perform the analysis on Columbus.

Input Image	**Stack Processing:** Individual Planes		
	Flatfield Correction: None		
Find Nuclei	**Channel:** Exp1Cam1	**Method:** B	
	ROI: None	Common Threshold: 0.15	
		Area: > 100 µm²	Output Population: Nuclei
		Split Factor: 10	
		Individual Threshold: 0.3	
		Contrast: > 0.1	
Select Population		**Method:** Common Filters	
	Population: Nuclei	Remove Border Objects	Output Population: Nuclei Selected
		Region: Nucleus	
Find Cytoplasm	**Channel:** Exp2Cam1	**Method:** A	
	Nuclei: Nuclei Selected	Individual Threshold: 0.2	
Select Population (2)		**Method:** Common Filters	
	Population: Nuclei Selected	Remove Border Objects	Output Population: SELECTED CELLS
		Region: Cell	

Select Cell Region		**Method:** Resize Region [%]	
	Population: SELECTED CELLS	Region Type: Cytoplasm Region	Output Region: ALL Cytoplasm
		Outer Border: 0 %	
		Inner Border: 45 %	
Calculate Intensity Properties (3)	**Channel:** Exp2Cam1	**Method:** Standard	
	Population: SELECTED CELLS	Mean	Output Properties: TFEB INT NUCLEUS
	Region: Nucleus		
Calculate Intensity Properties (4)	**Channel:** Exp2Cam1	**Method:** Standard	
	Population: SELECTED CELLS	Mean	Output Properties: TFEB INT CYTOPLASM
	Region: Cytoplasm		
Select Population (3)		**Method:** Filter by Property	
	Population: SELECTED CELLS		Output Population: Cells Nuclear TFEB
		TFEB INT NUCLEUS Mean: >= 350	
Calculate Properties	**Population:** SELECTED CELLS	**Method:** By Formula	Output Property: ratio NUC/Cyt per cell
		Formula: a/b	

		Variable A: TFEB INT NUCLEUS Mean Variable B: TFEB INT CYTOPLASM Mean
Define Results	**Method:** List of Outputs **Population: Nuclei Selected** **Population: Nuclei** **Population: Cells Nuclear TFEB** **Population: SELECTED CELLS** Number of Objects TFEB INT NUCLEUS Mean: Mean TFEB INT CYTOPLASM Mean: Mean Cells Nuclear TFEB: Mean	

ratio NUC/Cyt per cell: Mean

Method: Formula Output

Formula: (a/b)*100

Population Type: Objects

Variable A: Cells Nuclear TFEB - Number of Objects

Variable B: SELECTED CELLS - Number of Objects

Output Name: % cells with Nuclear TFEB

Single Cell Results: None

Table 6: Script sequence used for the (HC)-screening of results sub-paragraph 2. In the table below are listed in sequence all the steps and parameters used to perform the analysis on Columbus.

Input Image	**Stack Processing:** Individual Planes **Flatfield Correction:** None		
Find Nuclei	**Channel:** Exp1Cam1	**Method:** B	
	ROI: None	Common Threshold: 0.8	
		Area: > 30 µm²	Output Population: Nuclei
		Split Factor: 7.0	
		Individual Threshold: 0.4	
		Contrast: > 0.1	
Find Cytoplasm	**Channel:** Exp2Cam3	**Method:** F	
	Nuclei: Nuclei	Membrane Channel: Exp2Cam3	
		Individual Threshold: 0.15	
Select Population		**Method:** Common Filters	
	Population: Nuclei	Remove Border Objects	Output Population: Nuclei Selected
		Region: Cell	
Find Spots	**Channel:** Exp2Cam1	**Method:** B	
	ROI: Nuclei Selected	Detection Sensitivity: 0.5	Output Population: Spots
		Splitting Coefficient: 0.07	
		Calculate Spot Properties	
Calculate Intensity Properties	**Channel:** Exp2Cam1	**Method:** Standard	
	Population: Nuclei Selected	Mean	Output Properties: Intensity Cytoplasm Exp2Cam1
	Region: Cytoplasm		
Calculate Morphology Properties	**Population:** Nuclei Selected	**Method:** Standard	
	Region: Cytoplasm	Area	Output Properties: Cytoplasm
		Roundness	

Select Cell Region		**Method:** Resize Region [%]	
	Population: Nuclei	Region Type: Cytoplasm Region	Output Region: Cytoplasm Region
		Outer Border: 5 %	
		Inner Border: 50 %	
Find Spots (2)	**Channel:** Exp2Cam1	**Method:** B	
	ROI: Nuclei	Detection Sensitivity: 0.5	
		Splitting Coefficient: 0.5	Output Population: Spots ring
		Calculate Spot Properties	
Calculate Intensity Properties (2)	**Channel:** Exp2Cam1	**Method:** Standard	
	Population: Nuclei	Mean	Output Properties: Intensity Cytoplasm Region Exp2Cam1
	Region: Cytoplasm Region		
Select Population (2)		**Method:** Filter by Property	
		Corrected Spot Intensity: > 600	
	Population: Spots		Output Population: Spots Selected
		Spot Area [px²]: > 50	
		Boolean Operations: F1 and F2	
Define Results	**Method:** List of Outputs		
	Population: Spots ring		
	Population: Nuclei		
	Intensity Cytoplasm Region Exp2Cam1 Mean: Mean		

Population: Spots

Population: Nuclei Selected

Number of Objects

Total Spot Area: Mean

Relative Spot Intensity: Mean

Number of Spots: Mean

Number of Spots per Area of Cytoplasm: Mean

Intensity Cytoplasm Exp2Cam1 Mean: Mean

Population: Spots Selected

Method: Formula Output

Formula: a*b

Population Type: Objects

Variable A: Nuclei Selected - Total Spot Area Mean

Variable B: Nuclei Selected - Relative Spot Intensity Mean

Output Name: area*intensity

Method: Formula Output

Formula: a/b

Population Type: Objects

Variable A: Spots Selected - Number of Objects

Variable B: Nuclei Selected - Number of Objects

Output Name: aggregate/n cells

Method: Formula Output

Formula: a/b

Population Type: Objects

Variable A: Spots Selected - Spot Area [px²] Sum

Variable B: Nuclei Selected - Cytoplasm Area [µm²] Sum

Output Name: Area spot /area cyt

Method: Formula Output

Formula: a/b

Population Type: Objects

Variable A: Nuclei Selected - Intensity Cytoplasm Exp2Cam1 Mean Sum

Variable B: Nuclei Selected - Cytoplasm Area [µm²] Sum

Output Name: intensity/area cyto

Method: Formula Output

Formula: a/b

Population Type: Objects

Variable A: Spots ring - Spot Area [px²] Sum

Variable B: Nuclei - Number of Objects

Output Name: ring spot area mean

Single Cell Results: None

List of Figures

List of Tables

References

ALI, E. S., HUA, J., WILSON, C. H., TALLIS, G. A., ZHOU, F. H., RYCHKOV, G. Y. & BARRITT, G. J. 2016. The glucagon-like peptide-1 analogue exendin-4 reverses impaired intracellular Ca(2+) signalling in steatotic hepatocytes. *Biochim Biophys Acta,* 1863**,** 2135-46.

ALTARESCU, G., SUN, M., MOORE, D. F., SMITH, J. A., WIGGS, E. A., SOLOMON, B. I., PATRONAS, N. J., FREI, K. P., GUPTA, S., KANESKI, C. R., QUARRELL, O. W., SLAUGENHAUPT, S. A., GOLDIN, E. & SCHIFFMANN, R. 2002. The neurogenetics of mucolipidosis type IV. *Neurology,* 59**,** 306-13.

AMIR, N., ZLOTOGORA, J. & BACH, G. 1987. Mucolipidosis type IV: clinical spectrum and natural history. *Pediatrics,* 79**,** 953-9.

AXE, E. L., WALKER, S. A., MANIFAVA, M., CHANDRA, P., RODERICK, H. L., HABERMANN, A., GRIFFITHS, G. & KTISTAKIS, N. T. 2008. Autophagosome formation from membrane compartments enriched in phosphatidylinositol 3-phosphate and dynamically connected to the endoplasmic reticulum. *J Cell Biol,* 182**,** 685-701.

BACH, G. 2001. Mucolipidosis type IV. *Mol Genet Metab,* 73**,** 197-203.

BAE, M., PATEL, N., XU, H., LEE, M., TOMINAGA-YAMANAKA, K., NATH, A., GEIGER, J., GOROSPE, M., MATTSON, M. P. & HAUGHEY, N. J. 2014. Activation of TRPML1 clears intraneuronal Abeta in preclinical models of HIV infection. *J Neurosci,* 34**,** 11485-503.

BARGAL, R., AVIDAN, N., BEN-ASHER, E., OLENDER, Z., ZEIGLER, M., FRUMKIN, A., RAAS-ROTHSCHILD, A., GLUSMAN, G., LANCET, D. & BACH, G. 2000. Identification of the gene causing mucolipidosis type IV. *Nat Genet,* 26**,** 118-23.

BARGAL, R. & BACH, G. 1988. Phospholipids accumulation in mucolipidosis IV cultured fibroblasts. *J Inherit Metab Dis,* 11**,** 144-50.

BARGAL, R. & BACH, G. 1989. Phosphatidylcholine storage in mucolipidosis IV. *Clin Chim Acta,* 181**,** 167-74.

BARGAL, R. & BACH, G. 1997. Mucolipidosis type IV: abnormal transport of lipids to lysosomes. *J Inherit Metab Dis,* 20**,** 625-32.

BARGAL, R., GOEBEL, H. H., LATTA, E. & BACH, G. 2002. Mucolipidosis IV: novel mutation and diverse ultrastructural spectrum in the skin. *Neuropediatrics,* 33**,** 199-202.

BASSI, M. T., MANZONI, M., MONTI, E., PIZZO, M. T., BALLABIO, A. & BORSANI, G. 2000. Cloning of the gene encoding a novel integral membrane protein, mucolipidin-and identification of the two major founder mutations causing mucolipidosis type IV. *Am J Hum Genet,* 67**,** 1110-20.

BERMAN, E. R., LIVNI, N., SHAPIRA, E., MERIN, S. & LEVIJ, I. S. 1974. Congenital corneal clouding with abnormal systemic storage bodies: a new variant of mucolipidosis. *J Pediatr,* 84**,** 519-26.

BERRIDGE, M. J. 2009. Inositol trisphosphate and calcium signalling mechanisms. *Biochim Biophys Acta,* 1793**,** 933-40.

BERRIDGE, M. J., BOOTMAN, M. D. & RODERICK, H. L. 2003. Calcium signalling: dynamics, homeostasis and remodelling. *Nat Rev Mol Cell Biol,* 4**,** 517-29.

BERRIDGE, M. J., LIPP, P. & BOOTMAN, M. D. 2000. The versatility and universality of calcium signalling. *Nat Rev Mol Cell Biol,* 1**,** 11-21.

BHAVE, G., HU, H. J., GLAUNER, K. S., ZHU, W., WANG, H., BRASIER, D. J., OXFORD, G. S. & GEREAU, R. W. T. 2003. Protein kinase C phosphorylation sensitizes but does not activate the capsaicin receptor transient receptor potential vanilloid 1 (TRPV1). *Proc Natl Acad Sci U S A,* 100**,** 12480-5.

BIAZIK, J., YLA-ANTTILA, P., VIHINEN, H., JOKITALO, E. & ESKELINEN, E. L. 2015. Ultrastructural relationship of the phagophore with surrounding organelles. *Autophagy,* 11**,** 439-51.

BURMAN, C. & KTISTAKIS, N. T. 2010. Regulation of autophagy by phosphatidylinositol 3-phosphate. *FEBS Lett,* 584**,** 1302-12.

CAMPBELL, E. M. & FARES, H. 2010. Roles of CUP-5, the Caenorhabditis elegans orthologue of human TRPML1, in lysosome and gut granule biogenesis. *BMC Cell Biol,* 11**,** 40.
CANTIELLO, H. F., MONTALBETTI, N., GOLDMANN, W. H., RAYCHOWDHURY, M. K., GONZALEZ-PERRETT, S., TIMPANARO, G. A. & CHASAN, B. 2005. Cation channel activity of mucolipin-1: the effect of calcium. *Pflugers Arch,* 451**,** 304-12.
CAO, Q., YANG, Y., ZHONG, X. Z. & DONG, X. P. 2017. The lysosomal Ca2+ release channel TRPML1 regulates lysosome size by activating calmodulin. *J Biol Chem,* 292**,** 8424-8435.
CARDENAS, C. & FOSKETT, J. K. 2012. Mitochondrial Ca(2+) signals in autophagy. *Cell Calcium,* 52**,** 44-51.
CARDENAS, C., MILLER, R. A., SMITH, I., BUI, T., MOLGO, J., MULLER, M., VAIS, H., CHEUNG, K. H., YANG, J., PARKER, I., THOMPSON, C. B., BIRNBAUM, M. J., HALLOWS, K. R. & FOSKETT, J. K. 2010. Essential regulation of cell bioenergetics by constitutive InsP3 receptor Ca2+ transfer to mitochondria. *Cell,* 142**,** 270-83.
CARRELLA, D., NAPOLITANO, F., RISPOLI, R., MIGLIETTA, M., CARISSIMO, A., CUTILLO, L., SIRCI, F., GREGORETTI, F. & DI BERNARDO, D. 2014. Mantra 2.0: an online collaborative resource for drug mode of action and repurposing by network analysis. *Bioinformatics,* 30**,** 1787-8.
CATERINA, M. J., SCHUMACHER, M. A., TOMINAGA, M., ROSEN, T. A., LEVINE, J. D. & JULIUS, D. 1997. The capsaicin receptor: a heat-activated ion channel in the pain pathway. *Nature,* 389**,** 816-24.
CENEDELLA, R. J. 2009. Cholesterol synthesis inhibitor U18666A and the role of sterol metabolism and trafficking in numerous pathophysiological processes. *Lipids,* 44**,** 477-87.
CHEN, C. C., KELLER, M., HESS, M., SCHIFFMANN, R., URBAN, N., WOLFGARDT, A., SCHAEFER, M., BRACHER, F., BIEL, M., WAHL-SCHOTT, C. & GRIMM, C. 2014. A small molecule restores function to TRPML1 mutant isoforms responsible for mucolipidosis type IV. *Nat Commun,* 5**,** 4681.
CHEN, C. S., BACH, G. & PAGANO, R. E. 1998. Abnormal transport along the lysosomal pathway in mucolipidosis, type IV disease. *Proc Natl Acad Sci U S A,* 95**,** 6373-8.
CHENG, X., ZHANG, X., GAO, Q., ALI SAMIE, M., AZAR, M., TSANG, W. L., DONG, L., SAHOO, N., LI, X., ZHUO, Y., GARRITY, A. G., WANG, X., FERRER, M., DOWLING, J., XU, L., HAN, R. & XU, H. 2014. The intracellular Ca(2)(+) channel MCOLN1 is required for sarcolemma repair to prevent muscular dystrophy. *Nat Med,* 20**,** 1187-92.
CHOI, S. & KIM, H. J. 2014. The Ca2+ channel TRPML3 specifically interacts with the mammalian ATG8 homologue GATE16 to regulate autophagy. *Biochem Biophys Res Commun,* 443**,** 56-61.
CHRISTENSEN, K. A., MYERS, J. T. & SWANSON, J. A. 2002. pH-dependent regulation of lysosomal calcium in macrophages. *J Cell Sci,* 115**,** 599-607.
CHUNG, M. K., LEE, H., MIZUNO, A., SUZUKI, M. & CATERINA, M. J. 2004. 2-aminoethoxydiphenyl borate activates and sensitizes the heat-gated ion channel TRPV3. *J Neurosci,* 24**,** 5177-82.
CLAPHAM, D. E. 2007. Calcium signaling. *Cell,* 131**,** 1047-58.
CLARK, R. & GRIFFITHS, G. M. 2003. Lytic granules, secretory lysosomes and disease. *Curr Opin Immunol,* 15**,** 516-21.
COBLENTZ, J., ST CROIX, C. & KISELYOV, K. 2014. Loss of TRPML1 promotes production of reactive oxygen species: is oxidative damage a factor in mucolipidosis type IV? *Biochem J,* 457**,** 361-8.
COOPER, S. T. & MCNEIL, P. L. 2015. Membrane Repair: Mechanisms and Pathophysiology. *Physiol Rev,* 95**,** 1205-40.
CUAJUNGCO, M. P., BASILIO, L. C., SILVA, J., HART, T., TRINGALI, J., CHEN, C. C., BIEL, M. & GRIMM, C. 2014. Cellular zinc levels are modulated by TRPML1-TMEM163 interaction. *Traffic,* 15**,** 1247-65.
CUAJUNGCO, M. P., GRIMM, C., OSHIMA, K., D'HOEDT, D., NILIUS, B., MENSENKAMP, A. R., BINDELS, R. J., PLOMANN, M. & HELLER, S. 2006. PACSINs bind to the TRPV4 cation

channel. PACSIN 3 modulates the subcellular localization of TRPV4. *J Biol Chem,* 281**,** 18753-62.

CURCIO-MORELLI, C., CHARLES, F. A., MICSENYI, M. C., CAO, Y., VENUGOPAL, B., BROWNING, M. F., DOBRENIS, K., COTMAN, S. L., WALKLEY, S. U. & SLAUGENHAUPT, S. A. 2010a. Macroautophagy is defective in mucolipin-1-deficient mouse neurons. *Neurobiol Dis,* 40**,** 370-7.

CURCIO-MORELLI, C., ZHANG, P., VENUGOPAL, B., CHARLES, F. A., BROWNING, M. F., CANTIELLO, H. F. & SLAUGENHAUPT, S. A. 2010b. Functional multimerization of mucolipin channel proteins. *J Cell Physiol,* 222**,** 328-35.

D'HOEDT, D., OWSIANIK, G., PRENEN, J., CUAJUNGCO, M. P., GRIMM, C., HELLER, S., VOETS, T. & NILIUS, B. 2008. Stimulus-specific modulation of the cation channel TRPV4 by PACSIN 3. *J Biol Chem,* 283**,** 6272-80.

DAYAM, R. M., SARIC, A., SHILLIDAY, R. E. & BOTELHO, R. J. 2015. The Phosphoinositide-Gated Lysosomal Ca(2+) Channel, TRPML1, Is Required for Phagosome Maturation. *Traffic,* 16**,** 1010-26.

DE DUVE, C. 2005. The lysosome turns fifty. *Nat Cell Biol,* 7**,** 847-9.

DE LEO, M. G., STAIANO, L., VICINANZA, M., LUCIANI, A., CARISSIMO, A., MUTARELLI, M., DI CAMPLI, A., POLISHCHUK, E., DI TULLIO, G., MORRA, V., LEVTCHENKO, E., OLTRABELLA, F., STARBORG, T., SANTORO, M., DI BERNARDO, D., DEVUYST, O., LOWE, M., MEDINA, D. L., BALLABIO, A. & DE MATTEIS, M. A. 2016. Autophagosome-lysosome fusion triggers a lysosomal response mediated by TLR9 and controlled by OCRL. *Nat Cell Biol,* 18**,** 839-50.

DECUYPERE, J. P., BULTYNCK, G. & PARYS, J. B. 2011a. A dual role for Ca(2+) in autophagy regulation. *Cell Calcium,* 50**,** 242-50.

DECUYPERE, J. P., MONACO, G., BULTYNCK, G., MISSIAEN, L., DE SMEDT, H. & PARYS, J. B. 2011b. The IP(3) receptor-mitochondria connection in apoptosis and autophagy. *Biochim Biophys Acta,* 1813**,** 1003-13.

DI PALMA, F., BELYANTSEVA, I. A., KIM, H. J., VOGT, T. F., KACHAR, B. & NOBEN-TRAUTH, K. 2002. Mutations in Mcoln3 associated with deafness and pigmentation defects in varitint-waddler (Va) mice. *Proc Natl Acad Sci U S A,* 99**,** 14994-9.

DI PAOLA, S., SCOTTO-ROSATO, A. & MEDINA, D. L. 2017. TRPML1: The Ca(2+)retaker of the lysosome. *Cell Calcium*.

DI PAOLO, G. & DE CAMILLI, P. 2006. Phosphoinositides in cell regulation and membrane dynamics. *Nature,* 443**,** 651-7.

DONG, X. P., CHENG, X., MILLS, E., DELLING, M., WANG, F., KURZ, T. & XU, H. 2008. The type IV mucolipidosis-associated protein TRPML1 is an endolysosomal iron release channel. *Nature,* 455**,** 992-6.

DONG, X. P., SHEN, D., WANG, X., DAWSON, T., LI, X., ZHANG, Q., CHENG, X., ZHANG, Y., WEISMAN, L. S., DELLING, M. & XU, H. 2010. PI(3,5)P(2) controls membrane trafficking by direct activation of mucolipin Ca(2+) release channels in the endolysosome. *Nat Commun,* 1**,** 38.

DONG, X. P., WANG, X., SHEN, D., CHEN, S., LIU, M., WANG, Y., MILLS, E., CHENG, X., DELLING, M. & XU, H. 2009. Activating mutations of the TRPML1 channel revealed by proline-scanning mutagenesis. *J Biol Chem,* 284**,** 32040-52.

DOOLEY, H. C., RAZI, M., POLSON, H. E., GIRARDIN, S. E., WILSON, M. I. & TOOZE, S. A. 2014. WIPI2 links LC3 conjugation with PI3P, autophagosome formation, and pathogen clearance by recruiting Atg12-5-16L1. *Mol Cell,* 55**,** 238-52.

EAST, D. A. & CAMPANELLA, M. 2013. Ca2+ in quality control: an unresolved riddle critical to autophagy and mitophagy. *Autophagy,* 9**,** 1710-9.

EDEN, E. R. 2016. The formation and function of ER-endosome membrane contact sites. *Biochim Biophys Acta,* 1861**,** 874-879.

EGAN, D., KIM, J., SHAW, R. J. & GUAN, K. L. 2011a. The autophagy initiating kinase ULK1 is regulated via opposing phosphorylation by AMPK and mTOR. *Autophagy,* 7**,** 643-4.

EGAN, D. F., SHACKELFORD, D. B., MIHAYLOVA, M. M., GELINO, S., KOHNZ, R. A., MAIR, W., VASQUEZ, D. S., JOSHI, A., GWINN, D. M., TAYLOR, R., ASARA, J. M., FITZPATRICK, J., DILLIN, A., VIOLLET, B., KUNDU, M., HANSEN, M. & SHAW, R. J. 2011b. Phosphorylation of ULK1 (hATG1) by AMP-activated protein kinase connects energy sensing to mitophagy. *Science,* 331**,** 456-61.

EICHELSDOERFER, J. L., EVANS, J. A., SLAUGENHAUPT, S. A. & CUAJUNGCO, M. P. 2010. Zinc dyshomeostasis is linked with the loss of mucolipidosis IV-associated TRPML1 ion channel. *J Biol Chem,* 285**,** 34304-8.

EZEANI, M. & OMABE, M. 2016. A New Perspective of Lysosomal Cation Channel-Dependent Homeostasis in Alzheimer's Disease. *Mol Neurobiol,* 53**,** 1672-1678.

FALARDEAU, J. L., KENNEDY, J. C., ACIERNO, J. S., JR., SUN, M., STAHL, S., GOLDIN, E. & SLAUGENHAUPT, S. A. 2002. Cloning and characterization of the mouse Mcoln1 gene reveals an alternatively spliced transcript not seen in humans. *BMC Genomics,* 3**,** 3.

FARES, H. & GREENWALD, I. 2001. Regulation of endocytosis by CUP-5, the Caenorhabditis elegans mucolipin-1 homolog. *Nat Genet,* 28**,** 64-8.

FILIPPI-CHIELA, E. C., VIEGAS, M. S., THOME, M. P., BUFFON, A., WINK, M. R. & LENZ, G. 2016. Modulation of Autophagy by Calcium Signalosome in Human Disease. *Mol Pharmacol,* 90**,** 371-84.

FREI, K. P., PATRONAS, N. J., CRUTCHFIELD, K. E., ALTARESCU, G. & SCHIFFMANN, R. 1998. Mucolipidosis type IV: characteristic MRI findings. *Neurology,* 51**,** 565-9.

FULLGRABE, J., KLIONSKY, D. J. & JOSEPH, B. 2014. The return of the nucleus: transcriptional and epigenetic control of autophagy. *Nat Rev Mol Cell Biol,* 15**,** 65-74.

FUNK, K. E. & KURET, J. 2012. Lysosomal fusion dysfunction as a unifying hypothesis for Alzheimer's disease pathology. *Int J Alzheimers Dis,* 2012**,** 752894.

GALLUZZI, L., PIETROCOLA, F., BRAVO-SAN PEDRO, J. M., AMARAVADI, R. K., BAEHRECKE, E. H., CECCONI, F., CODOGNO, P., DEBNATH, J., GEWIRTZ, D. A., KARANTZA, V., KIMMELMAN, A., KUMAR, S., LEVINE, B., MAIURI, M. C., MARTIN, S. J., PENNINGER, J., PIACENTINI, M., RUBINSZTEIN, D. C., SIMON, H. U., SIMONSEN, A., THORBURN, A. M., VELASCO, G., RYAN, K. M. & KROEMER, G. 2015. Autophagy in malignant transformation and cancer progression. *EMBO J,* 34**,** 856-80.

GARY, J. D., SATO, T. K., STEFAN, C. J., BONANGELINO, C. J., WEISMAN, L. S. & EMR, S. D. 2002. Regulation of Fab1 phosphatidylinositol 3-phosphate 5-kinase pathway by Vac7 protein and Fig4, a polyphosphoinositide phosphatase family member. *Mol Biol Cell,* 13**,** 1238-51.

GASTALDELLO, A., CALLAGHAN, H., GAMI, P. & CAMPANELLA, M. 2010. Ca 2+ -dependent autophagy is enhanced by the pharmacological agent PK11195. *Autophagy,* 6**,** 607-13.

GAUDET, R. 2008. A primer on ankyrin repeat function in TRP channels and beyond. *Mol Biosyst,* 4**,** 372-9.

GIETZEN, K. 1983. Comparison of the calmodulin antagonists compound 48/80 and calmidazolium. *Biochem J,* 216**,** 611-6.

GOLDIN, E., CARUSO, R. C., BENKO, W., KANESKI, C. R., STAHL, S. & SCHIFFMANN, R. 2008. Isolated ocular disease is associated with decreased mucolipin-1 channel conductance. *Invest Ophthalmol Vis Sci,* 49**,** 3134-42.

GORDON, J. N., SHU, W. P., SCHLUSSEL, R. N., DROLLER, M. J. & LIU, B. C. 1993. Altered extracellular matrices influence cellular processes and nuclear matrix organizations of overlying human bladder urothelial cells. *Cancer Res,* 53**,** 4971-7.

GRIMM, C., CUAJUNGCO, M. P., VAN AKEN, A. F., SCHNEE, M., JORS, S., KROS, C. J., RICCI, A. J. & HELLER, S. 2007. A helix-breaking mutation in TRPML3 leads to constitutive activity underlying deafness in the varitint-waddler mouse. *Proc Natl Acad Sci U S A,* 104**,** 19583-8.

GRIMM, C., JORS, S., GUO, Z., OBUKHOV, A. G. & HELLER, S. 2012. Constitutive activity of TRPML2 and TRPML3 channels versus activation by low extracellular sodium and small molecules. *J Biol Chem,* 287**,** 22701-8.

GRIMM, C., JORS, S., SALDANHA, S. A., OBUKHOV, A. G., PAN, B., OSHIMA, K., CUAJUNGCO, M. P., CHASE, P., HODDER, P. & HELLER, S. 2010. Small molecule activators of TRPML3. *Chem Biol,* 17**,** 135-48.

GRUMATI, P., COLETTO, L., SCHIAVINATO, A., CASTAGNARO, S., BERTAGGIA, E., SANDRI, M. & BONALDO, P. 2011. Physical exercise stimulates autophagy in normal skeletal muscles but is detrimental for collagen VI-deficient muscles. *Autophagy,* 7**,** 1415-23.

HAWLEY, S. A., PAN, D. A., MUSTARD, K. J., ROSS, L., BAIN, J., EDELMAN, A. M., FRENGUELLI, B. G. & HARDIE, D. G. 2005. Calmodulin-dependent protein kinase kinase-beta is an alternative upstream kinase for AMP-activated protein kinase. *Cell Metab,* 2**,** 9-19.

HE, C., BASSIK, M. C., MORESI, V., SUN, K., WEI, Y., ZOU, Z., AN, Z., LOH, J., FISHER, J., SUN, Q., KORSMEYER, S., PACKER, M., MAY, H. I., HILL, J. A., VIRGIN, H. W., GILPIN, C., XIAO, G., BASSEL-DUBY, R., SCHERER, P. E. & LEVINE, B. 2012. Exercise-induced BCL2-regulated autophagy is required for muscle glucose homeostasis. *Nature,* 481**,** 511-5.

HE, C. & KLIONSKY, D. J. 2009. Regulation mechanisms and signaling pathways of autophagy. *Annu Rev Genet,* 43**,** 67-93.

HERSH, B. M., HARTWIEG, E. & HORVITZ, H. R. 2002. The Caenorhabditis elegans mucolipin-like gene cup-5 is essential for viability and regulates lysosomes in multiple cell types. *Proc Natl Acad Sci U S A,* 99**,** 4355-60.

HOYER-HANSEN, M., BASTHOLM, L., SZYNIAROWSKI, P., CAMPANELLA, M., SZABADKAI, G., FARKAS, T., BIANCHI, K., FEHRENBACHER, N., ELLING, F., RIZZUTO, R., MATHIASEN, I. S. & JAATTELA, M. 2007. Control of macroautophagy by calcium, calmodulin-dependent kinase kinase-beta, and Bcl-2. *Mol Cell,* 25**,** 193-205.

HU, H. Z., GU, Q., WANG, C., COLTON, C. K., TANG, J., KINOSHITA-KAWADA, M., LEE, L. Y., WOOD, J. D. & ZHU, M. X. 2004. 2-aminoethoxydiphenyl borate is a common activator of TRPV1, TRPV2, and TRPV3. *J Biol Chem,* 279**,** 35741-8.

IIDA, T., MORIYAMA, T., KOBATA, K., MORITA, A., MURAYAMA, N., HASHIZUME, S., FUSHIKI, T., YAZAWA, S., WATANABE, T. & TOMINAGA, M. 2003. TRPV1 activation and induction of nociceptive response by a non-pungent capsaicin-like compound, capsiate. *Neuropharmacology,* 44**,** 958-67.

JAMART, C., NASLAIN, D., GILSON, H. & FRANCAUX, M. 2013. Higher activation of autophagy in skeletal muscle of mice during endurance exercise in the fasted state. *Am J Physiol Endocrinol Metab,* 305**,** E964-74.

JANSEN, S. M., GROENER, J. E., BAX, W. & POORTHUIS, B. J. 2001. Delayed lysosomal metabolism of lipids in mucolipidosis type IV fibroblasts after LDL-receptor-mediated endocytosis. *J Inherit Metab Dis,* 24**,** 577-86.

JENNINGS, J. J., JR., ZHU, J. H., RBAIBI, Y., LUO, X., CHU, C. T. & KISELYOV, K. 2006. Mitochondrial aberrations in mucolipidosis Type IV. *J Biol Chem,* 281**,** 39041-50.

KARACSONYI, C., MIGUEL, A. S. & PUERTOLLANO, R. 2007. Mucolipin-2 localizes to the Arf6-associated pathway and regulates recycling of GPI-APs. *Traffic,* 8**,** 1404-14.

KARANASIOS, E., WALKER, S. A., OKKENHAUG, H., MANIFAVA, M., HUMMEL, E., ZIMMERMANN, H., AHMED, Q., DOMART, M. C., COLLINSON, L. & KTISTAKIS, N. T. 2016. Autophagy initiation by ULK complex assembly on ER tubulovesicular regions marked by ATG9 vesicles. *Nat Commun,* 7**,** 12420.

KARASHIMA, Y., PRENEN, J., MESEGUER, V., OWSIANIK, G., VOETS, T. & NILIUS, B. 2008. Modulation of the transient receptor potential channel TRPA1 by phosphatidylinositol 4,5-biphosphate manipulators. *Pflugers Arch,* 457**,** 77-89.

KASAHARA, A., CIPOLAT, S., CHEN, Y., DORN, G. W., 2ND & SCORRANO, L. 2013. Mitochondrial fusion directs cardiomyocyte differentiation via calcineurin and Notch signaling. *Science,* 342**,** 734-7.

KIM, A. Y., TANG, Z., LIU, Q., PATEL, K. N., MAAG, D., GENG, Y. & DONG, X. 2008. Pirt, a phosphoinositide-binding protein, functions as a regulatory subunit of TRPV1. *Cell,* 133**,** 475-85.

KIM, H. J., LI, Q., TJON-KON-SANG, S., SO, I., KISELYOV, K. & MUALLEM, S. 2007. Gain-of-function mutation in TRPML3 causes the mouse Varitint-Waddler phenotype. *J Biol Chem,* 282**,** 36138-42.

KIM, H. J., SOYOMBO, A. A., TJON-KON-SANG, S., SO, I. & MUALLEM, S. 2009. The Ca(2+) channel TRPML3 regulates membrane trafficking and autophagy. *Traffic,* 10**,** 1157-67.

KIM, J., KUNDU, M., VIOLLET, B. & GUAN, K. L. 2011. AMPK and mTOR regulate autophagy through direct phosphorylation of Ulk1. *Nat Cell Biol,* 13**,** 132-41.

KIRKIN, V., LAMARK, T., JOHANSEN, T. & DIKIC, I. 2009. NBR1 cooperates with p62 in selective autophagy of ubiquitinated targets. *Autophagy,* 5**,** 732-3.

KISELYOV, K., CHEN, J., RBAIBI, Y., OBERDICK, D., TJON-KON-SANG, S., SHCHEYNIKOV, N., MUALLEM, S. & SOYOMBO, A. 2005. TRP-ML1 is a lysosomal monovalent cation channel that undergoes proteolytic cleavage. *J Biol Chem,* 280**,** 43218-23.

KLAUSEN, T. K., PAGANI, A., MINASSI, A., ECH-CHAHAD, A., PRENEN, J., OWSIANIK, G., HOFFMANN, E. K., PEDERSEN, S. F., APPENDINO, G. & NILIUS, B. 2009. Modulation of the transient receptor potential vanilloid channel TRPV4 by 4alpha-phorbol esters: a structure-activity study. *J Med Chem,* 52**,** 2933-9.

KNAEVELSRUD, H., SORENG, K., RAIBORG, C., HABERG, K., RASMUSON, F., BRECH, A., LIESTOL, K., RUSTEN, T. E., STENMARK, H., NEUFELD, T. P., CARLSSON, S. R. & SIMONSEN, A. 2013. Membrane remodeling by the PX-BAR protein SNX18 promotes autophagosome formation. *J Cell Biol,* 202**,** 331-49.

KOGOT-LEVIN, A., ZEIGLER, M., ORNOY, A. & BACH, G. 2009. Mucolipidosis type IV: the effect of increased lysosomal pH on the abnormal lysosomal storage. *Pediatr Res,* 65**,** 686-90.

KONDRATSKYI, A., YASSINE, M., KONDRATSKA, K., SKRYMA, R., SLOMIANNY, C. & PREVARSKAYA, N. 2013. Calcium-permeable ion channels in control of autophagy and cancer. *Front Physiol,* 4**,** 272.

KOROLCHUK, V. I., SAIKI, S., LICHTENBERG, M., SIDDIQI, F. H., ROBERTS, E. A., IMARISIO, S., JAHREISS, L., SARKAR, S., FUTTER, M., MENZIES, F. M., O'KANE, C. J., DERETIC, V. & RUBINSZTEIN, D. C. 2011. Lysosomal positioning coordinates cellular nutrient responses. *Nat Cell Biol,* 13**,** 453-60.

KROEMER, G., MARINO, G. & LEVINE, B. 2010. Autophagy and the integrated stress response. *Mol Cell,* 40**,** 280-93.

KUBALLA, P., NOLTE, W. M., CASTORENO, A. B. & XAVIER, R. J. 2012. Autophagy and the immune system. *Annu Rev Immunol,* 30**,** 611-46.

KUKIC, I., KELLEHER, S. L. & KISELYOV, K. 2014. Zn2+ efflux through lysosomal exocytosis prevents Zn2+-induced toxicity. *J Cell Sci,* 127**,** 3094-103.

KUKIC, I., LEE, J. K., COBLENTZ, J., KELLEHER, S. L. & KISELYOV, K. 2013. Zinc-dependent lysosomal enlargement in TRPML1-deficient cells involves MTF-1 transcription factor and ZnT4 (Slc30a4) transporter. *Biochem J,* 451**,** 155-63.

KWIATKOWSKA, K., MARSZALEK-SADOWSKA, E., TRACZYK, G., KOPROWSKI, P., MUSIELAK, M., LUGOWSKA, A., KULMA, M., GRZELCZYK, A. & SOBOTA, A. 2014. Visualization of cholesterol deposits in lysosomes of Niemann-Pick type C fibroblasts using recombinant perfringolysin O. *Orphanet J Rare Dis,* 9**,** 64.

LA ROVERE, R. M., ROEST, G., BULTYNCK, G. & PARYS, J. B. 2016. Intracellular Ca(2+) signaling and Ca(2+) microdomains in the control of cell survival, apoptosis and autophagy. *Cell Calcium,* 60**,** 74-87.

LAMARK, T., KIRKIN, V., DIKIC, I. & JOHANSEN, T. 2009. NBR1 and p62 as cargo receptors for selective autophagy of ubiquitinated targets. *Cell Cycle,* 8**,** 1986-90.

LAPLANTE, J. M., FALARDEAU, J., SUN, M., KANAZIRSKA, M., BROWN, E. M., SLAUGENHAUPT, S. A. & VASSILEV, P. M. 2002. Identification and characterization of the single channel function of human mucolipin-1 implicated in mucolipidosis type IV, a disorder affecting the lysosomal pathway. *FEBS Lett,* 532**,** 183-7.

LAPLANTE, J. M., SUN, M., FALARDEAU, J., DAI, D., BROWN, E. M., SLAUGENHAUPT, S. A. & VASSILEV, P. M. 2006. Lysosomal exocytosis is impaired in mucolipidosis type IV. *Mol Genet Metab,* 89**,** 339-48.

LAPLANTE, J. M., YE, C. P., QUINN, S. J., GOLDIN, E., BROWN, E. M., SLAUGENHAUPT, S. A. & VASSILEV, P. M. 2004. Functional links between mucolipin-1 and Ca2+-dependent membrane trafficking in mucolipidosis IV. *Biochem Biophys Res Commun,* 322**,** 1384-91.

LEV, S., ZEEVI, D. A., FRUMKIN, A., OFFEN-GLASNER, V., BACH, G. & MINKE, B. 2010. Constitutive activity of the human TRPML2 channel induces cell degeneration. *J Biol Chem,* 285**,** 2771-82.

LI, M., YU, Y. & YANG, J. 2011. Structural biology of TRP channels. *Adv Exp Med Biol,* 704**,** 1-23.

LI, M., ZHANG, W. K., BENVIN, N. M., ZHOU, X., SU, D., LI, H., WANG, S., MICHAILIDIS, I. E., TONG, L., LI, X. & YANG, J. 2017. Structural basis of dual Ca2+/pH regulation of the endolysosomal TRPML1 channel. *Nat Struct Mol Biol,* 24**,** 205-213.

LI, X., GARRITY, A. G. & XU, H. 2013. Regulation of membrane trafficking by signalling on endosomal and lysosomal membranes. *J Physiol,* 591**,** 4389-401.

LI, X., RYDZEWSKI, N., HIDER, A., ZHANG, X., YANG, J., WANG, W., GAO, Q., CHENG, X. & XU, H. 2016. A molecular mechanism to regulate lysosome motility for lysosome positioning and tubulation. *Nat Cell Biol,* 18**,** 404-17.

LIANG, C., FENG, P., KU, B., DOTAN, I., CANAANI, D., OH, B. H. & JUNG, J. U. 2006. Autophagic and tumour suppressor activity of a novel Beclin1-binding protein UVRAG. *Nat Cell Biol,* 8**,** 688-99.

LINDVALL, J. M., BLOMBERG, K. E., BERGLOF, A., YANG, Q., SMITH, C. I. & ISLAM, T. C. 2004. Gene expression profile of B cells from Xid mice and Btk knockout mice. *Eur J Immunol,* 34**,** 1981-91.

LINDVALL, J. M., BLOMBERG, K. E., WENNBORG, A. & SMITH, C. I. 2005. Differential expression and molecular characterisation of Lmo7, Myo1e, Sash1, and Mcoln2 genes in Btk-defective B-cells. *Cell Immunol,* 235**,** 46-55.

LISCUM, L. & FAUST, J. R. 1989. The intracellular transport of low density lipoprotein-derived cholesterol is inhibited in Chinese hamster ovary cells cultured with 3-beta-[2-(diethylamino)ethoxy]androst-5-en-17-one. *J Biol Chem,* 264**,** 11796-806.

LIU, B. 2012. Therapeutic potential of cyclodextrins in the treatment of Niemann-Pick type C disease. *Clin Lipidol,* 7**,** 289-301.

LIU, B. & QIN, F. 2005. Functional control of cold- and menthol-sensitive TRPM8 ion channels by phosphatidylinositol 4,5-bisphosphate. *J Neurosci,* 25**,** 1674-81.

LLOYD-EVANS, E., MORGAN, A. J., HE, X., SMITH, D. A., ELLIOT-SMITH, E., SILLENCE, D. J., CHURCHILL, G. C., SCHUCHMAN, E. H., GALIONE, A. & PLATT, F. M. 2008. Niemann-Pick disease type C1 is a sphingosine storage disease that causes deregulation of lysosomal calcium. *Nat Med,* 14**,** 1247-55.

LUBENSKY, I. A., SCHIFFMANN, R., GOLDIN, E. & TSOKOS, M. 1999. Lysosomal inclusions in gastric parietal cells in mucolipidosis type IV: a novel cause of achlorhydria and hypergastrinemia. *Am J Surg Pathol,* 23**,** 1527-31.

LUM, J. J., BAUER, D. E., KONG, M., HARRIS, M. H., LI, C., LINDSTEN, T. & THOMPSON, C. B. 2005. Growth factor regulation of autophagy and cell survival in the absence of apoptosis. *Cell,* 120**,** 237-48.

LUZIO, J. P., PARKINSON, M. D., GRAY, S. R. & BRIGHT, N. A. 2009. The delivery of endocytosed cargo to lysosomes. *Biochem Soc Trans,* 37**,** 1019-21.

LUZIO, J. P., PRYOR, P. R. & BRIGHT, N. A. 2007. Lysosomes: fusion and function. *Nat Rev Mol Cell Biol,* 8**,** 622-32.

MACIAN, F. 2005. NFAT proteins: key regulators of T-cell development and function. *Nat Rev Immunol,* 5**,** 472-84.

MALLILANKARAMAN, K., CARDENAS, C., DOONAN, P. J., CHANDRAMOORTHY, H. C., IRRINKI, K. M., GOLENAR, T., CSORDAS, G., MADIREDDI, P., YANG, J., MULLER, M., MILLER, R., KOLESAR, J. E., MOLGO, J., KAUFMAN, B., HAJNOCZKY, G., FOSKETT, J. K. & MADESH, M. 2012. MCUR1 is an essential component of mitochondrial Ca2+ uptake that regulates cellular metabolism. *Nat Cell Biol,* 14**,** 1336-43.

MAMMUCARI, C., MILAN, G., ROMANELLO, V., MASIERO, E., RUDOLF, R., DEL PICCOLO, P., BURDEN, S. J., DI LISI, R., SANDRI, C., ZHAO, J., GOLDBERG, A. L., SCHIAFFINO, S. & SANDRI, M. 2007. FoxO3 controls autophagy in skeletal muscle in vivo. *Cell Metab,* 6**,** 458-71.

MANZONI, M., MONTI, E., BRESCIANI, R., BOZZATO, A., BARLATI, S., BASSI, M. T. & BORSANI, G. 2004. Overexpression of wild-type and mutant mucolipin proteins in mammalian cells: effects on the late endocytic compartment organization. *FEBS Lett,* 567**,** 219-24.

MARAT, A. L. & HAUCKE, V. 2016. Phosphatidylinositol 3-phosphates-at the interface between cell signalling and membrane traffic. *EMBO J,* 35**,** 561-79.

MARKS, D. L., HOLICKY, E. L., WHEATLEY, C. L., FRUMKIN, A., BACH, G. & PAGANO, R. E. 2012. Role of protein kinase d in Golgi exit and lysosomal targeting of the transmembrane protein, Mcoln1. *Traffic,* 13**,** 565-75.

MARTINA, J. A., LELOUVIER, B. & PUERTOLLANO, R. 2009. The calcium channel mucolipin-3 is a novel regulator of trafficking along the endosomal pathway. *Traffic,* 10**,** 1143-56.

MARTINEZ, I., CHAKRABARTI, S., HELLEVIK, T., MOREHEAD, J., FOWLER, K. & ANDREWS, N. W. 2000. Synaptotagmin VII regulates Ca(2+)-dependent exocytosis of lysosomes in fibroblasts. *J Cell Biol,* 148**,** 1141-49.

MATSUNAGA, K., MORITA, E., SAITOH, T., AKIRA, S., KTISTAKIS, N. T., IZUMI, T., NODA, T. & YOSHIMORI, T. 2010. Autophagy requires endoplasmic reticulum targeting of the PI3-kinase complex via Atg14L. *J Cell Biol,* 190**,** 511-21.

MAUTHE, M., JACOB, A., FREIBERGER, S., HENTSCHEL, K., STIERHOF, Y. D., CODOGNO, P. & PROIKAS-CEZANNE, T. 2011. Resveratrol-mediated autophagy requires WIPI-1-regulated LC3 lipidation in the absence of induced phagophore formation. *Autophagy,* 7**,** 1448-61.

MCKEMY, D. D., NEUHAUSSER, W. M. & JULIUS, D. 2002. Identification of a cold receptor reveals a general role for TRP channels in thermosensation. *Nature,* 416**,** 52-8.

MCNAMARA, F. N., RANDALL, A. & GUNTHORPE, M. J. 2005. Effects of piperine, the pungent component of black pepper, at the human vanilloid receptor (TRPV1). *Br J Pharmacol,* 144**,** 781-90.

MEDINA, D. L., DI PAOLA, S., PELUSO, I., ARMANI, A., DE STEFANI, D., VENDITTI, R., MONTEFUSCO, S., SCOTTO-ROSATO, A., PREZIOSO, C., FORRESTER, A., SETTEMBRE, C., WANG, W., GAO, Q., XU, H., SANDRI, M., RIZZUTO, R., DE MATTEIS, M. A. & BALLABIO, A. 2015. Lysosomal calcium signalling regulates autophagy through calcineurin and TFEB. *Nat Cell Biol,* 17**,** 288-99.

MEDINA, D. L., FRALDI, A., BOUCHE, V., ANNUNZIATA, F., MANSUETO, G., SPAMPANATO, C., PURI, C., PIGNATA, A., MARTINA, J. A., SARDIELLO, M., PALMIERI, M., POLISHCHUK, R., PUERTOLLANO, R. & BALLABIO, A. 2011. Transcriptional activation of lysosomal exocytosis promotes cellular clearance. *Dev Cell,* 21**,** 421-30.

MIAO, Y., LI, G., ZHANG, X., XU, H. & ABRAHAM, S. N. 2015. A TRP Channel Senses Lysosome Neutralization by Pathogens to Trigger Their Expulsion. *Cell,* 161**,** 1306-19.

MICSENYI, M. C., DOBRENIS, K., STEPHNEY, G., PICKEL, J., VANIER, M. T., SLAUGENHAUPT, S. A. & WALKLEY, S. U. 2009. Neuropathology of the Mcoln1(-/-) knockout mouse model of mucolipidosis type IV. *J Neuropathol Exp Neurol,* 68**,** 125-35.

MIEDEL, M. T., RBAIBI, Y., GUERRIERO, C. J., COLLETTI, G., WEIXEL, K. M., WEISZ, O. A. & KISELYOV, K. 2008. Membrane traffic and turnover in TRP-ML1-deficient cells: a revised model for mucolipidosis type IV pathogenesis. *J Exp Med,* 205**,** 1477-90.

MIEDEL, M. T., WEIXEL, K. M., BRUNS, J. R., TRAUB, L. M. & WEISZ, O. A. 2006. Posttranslational cleavage and adaptor protein complex-dependent trafficking of mucolipin-1. *J Biol Chem,* 281**,** 12751-9.

MILLER, A., SCHAFER, J., UPCHURCH, C., SPOONER, E., HUYNH, J., HERNANDEZ, S., MCLAUGHLIN, B., ODEN, L. & FARES, H. 2015. Mucolipidosis type IV protein TRPML1-dependent lysosome formation. *Traffic,* 16**,** 284-97.

MIZUSHIMA, N. & KOMATSU, M. 2011. Autophagy: renovation of cells and tissues. *Cell,* 147**,** 728-41.

MIZUSHIMA, N., LEVINE, B., CUERVO, A. M. & KLIONSKY, D. J. 2008. Autophagy fights disease through cellular self-digestion. *Nature,* 451**,** 1069-75.

MIZUSHIMA, N., YOSHIMORI, T. & OHSUMI, Y. 2011. The role of Atg proteins in autophagosome formation. *Annu Rev Cell Dev Biol,* 27**,** 107-32.

MONTELL, C. & RUBIN, G. M. 1989. Molecular characterization of the Drosophila trp locus: a putative integral membrane protein required for phototransduction. *Neuron,* 2**,** 1313-23.

MORGAN, A. J., DAVIS, L. C., WAGNER, S. K., LEWIS, A. M., PARRINGTON, J., CHURCHILL, G. C. & GALIONE, A. 2013. Bidirectional Ca(2)(+) signaling occurs between the endoplasmic reticulum and acidic organelles. *J Cell Biol,* 200**,** 789-805.

MORGAN, A. J., PLATT, F. M., LLOYD-EVANS, E. & GALIONE, A. 2011. Molecular mechanisms of endolysosomal Ca2+ signalling in health and disease. *Biochem J,* 439**,** 349-74.

NAGATA, K., ZHENG, L., MADATHANY, T., CASTIGLIONI, A. J., BARTLES, J. R. & GARCIA-ANOVEROS, J. 2008. The varitint-waddler (Va) deafness mutation in TRPML3 generates constitutive, inward rectifying currents and causes cell degeneration. *Proc Natl Acad Sci U S A,* 105**,** 353-8.

NAPOLITANO, G. & BALLABIO, A. 2016. TFEB at a glance. *J Cell Sci,* 129**,** 2475-81.

NILIUS, B., MAHIEU, F., PRENEN, J., JANSSENS, A., OWSIANIK, G., VENNEKENS, R. & VOETS, T. 2006. The Ca2+-activated cation channel TRPM4 is regulated by phosphatidylinositol 4,5-biphosphate. *EMBO J,* 25**,** 467-78.

NILIUS, B. & OWSIANIK, G. 2011. The transient receptor potential family of ion channels. *Genome Biol,* 12**,** 218.

NILIUS, B., PRENEN, J., DROOGMANS, G., VOETS, T., VENNEKENS, R., FREICHEL, M., WISSENBACH, U. & FLOCKERZI, V. 2003. Voltage dependence of the Ca2+-activated cation channel TRPM4. *J Biol Chem,* 278**,** 30813-20.

NILIUS, B., TALAVERA, K., OWSIANIK, G., PRENEN, J., DROOGMANS, G. & VOETS, T. 2005. Gating of TRP channels: a voltage connection? *J Physiol,* 567**,** 35-44.

ONODERA, J. & OHSUMI, Y. 2005. Autophagy is required for maintenance of amino acid levels and protein synthesis under nitrogen starvation. *J Biol Chem,* 280**,** 31582-6.

ONYENWOKE, R. U., SEXTON, J. Z., YAN, F., DIAZ, M. C., FORSBERG, L. J., MAJOR, M. B. & BRENMAN, J. E. 2015. The mucolipidosis IV Ca2+ channel TRPML1 (MCOLN1) is regulated by the TOR kinase. *Biochem J,* 470**,** 331-42.

OWSIANIK, G., D'HOEDT, D., VOETS, T. & NILIUS, B. 2006. Structure-function relationship of the TRP channel superfamily. *Rev Physiol Biochem Pharmacol,* 156**,** 61-90.

PALMIERI, M., IMPEY, S., KANG, H., DI RONZA, A., PELZ, C., SARDIELLO, M. & BALLABIO, A. 2011. Characterization of the CLEAR network reveals an integrated control of cellular clearance pathways. *Hum Mol Genet,* 20**,** 3852-66.

PERRAUD, A. L., FLEIG, A., DUNN, C. A., BAGLEY, L. A., LAUNAY, P., SCHMITZ, C., STOKES, A. J., ZHU, Q., BESSMAN, M. J., PENNER, R., KINET, J. P. & SCHARENBERG, A. M. 2001. ADP-ribose gating of the calcium-permeable LTRPC2 channel revealed by Nudix motif homology. *Nature,* 411**,** 595-9.

POLSON, H. E., DE LARTIGUE, J., RIGDEN, D. J., REEDIJK, M., URBE, S., CLAGUE, M. J. & TOOZE, S. A. 2010. Mammalian Atg18 (WIPI2) localizes to omegasome-anchored phagophores and positively regulates LC3 lipidation. *Autophagy,* 6**,** 506-22.

POWIS, G., BONJOUKLIAN, R., BERGGREN, M. M., GALLEGOS, A., ABRAHAM, R., ASHENDEL, C., ZALKOW, L., MATTER, W. F., DODGE, J., GRINDEY, G. & ET AL. 1994. Wortmannin, a potent and selective inhibitor of phosphatidylinositol-3-kinase. *Cancer Res,* 54**,** 2419-23.

PREMKUMAR, L. S. & AHERN, G. P. 2000. Induction of vanilloid receptor channel activity by protein kinase C. *Nature,* 408**,** 985-90.

PREMKUMAR, L. S., RAISINGHANI, M., PINGLE, S. C., LONG, C. & PIMENTEL, F. 2005. Downregulation of transient receptor potential melastatin 8 by protein kinase C-mediated dephosphorylation. *J Neurosci,* 25**,** 11322-9.

PROIKAS-CEZANNE, T., RUCKERBAUER, S., STIERHOF, Y. D., BERG, C. & NORDHEIM, A. 2007. Human WIPI-1 puncta-formation: a novel assay to assess mammalian autophagy. *FEBS Lett,* 581**,** 3396-404.

PROIKAS-CEZANNE, T., TAKACS, Z., DONNES, P. & KOHLBACHER, O. 2015. WIPI proteins: essential PtdIns3P effectors at the nascent autophagosome. *J Cell Sci,* 128**,** 207-17.

PROIKAS-CEZANNE, T., WADDELL, S., GAUGEL, A., FRICKEY, T., LUPAS, A. & NORDHEIM, A. 2004. WIPI-1alpha (WIPI49), a member of the novel 7-bladed WIPI protein family, is aberrantly expressed in human cancer and is linked to starvation-induced autophagy. *Oncogene,* 23**,** 9314-25.

PRYOR, P. R., MULLOCK, B. M., BRIGHT, N. A., GRAY, S. R. & LUZIO, J. P. 2000. The role of intraorganellar Ca(2+) in late endosome-lysosome heterotypic fusion and in the reformation of lysosomes from hybrid organelles. *J Cell Biol,* 149**,** 1053-62.

PRYOR, P. R., REIMANN, F., GRIBBLE, F. M. & LUZIO, J. P. 2006. Mucolipin-1 is a lysosomal membrane protein required for intracellular lactosylceramide traffic. *Traffic,* 7**,** 1388-98.

RAYCHOWDHURY, M. K., GONZALEZ-PERRETT, S., MONTALBETTI, N., TIMPANARO, G. A., CHASAN, B., GOLDMANN, W. H., STAHL, S., COONEY, A., GOLDIN, E. & CANTIELLO, H. F. 2004. Molecular pathophysiology of mucolipidosis type IV: pH dysregulation of the mucolipin-1 cation channel. *Hum Mol Genet,* 13**,** 617-27.

REDDY, A., CALER, E. V. & ANDREWS, N. W. 2001. Plasma membrane repair is mediated by Ca(2+)-regulated exocytosis of lysosomes. *Cell,* 106**,** 157-69.

RIDLEY, S. H., KTISTAKIS, N., DAVIDSON, K., ANDERSON, K. E., MANIFAVA, M., ELLSON, C. D., LIPP, P., BOOTMAN, M., COADWELL, J., NAZARIAN, A., ERDJUMENT-BROMAGE, H., TEMPST, P., COOPER, M. A., THURING, J. W., LIM, Z. Y., HOLMES, A. B., STEPHENS, L. R. & HAWKINS, P. T. 2001. FENS-1 and DFCP1 are FYVE domain-containing proteins with distinct functions in the endosomal and Golgi compartments. *J Cell Sci,* 114**,** 3991-4000.

ROBERTS, R. & KTISTAKIS, N. T. 2013. Omegasomes: PI3P platforms that manufacture autophagosomes. *Essays Biochem,* 55**,** 17-27.

RODRIGUEZ, A., WEBSTER, P., ORTEGO, J. & ANDREWS, N. W. 1997. Lysosomes behave as Ca2+-regulated exocytic vesicles in fibroblasts and epithelial cells. *J Cell Biol,* 137**,** 93-104.

ROHACS, T. 2014. Phosphoinositide regulation of TRP channels. *Handb Exp Pharmacol,* 223**,** 1143-76.

ROHACS, T. & NILIUS, B. 2007. Regulation of transient receptor potential (TRP) channels by phosphoinositides. *Pflugers Arch,* 455**,** 157-68.

ROSENBAUM, A. I., ZHANG, G., WARREN, J. D. & MAXFIELD, F. R. 2010. Endocytosis of beta-cyclodextrins is responsible for cholesterol reduction in Niemann-Pick type C mutant cells. *Proc Natl Acad Sci U S A,* 107**,** 5477-82.

RUBINSZTEIN, D. C., SHPILKA, T. & ELAZAR, Z. 2012. Mechanisms of autophagosome biogenesis. *Curr Biol,* 22**,** R29-34.

RUSNAK, F. & MERTZ, P. 2000. Calcineurin: form and function. *Physiol Rev,* 80**,** 1483-521.

SAFTIG, P. & KLUMPERMAN, J. 2009. Lysosome biogenesis and lysosomal membrane proteins: trafficking meets function. *Nat Rev Mol Cell Biol,* 10**,** 623-35.

SALDANHA, S. A., GRIMM, C., ALLAIS, C., SMITH, E., OUIZEM, S., MERCER, B. A., ROUSH, W. R., HELLER, S. & HODDER, P. 2010. Identification of Selective Agonists of the Transient Receptor Potential Channels 3 (TRPML3). *Probe Reports from the NIH Molecular Libraries Program.* Bethesda (MD).

SAMIE, M., WANG, X., ZHANG, X., GOSCHKA, A., LI, X., CHENG, X., GREGG, E., AZAR, M., ZHUO, Y., GARRITY, A. G., GAO, Q., SLAUGENHAUPT, S., PICKEL, J., ZOLOV, S. N., WEISMAN, L. S., LENK, G. M., TITUS, S., BRYANT-GENEVIER, M., SOUTHALL, N., JUAN, M., FERRER, M. & XU, H. 2013. A TRP channel in the lysosome regulates large particle phagocytosis via focal exocytosis. *Dev Cell,* 26**,** 511-24.

SAMIE, M. A., GRIMM, C., EVANS, J. A., CURCIO-MORELLI, C., HELLER, S., SLAUGENHAUPT, S. A. & CUAJUNGCO, M. P. 2009. The tissue-specific expression of TRPML2 (MCOLN-2) gene is influenced by the presence of TRPML1. *Pflugers Arch,* 459**,** 79-91.

SARDIELLO, M., PALMIERI, M., DI RONZA, A., MEDINA, D. L., VALENZA, M., GENNARINO, V. A., DI MALTA, C., DONAUDY, F., EMBRIONE, V., POLISHCHUK, R. S., BANFI, S., PARENTI, G., CATTANEO, E. & BALLABIO, A. 2009. A gene network regulating lysosomal biogenesis and function. *Science,* 325**,** 473-7.

SCHAHEEN, L., DANG, H. & FARES, H. 2006. Basis of lethality in C. elegans lacking CUP-5, the Mucolipidosis Type IV orthologue. *Dev Biol,* 293**,** 382-91.

SCHINK, K. O., TAN, K. W. & STENMARK, H. 2016. Phosphoinositides in Control of Membrane Dynamics. *Annu Rev Cell Dev Biol,* 32**,** 143-171.

SETTEMBRE, C., DI MALTA, C., POLITO, V. A., GARCIA ARENCIBIA, M., VETRINI, F., ERDIN, S., ERDIN, S. U., HUYNH, T., MEDINA, D., COLELLA, P., SARDIELLO, M., RUBINSZTEIN, D. C. & BALLABIO, A. 2011. TFEB links autophagy to lysosomal biogenesis. *Science,* 332**,** 1429-33.

SETTEMBRE, C., FRALDI, A., MEDINA, D. L. & BALLABIO, A. 2013. Signals from the lysosome: a control centre for cellular clearance and energy metabolism. *Nat Rev Mol Cell Biol,* 14**,** 283-96.

SETTEMBRE, C., ZONCU, R., MEDINA, D. L., VETRINI, F., ERDIN, S., ERDIN, S., HUYNH, T., FERRON, M., KARSENTY, G., VELLARD, M. C., FACCHINETTI, V., SABATINI, D. M. & BALLABIO, A. 2012. A lysosome-to-nucleus signalling mechanism senses and regulates the lysosome via mTOR and TFEB. *EMBO J,* 31**,** 1095-108.

SHEN, D., WANG, X., LI, X., ZHANG, X., YAO, Z., DIBBLE, S., DONG, X. P., YU, T., LIEBERMAN, A. P., SHOWALTER, H. D. & XU, H. 2012. Lipid storage disorders block lysosomal trafficking by inhibiting a TRP channel and lysosomal calcium release. *Nat Commun,* 3**,** 731.

SHIGETOMI, E., PATEL, S. & KHAKH, B. S. 2016. Probing the Complexities of Astrocyte Calcium Signaling. *Trends Cell Biol,* 26**,** 300-12.

SMAILI, S. S., PEREIRA, G. J., COSTA, M. M., ROCHA, K. K., RODRIGUES, L., DO CARMO, L. G., HIRATA, H. & HSU, Y. T. 2013. The role of calcium stores in apoptosis and autophagy. *Curr Mol Med,* 13**,** 252-65.

SONG, Y., DAYALU, R., MATTHEWS, S. A. & SCHARENBERG, A. M. 2006. TRPML cation channels regulate the specialized lysosomal compartment of vertebrate B-lymphocytes. *Eur J Cell Biol,* 85**,** 1253-64.

SOYOMBO, A. A., TJON-KON-SANG, S., RBAIBI, Y., BASHLLARI, E., BISCEGLIA, J., MUALLEM, S. & KISELYOV, K. 2006. TRP-ML1 regulates lysosomal pH and acidic lysosomal lipid hydrolytic activity. *J Biol Chem,* 281**,** 7294-301.

SPOONER, E., MCLAUGHLIN, B. M., LEPOW, T., DURNS, T. A., RANDALL, J., UPCHURCH, C., MILLER, K., CAMPBELL, E. M. & FARES, H. 2013. Systematic screens for proteins that interact with the mucolipidosis type IV protein TRPML1. *PLoS One,* 8**,** e56780.

STORY, G. M., PEIER, A. M., REEVE, A. J., EID, S. R., MOSBACHER, J., HRICIK, T. R., EARLEY, T. J., HERGARDEN, A. C., ANDERSSON, D. A., HWANG, S. W., MCINTYRE, P., JEGLA, T., BEVAN, S. & PATAPOUTIAN, A. 2003. ANKTM1, a TRP-like channel expressed in nociceptive neurons, is activated by cold temperatures. *Cell,* 112**,** 819-29.

SU, J., ZHOU, L., KONG, X., YANG, X., XIANG, X., ZHANG, Y., LI, X. & SUN, L. 2013. Endoplasmic reticulum is at the crossroads of autophagy, inflammation, and apoptosis signaling pathways and participates in the pathogenesis of diabetes mellitus. *J Diabetes Res,* 2013**,** 193461.

SUDHOF, T. C. & ROTHMAN, J. E. 2009. Membrane fusion: grappling with SNARE and SM proteins. *Science,* 323**,** 474-7.

SUN, L., HUA, Y., VERGARAJAUREGUI, S., DIAB, H. I. & PUERTOLLANO, R. 2015. Novel Role of TRPML2 in the Regulation of the Innate Immune Response. *J Immunol,* 195**,** 4922-32.

SUN, M., GOLDIN, E., STAHL, S., FALARDEAU, J. L., KENNEDY, J. C., ACIERNO, J. S., JR., BOVE, C., KANESKI, C. R., NAGLE, J., BROMLEY, M. C., COLMAN, M., SCHIFFMANN, R. &

SLAUGENHAUPT, S. A. 2000. Mucolipidosis type IV is caused by mutations in a gene encoding a novel transient receptor potential channel. *Hum Mol Genet,* 9**,** 2471-8.
SUN, T., WANG, X., LU, Q., REN, H. & ZHANG, H. 2011. CUP-5, the C. elegans ortholog of the mammalian lysosomal channel protein MLN1/TRPML1, is required for proteolytic degradation in autolysosomes. *Autophagy,* 7**,** 1308-15.
SZALLASI, A., SZABO, T., BIRO, T., MODARRES, S., BLUMBERG, P. M., KRAUSE, J. E., CORTRIGHT, D. N. & APPENDINO, G. 1999. Resiniferatoxin-type phorboid vanilloids display capsaicin-like selectivity at native vanilloid receptors on rat DRG neurons and at the cloned vanilloid receptor VR1. *Br J Pharmacol,* 128**,** 428-34.
THOMPSON, E. G., SCHAHEEN, L., DANG, H. & FARES, H. 2007. Lysosomal trafficking functions of mucolipin-1 in murine macrophages. *BMC Cell Biol,* 8**,** 54.
THORNELOE, K. S., SULPIZIO, A. C., LIN, Z., FIGUEROA, D. J., CLOUSE, A. K., MCCAFFERTY, G. P., CHENDRIMADA, T. P., LASHINGER, E. S., GORDON, E., EVANS, L., MISAJET, B. A., DEMARINI, D. J., NATION, J. H., CASILLAS, L. N., MARQUIS, R. W., VOTTA, B. J., SHEARDOWN, S. A., XU, X., BROOKS, D. P., LAPING, N. J. & WESTFALL, T. D. 2008. N-((1S)-1-{[4-((2S)-2-{[(2,4-dichlorophenyl)sulfonyl]amino}-3-hydroxypropanoyl)-1 -piperazinyl]carbonyl}-3-methylbutyl)-1-benzothiophene-2-carboxamide (GSK1016790A), a novel and potent transient receptor potential vanilloid 4 channel agonist induces urinary bladder contraction and hyperactivity: Part I. *J Pharmacol Exp Ther,* 326**,** 432-42.
TOKUMITSU, H., INUZUKA, H., ISHIKAWA, Y., IKEDA, M., SAJI, I. & KOBAYASHI, R. 2002. STO-609, a specific inhibitor of the Ca(2+)/calmodulin-dependent protein kinase kinase. *J Biol Chem,* 277**,** 15813-8.
TREUSCH, S., KNUTH, S., SLAUGENHAUPT, S. A., GOLDIN, E., GRANT, B. D. & FARES, H. 2004. Caenorhabditis elegans functional orthologue of human protein h-mucolipin-1 is required for lysosome biogenesis. *Proc Natl Acad Sci U S A,* 101**,** 4483-8.
TRONCHERE, H., LAPORTE, J., PENDARIES, C., CHAUSSADE, C., LIAUBET, L., PIROLA, L., MANDEL, J. L. & PAYRASTRE, B. 2004. Production of phosphatidylinositol 5-phosphate by the phosphoinositide 3-phosphatase myotubularin in mammalian cells. *J Biol Chem,* 279**,** 7304-12.
TSURUTA, F. 2016. New insights into the functions of PtdIns(3,5)P2 in the pathogenisis of neurodegenerative disorders. *Neural Regen Res,* 11**,** 240-1.
VALADEZ, J. A. & CUAJUNGCO, M. P. 2015. PAX5 is the transcriptional activator of mucolipin-2 (MCOLN2) gene. *Gene,* 555**,** 194-202.
VENKATACHALAM, K., HOFMANN, T. & MONTELL, C. 2006. Lysosomal localization of TRPML3 depends on TRPML2 and the mucolipidosis-associated protein TRPML1. *J Biol Chem,* 281**,** 17517-27.
VENKATACHALAM, K., LONG, A. A., ELSAESSER, R., NIKOLAEVA, D., BROADIE, K. & MONTELL, C. 2008. Motor deficit in a Drosophila model of mucolipidosis type IV due to defective clearance of apoptotic cells. *Cell,* 135**,** 838-51.
VENUGOPAL, B., BROWNING, M. F., CURCIO-MORELLI, C., VARRO, A., MICHAUD, N., NANTHAKUMAR, N., WALKLEY, S. U., PICKEL, J. & SLAUGENHAUPT, S. A. 2007. Neurologic, gastric, and opthalmologic pathologies in a murine model of mucolipidosis type IV. *Am J Hum Genet,* 81**,** 1070-83.
VERGARAJAUREGUI, S., CONNELLY, P. S., DANIELS, M. P. & PUERTOLLANO, R. 2008a. Autophagic dysfunction in mucolipidosis type IV patients. *Hum Mol Genet,* 17**,** 2723-37.
VERGARAJAUREGUI, S., MARTINA, J. A. & PUERTOLLANO, R. 2009. Identification of the penta-EF-hand protein ALG-2 as a Ca2+-dependent interactor of mucolipin-1. *J Biol Chem,* 284**,** 36357-66.
VERGARAJAUREGUI, S., OBERDICK, R., KISELYOV, K. & PUERTOLLANO, R. 2008b. Mucolipin 1 channel activity is regulated by protein kinase A-mediated phosphorylation. *Biochem J,* 410**,** 417-25.

VERGARAJAUREGUI, S. & PUERTOLLANO, R. 2006. Two di-leucine motifs regulate trafficking of mucolipin-1 to lysosomes. *Traffic,* 7**,** 337-53.

VOETS, T. & NILIUS, B. 2007. Modulation of TRPs by PIPs. *J Physiol,* 582**,** 939-44.

VOETS, T., OWSIANIK, G., JANSSENS, A., TALAVERA, K. & NILIUS, B. 2007. TRPM8 voltage sensor mutants reveal a mechanism for integrating thermal and chemical stimuli. *Nat Chem Biol,* 3**,** 174-82.

WANG, W., GAO, Q., YANG, M., ZHANG, X., YU, L., LAWAS, M., LI, X., BRYANT-GENEVIER, M., SOUTHALL, N. T., MARUGAN, J., FERRER, M. & XU, H. 2015. Up-regulation of lysosomal TRPML1 channels is essential for lysosomal adaptation to nutrient starvation. *Proc Natl Acad Sci U S A,* 112**,** E1373-81.

WANG, W., ZHANG, X., GAO, Q. & XU, H. 2014. TRPML1: an ion channel in the lysosome. *Handb Exp Pharmacol,* 222**,** 631-45.

WATANABE, H., DAVIS, J. B., SMART, D., JERMAN, J. C., SMITH, G. D., HAYES, P., VRIENS, J., CAIRNS, W., WISSENBACH, U., PRENEN, J., FLOCKERZI, V., DROOGMANS, G., BENHAM, C. D. & NILIUS, B. 2002. Activation of TRPV4 channels (hVRL-2/mTRP12) by phorbol derivatives. *J Biol Chem,* 277**,** 13569-77.

WEIDBERG, H., SHVETS, E. & ELAZAR, Z. 2011. Biogenesis and cargo selectivity of autophagosomes. *Annu Rev Biochem,* 80**,** 125-56.

WILLIAMS, G. S., BOYMAN, L., CHIKANDO, A. C., KHAIRALLAH, R. J. & LEDERER, W. J. 2013. Mitochondrial calcium uptake. *Proc Natl Acad Sci U S A,* 110**,** 10479-86.

WONG, C. O., LI, R., MONTELL, C. & VENKATACHALAM, K. 2012. Drosophila TRPML is required for TORC1 activation. *Curr Biol,* 22**,** 1616-21.

WONG, P. M., PUENTE, C., GANLEY, I. G. & JIANG, X. 2013. The ULK1 complex: sensing nutrient signals for autophagy activation. *Autophagy,* 9**,** 124-37.

WOODS, A., DICKERSON, K., HEATH, R., HONG, S. P., MOMCILOVIC, M., JOHNSTONE, S. R., CARLSON, M. & CARLING, D. 2005. Ca2+/calmodulin-dependent protein kinase kinase-beta acts upstream of AMP-activated protein kinase in mammalian cells. *Cell Metab,* 2**,** 21-33.

WU, H., ROTHERMEL, B., KANATOUS, S., ROSENBERG, P., NAYA, F. J., SHELTON, J. M., HUTCHESON, K. A., DIMAIO, J. M., OLSON, E. N., BASSEL-DUBY, R. & WILLIAMS, R. S. 2001. Activation of MEF2 by muscle activity is mediated through a calcineurin-dependent pathway. *EMBO J,* 20**,** 6414-23.

XU, H., BLAIR, N. T. & CLAPHAM, D. E. 2005. Camphor activates and strongly desensitizes the transient receptor potential vanilloid subtype 1 channel in a vanilloid-independent mechanism. *J Neurosci,* 25**,** 8924-37.

XU, H., DELLING, M., LI, L., DONG, X. & CLAPHAM, D. E. 2007. Activating mutation in a mucolipin transient receptor potential channel leads to melanocyte loss in varitint-waddler mice. *Proc Natl Acad Sci U S A,* 104**,** 18321-6.

XU, H. & REN, D. 2015. Lysosomal physiology. *Annu Rev Physiol,* 77**,** 57-80.

YANG, Z. & KLIONSKY, D. J. 2010. Mammalian autophagy: core molecular machinery and signaling regulation. *Curr Opin Cell Biol,* 22**,** 124-31.

YAO, Z. & KLIONSKY, D. J. 2015. The symphony of autophagy and calcium signaling. *Autophagy,* 11**,** 973-4.

YLA-ANTTILA, P., VIHINEN, H., JOKITALO, E. & ESKELINEN, E. L. 2009. 3D tomography reveals connections between the phagophore and endoplasmic reticulum. *Autophagy,* 5**,** 1180-5.

YORIMITSU, T. & KLIONSKY, D. J. 2005. Autophagy: molecular machinery for self-eating. *Cell Death Differ,* 12 Suppl 2**,** 1542-52.

ZEEVI, D. A., FRUMKIN, A., OFFEN-GLASNER, V., KOGOT-LEVIN, A. & BACH, G. 2009. A potentially dynamic lysosomal role for the endogenous TRPML proteins. *J Pathol,* 219**,** 153-62.

ZEEVI, D. A., LEV, S., FRUMKIN, A., MINKE, B. & BACH, G. 2010. Heteromultimeric TRPML channel assemblies play a crucial role in the regulation of cell viability models and starvation-induced autophagy. *J Cell Sci,* 123**,** 3112-24.

ZEIGLER, M., BARGAL, R., SURI, V., MEIDAN, B. & BACH, G. 1992. Mucolipidosis type IV: accumulation of phospholipids and gangliosides in cultured amniotic cells. A tool for prenatal diagnosis. *Prenat Diagn,* 12**,** 1037-42.

ZHANG, X., CHENG, X., YU, L., YANG, J., CALVO, R., PATNAIK, S., HU, X., GAO, Q., YANG, M., LAWAS, M., DELLING, M., MARUGAN, J., FERRER, M. & XU, H. 2016. MCOLN1 is a ROS sensor in lysosomes that regulates autophagy. *Nat Commun,* 7**,** 12109.

ZHANG, X., LI, X. & XU, H. 2012. Phosphoinositide isoforms determine compartment-specific ion channel activity. *Proc Natl Acad Sci U S A,* 109**,** 11384-9.

ZOLOV, S. N., BRIDGES, D., ZHANG, Y., LEE, W. W., RIEHLE, E., VERMA, R., LENK, G. M., CONVERSO-BARAN, K., WEIDE, T., ALBIN, R. L., SALTIEL, A. R., MEISLER, M. H., RUSSELL, M. W. & WEISMAN, L. S. 2012. In vivo, Pikfyve generates PI(3,5)P2, which serves as both a signaling lipid and the major precursor for PI5P. *Proc Natl Acad Sci U S A,* 109**,** 17472-7.